ELECTRONIC STRUCTURE OF COMPLEXES OF THE LIGAND O-PHENYLENEBISDIMETHYLARSINE

Thesis by

Paula K. Bernstein

In Partial Fulfillment of the Requirements

For the Degree of

Doctor of Philosophy

California Institute of Technology

Pasadena, California

1971

(Submitted September 23, 1970)

This thesis is dedicated to my husband, Uri.

ACKNOWLEDGMENTS

A number of people have contributed both directly and indirectly to the completion of this work.

I gratefully acknowledge the direction of my adviser, Dr. Harry B. Gray. His enthusiasm, encouragement, and ready availability for discussions have greatly contributed to this research.

I thank Dr. Gordon Rodley for his invaluable collaboration over the past year. I also thank Dr. Richard Marsh for his contributions to the crystallography portions of this work.

Several of my colleagues in the Gray group have given their advice and help as well as their companionship over the past four years. In particular, I thank Drs. Fred Tsay, James Preer, Diane Gutterman, and Robert Levenson.

I am grateful to Dr. Barbara Low for the use of her equipment and to Dr. Jerry Swalen for his spectral simulation program.

I thank the California Institute of Technology for its grant of an NDEA Fellowship during one year, and Dr. Gray for the Research Assistantship which has supported me for the remaining time.

My parents, Mr. and Mrs. Meyer Kreisman, have always encouraged my endeavors. I thank them for their confidence and support.

I am grateful to Mrs. Susan Brittenham for the excellent job she has done in typing this manuscript.

Finally, I wish to express my gratitude to my husband, Uri, for his patience and understanding during the more difficult portions of this work.

ABSTRACT

Various studies have been carried out to elucidate the detailed electronic structure of the unusual spin doublet complex $[Ni(diars)_2X_2]Y$ (X = Cl, Br, -NCS; Y = Cl, Br, -NCS, ClO_4^-). An X-ray crystallographic study has been done which confirmed its coordination number of six. U. v. and visible spectra have been taken of it and of other closely related cobalt and nickel complexes. Assignments for the charge transfer and ligand field spectra are suggested. ESR studies have been done in solution, powder, and single crystal to extract the components of the ligand superhyperfine splitting tensors. A semi-quantitative MO scheme, consistent with these tensor values, has been used to explain some of the unusual properties of this complex.

We have concluded from these studies that the energy level ordering in $Ni(diarsine)_2X_2^+$ is $x^2 - y^2 < xz, yz < z^2 < xy$ and that the ground state is ^2A_g. The ground state is highly delocalized, consisting of approximately 50% ligand character distributed over all six ligands. The tipping of the benzene rings and the distortion of the axial ligands permits an admixture of chlorine p_x orbitals into the ground state molecular orbital which serves to further stabilize this system.

TABLE OF CONTENTS

I. INTRODUCTION

The arsenic donor ligand o-phenylene-bis dimethylarsine

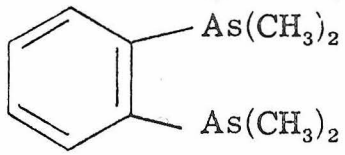

(diarsine) forms complexes with a large number of transition metals and stabilizes a variety of different oxidation states. The bulk of the work on diarsine transition metal chemistry has been done over the past few years by Nyholm and co-workers at University College, London.[1-3] Their work consisted primarily of the synthesis and characterization of various complexes and did not include any attempt to treat structural properties in detail.

Diarsine is an extremely versatile chelating agent. Its complexes vary in geometry from 8 coordinate dodecahedra[4] to 4 coordinate square planes,[3] and it stabilizes metal oxidation states from 0 to +4. Some of the more unusual diarsine complexes include the 8 coordinate compounds of Ti, Zr, and Hf[4]; the strong field-paramagnetic Mo(II) complex, $Mo(diars)_2X_2$[5]; the Tc(II) and Tc(III) complexes[6]; the Fe(IV)[7] and Os(IV) compounds[8]; an octahedral Au(III) complex, $Au(diars)_2I_3$[9]; and the four coordinate Au(I) compounds.[10] The spectra of the d^3 Cr(III),[11] d^5 Fe(III),[12] and d^6 Co(III) and Fe(II)[11] complexes have recently been studied and assigned.

Of particular interest are the complexes of the nickel group. Diamagnetic species of the form $M(diars)_2X_2$, where M = Ni(II), Pd(II), Pt(II) and X = Cl, Br, I, SCN^-, and ClO_4^- were prepared and

and studied by Dr. James Preer.[13]

When $Ni(diars)_2Cl_2$ is oxidized by air in the presence of HCl, the paramagnetic compound $[Ni(diars)_2Cl_2]Cl$ is obtained. Bromide, thiocyanate, and perchlorate derivatives also exist.[1] For a long time this compound had been cited as one of the very few authentic examples of a stabilized Ni(III) d^7 complex.

From the point of view of crystal field theory, it is easy to see why a Ni(III) state is difficult to stabilize. The value of Δ in an octahedral complex (i.e., the separation between the t_{2g} and e_g levels for a given ligand) generally increases with the change on the central metal. This would make the $(t_{2g})^6 e_g^1$ configuration required by octahedral Ni(III) extremely unstable and one would ordinarily expect either loss of one ligand or the formation of a metal-metal bond to occur. Despite such predictions, $Ni(diars)_2Cl_3$ has been shown by analytical, conductometric, chemical,[1] and X-ray evidence[14] to be an extremely stable six-coordinate monomer.

Several examples are available in the literature of so called Ni(III) compounds. Several sulfur donor ligands with this general structure

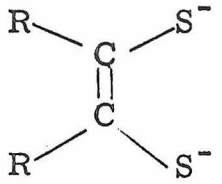

$R = \phi,\ CN^-,\ CF_3$

form complexes which formally at least contain Ni(III).[15] Recently Olson and Vasilevskis[16] reported the isolation of some square planar Ni(III) cyclic amine complexes, and Wolberg and Manassen reported

the ESR spectrum of a Ni(III) tetraphenyl porphyrin complex.[17]

With the exception of $Ni(diars)_2X_3$, all these Ni(III) complexes share in common a square planar structure. This means that these systems can be stabilized by a delocalized network of out-of-plane π bonds.[15] In the $Ni(diars)_2Cl_2^+$ cation, the arsenic orbitals which would be needed for such a system are already involved in bonding with the methyl groups and cannot π bond elsewhere. It has been suggested that arsenic $d\pi$ orbitals may play a role in stabilization of the complex,[1] however, their extremely high energies make such participation of doubtful importance.

The paramagnetism of $Ni(diars)_2X_2^+$ makes it particularly suitable for electronic structural studies. A research plan to elucidate its electronic structure was formulated and carried out as follows:

1. An X-ray crystal structure was done to confirm the six-coordinate octahedral structure of the compound and to obtain bond lengths for further electronic studies.

2. U. v. and visible spectra were taken of the known Ni(III), Ni(IV), and Co(III) complexes both at room temperature and at liquid nitrogen temperature.

3. Powder, solution, and single crystal ESR spectra were taken to obtain the components of the "g" and "A" tensors.

4. The experimental ESR results were treated theoretically in order to obtain a molecular orbital model for the ground state.

II. X-RAY CRYSTAL STRUCTURES OF THE PARAMAGNETIC COMPLEX DICHLOROBIS(DIARSINE)NICKEL MONOCHLORIDE AND THE DIAMAGNETIC COMPLEX DICHLOROBIS(DIARSINE) COBALT MONOCHLORIDE

Introduction

The logical first step in the determination of the electronic structure of the unusual Ni(diarsine)$_2$Cl$_3$ complex was a complete crystal structure. This was begun at Columbia University. Using film data, the structure was solved and refined to an R value of 0.13. Subsequently, the R value was considerably improved by collecting diffractometer data. When Ni(diars)$_2$Cl$_2^+$ is doped into a matrix of the supposedly isomorphous Co(diarsine)$_2$Cl$_3$ or Co(diarsine)$_2$Cl$_2$ClO$_4$, some unusual changes occur in its ESR spectrum. (These will be described in detail in Part IV.) In order to account for these changes, Dr. Gordon Rodley did the structure of Co(diars)$_2$Cl$_3$. Data were collected on an automated diffractometer and refined using the coordinates of the Ni(diarsine)$_2$Cl$_3$ structure. Dr. Rodley's results will also be presented here and compared in detail to ours.

Unit Cell and Space Group Determination

Nickel(diarsine)$_2$Cl$_3$ was prepared by the method of Nyholm[1] and recrystallized from ethanol. The crystals are small golden brown rectangular parallelepipeds elongated along the "a" axis. The space group was determined from h0ℓ and 0kℓ Weissenberg photographs. The cell dimensions were determined by a least squares fit to 12 reflections measured on a Datex-Automated

General Electric diffractometer. The crystal is monoclinic with space group $P2_{1/c}$ and cell dimensions a = 9.170 ± .007, b = 9.592 ± .005, c = 14.986 ± .003, β = 97.96° ± 0.07°, and ρ = 1.84 g/cm^3.

Collection and Reduction of X-Ray Data

Partial data were collected using a Weissenberg camera and CuKα radiation. Multiple film photographs of layers 0 to 7 about the "a" axis were taken for 72 hours each. Intensities were measured visually. We recorded 1967 reflections of which 517 were unobservable.

Additional data were taken using a Datex-Automated General Electric diffractometer and iron filtered cobalt X-radiation. Intensities were measured using a θ-2θ scan speed of 2° per minute. Background was counted for 30 seconds before and after each scan.

Two strong reflections, 080 and 544, were used as "check" reflections and were remeasured alternately every 20 reflections. No adjustments of the goniometer head were necessary during the 7 days of 24 hour operation. Eight hundred and ninety-two reflections were measured twice and the weights were averaged during the initial data processing. Of a total of 1820 independent reflections, 1774 were calculated to be non-zero and were used in the refinement of the structure.

The initial processing of the film data consisted of the assignment of a standard deviation to each reflection, correction for Lorentz and polarization factors, and the scaling together of the reflections to give values of F^2 and σF^2 for each observation.

The values of the observed intensities for the diffractometer data were derived from the following formula

$$I_{obsd} = S - \frac{(B_1 + B_2)}{2} \left(\frac{t}{30}\right)$$

where S is the scan count, B_1 and B_2 are the two background counts, and t is the scan time in seconds. Negative values of I_{obsd}, calculated in this way, were set equal to zero.

The standard deviation for each reflection was calculated using

$$\sigma^2(I_{obsd}) = S + \frac{(B_1 + B_2)}{2} \left(\frac{t}{30}\right)^2 + (0.02S)^2$$

The intensities and standard deviations were corrected for Lorentz and polarization factors and were the basis of the weights used in the least squares refinement of the diffractometer data.

Solution and Refinement of the Structure

The $Ni(diarsine)_2Cl_3$ structure was initially solved using only film data. The positions of the nickel and both arsenic atoms were determined from a three-dimensional Patterson function. The nickel parameters are 000 and $0\frac{1}{2}\frac{1}{2}$. The heavy atom positions were refined through several least squares cycles to an initial R of 0.35. A three-dimensional Fourier map was then calculated with phases based on the heavy atoms and used to locate the chlorines and benzene ring. An overall scale factor and an isotropic temperature factor were calculated by Wilson's method and used in the original calculations.

In the second stage of refinement, all of the heavy atoms were given anisotropic temperature parameters. This reduced the

R value to 0.20. The methyl groups were then located by means of a three dimensional difference Fourier. In the least squares refinement of the film data, 80 parameters were varied, 3 coordinates and 6 temperature factors for three of the two heavy atoms, 6 temperature factors for each of the heavy atoms in special positions, 3 coordinates and one temperature factor for the 10 light atoms, and a scale factor. All except the scale factor were put into one matrix and were permitted to vary in the final two cycles. The structure converged to a final R of 0.14 for 1366 reflections.

After collecting diffractometer data, we proceeded to refine the structure further.

For the first least squares refinement of the diffractometer data, we included in the least squares matrix only the final atomic coordinates obtained from the film structure and a scale factor. This gave an R value of 0.096. The next two least squares cycles, which reduced R to 0.064, included 13 atomic position coordinates, a scale factor, and anisotropic temperature factors for all atoms.

At this point we located the hydrogen atoms. The positions of the four hydrogens on the benzene ring were calculated assuming sp^2 hybridization around each carbon atom. The methyl hydrogens were located by means of difference Fouriers calculated in the planes perpendicular to the arsenic-methylcarbon bonds. The methyl hydrogens showed up quite clearly in all four difference maps, indicating that the methyl groups do not rotate freely in the molecule.

In the first refinement including hydrogens, only the heavy atoms were allowed to vary. The hydrogens were included in the calculation with isotropic temperature factors but were held constant. A secondary extinction factor was included at this stage. This cycle reduced R to 0.055.

In the final least squares cycle, 179 parameters were put into one matrix and permitted to vary: 6 temperature factors for the 2 atoms in special positions, 3 coordinates and 6 temperature factors for all other non-hydrogen atoms, 3 coordinates for the hydrogen atoms, a secondary extinction parameter, and a scale factor. The final R value was 0.054 for 1774 reflections. The weighted R was 0.012 and the goodness of fit $(\Sigma w (Fo^2 - Fc^2)/(n - p)^{\frac{1}{2}})$ was 0.00837.

All calculations were done on the IBM 7094 and IBM 360-75 computers using subprograms of the CRYRM system.[18] The atomic form factors for Ni, Co, As, and C were taken from the standard literature tabulation,[19] and those for Ni and As were corrected for anomalous dispersion. The form factor for hydrogen was taken from Stewart, Davidson, and Simpson.[20] The least squares calculation minimized the function $\Sigma w (Fo^2 - Fc^2)^2$. The weighting function used was $1/\sigma^2 (F^2_{obsd})$.

Figure 1 is a projection of the three dimensional Fourier map down the y axis. Figure 2 is a perspective view of the structure with the labeling adopted for discussion. The observed and calculated structure factors are given in Tables I and II. Tables III and IV list

the final positional and thermal parameters with their standard deviations for $Ni(diars)_2Cl_3$ and $Co(diars)_2Cl_3$, respectively. Selected bond distances and angles are given in Tables V and VI, VII and VIII.

Description of the Structures

Both monocations $Ni(diars)_2Cl_2^+$ and $Co(diars)_2Cl_2^+$ are monomeric. Two diarsine ligands surround the metal atom in a square planar arrangement. The chlorides are located above and below the plane of the arsenic atoms in octahedral sites. The benzene rings are not coplanar with the metal-arsenic plane. The dihedral angle between them is 12°26' for the nickel and 12°42' for the cobalt. In both cations, as in $Ni(diars)_2I_2$,[21] the halide appears to be perturbed by the methyl groups. The distances between the chloride and methyl carbon are 3.56 Å and 3.47 Å in the respective nickel and cobalt structures. This is less than the sum of the Van der Waals radii for the two (1.8 + 2.0 = 3.8 Å). This interaction is further suggested by the observed methyl-arsenic-metal angles, 12-2-1, 14-2-1, 13-3-1, 15-3-1, which all considerably exceed the tetrahedral angle. All the other angles about arsenic are less than the tetrahedral angle. This effect we interpret as due to the methyl groups being pushed aside to facilitate M–Cl bonding.

The chlorides in both structures are distorted from an axial "octahedral" position by an angle of two degrees. A similar and larger distortion is observed in the $Ni(diars)_2I_2$ complex.[21] This has been explained by the asymmetry of non-bonded interactions between the iodide and carbon ring atoms in adjacent molecules.

Although this explanation is possible for iodide, it seems unlikely for chloride which is smaller than iodide and closer to the central metal. Rather than relying on intermolecular interactions to explain this distortion and the nonplanarity, we prefer to propose that both take place in order to stabilize the molecule electronically. The tipping of the benzene rings lowers the ideal symmetry from D_{2h} to C_{2h}, and the chloride distortion lowers it still further to C_i. If we assume that the ground state is A_{1g} (d_{z^2}), then this lower symmetry permits the admixture of p_x orbitals from the chlorine. We have strong ESR evidence that there is an appreciable contribution from these orbitals (see Part V). All of the d^7 and d^8 structures done to date[9, 21-24] are 6 coordinate in the solid and show evidence of these distortions. In Au(III)$(diars)_2I_3$, the dihedral angle between the benzene ring and arsenic plane is as large as 26°.[9] Only one structure has been done which exhibits the ideal D_{2h} symmetry.[26] This is the structure of Co(III)$(diars)_2Cl_2ClO_4$, which crystallizes in the space group C_2. Note, however, that Co(III) has the inherently stable d^6 configuration which does not benefit from distortion nearly so much as d^7 or d^8. We have determined the space group of Ni(III)$(diars)_2Cl_2ClO_4$. It is quite interesting that rather than being isomorphous to Co$(diars)_2Cl_2ClO_4$, the nickel crystallizes in $C222_1$, a space group which requires it to have only one twofold axis. Its ESR spectrum has been reported[27] and is identical to the spectrum of Ni$(diars)_2Cl_3$. Since g values are extremely sensitive to small distortions, these facts suggest that Ni$(diars)_2Cl_3$ and Ni$(diars)_2Cl_2ClO_4$ have identical structures in the solid.

A careful comparison of the structures of $Ni(diars)_2Cl_3$ and $Co(diars)_2Cl_3$ yields only one appreciable difference between them. The metal chloride distance is 2.29 Å for Co–Cl and 2.43 Å for Ni–Cl. This difference is much larger than the standard deviations in the bond lengths. When one dopes $Ni(diars)_2Cl_3$ into $Co(diars)_2Cl_3$, a dramatic change occurs in the powder ESR spectrum. Since the only difference in the structures is the metal-chloride bond length, it is reasonable to assume that the only change that occurs in the nickel structure upon doping is a contraction of the Ni–Cl bond. It will be seen in Part V that it is possible to account for the changes in the ESR spectrum on this basis.

Figure 1. Projection of the three-dimensional Fourier map down the y axis.

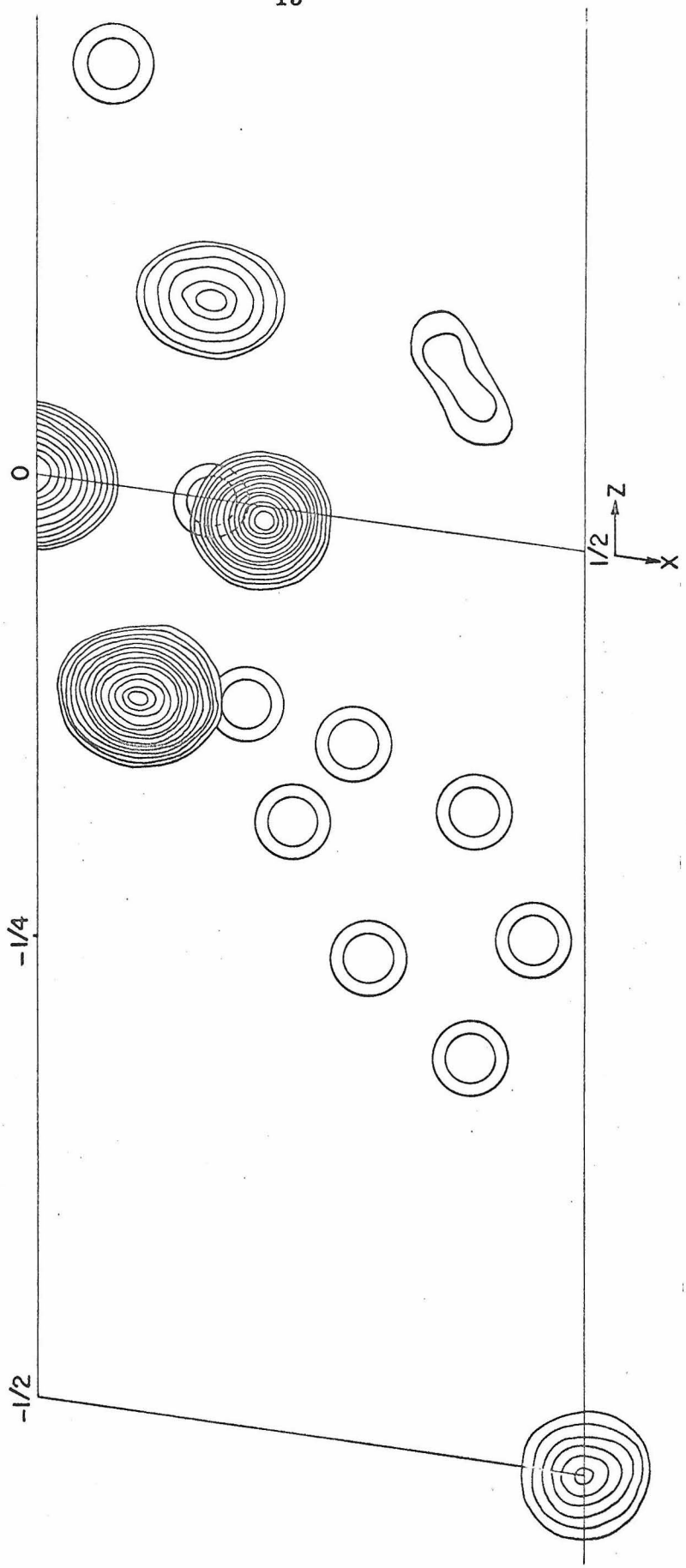
0
-1/4
-1/2
1/2
Z
X

Figure 2. Perspective view of the structure of $Ni(diars)_2Cl_2^+$.

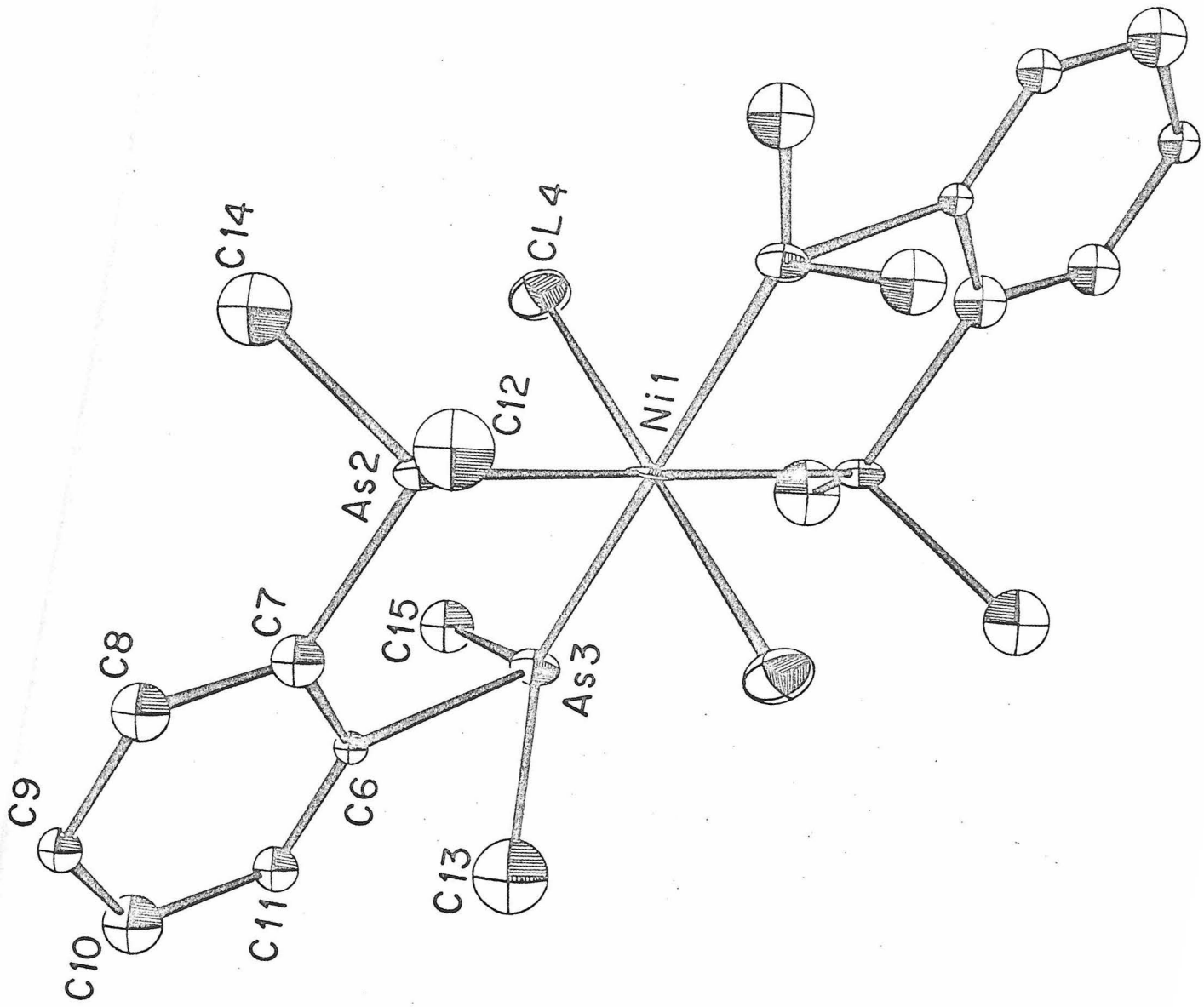
C14
CL4
C12
Ni1
As2
C7
C15
As3
C8
C9
C6
C13
C11
C10

Table I. Observed and Calculated Structure Factors for $Ni(diars)_2Cl_3$

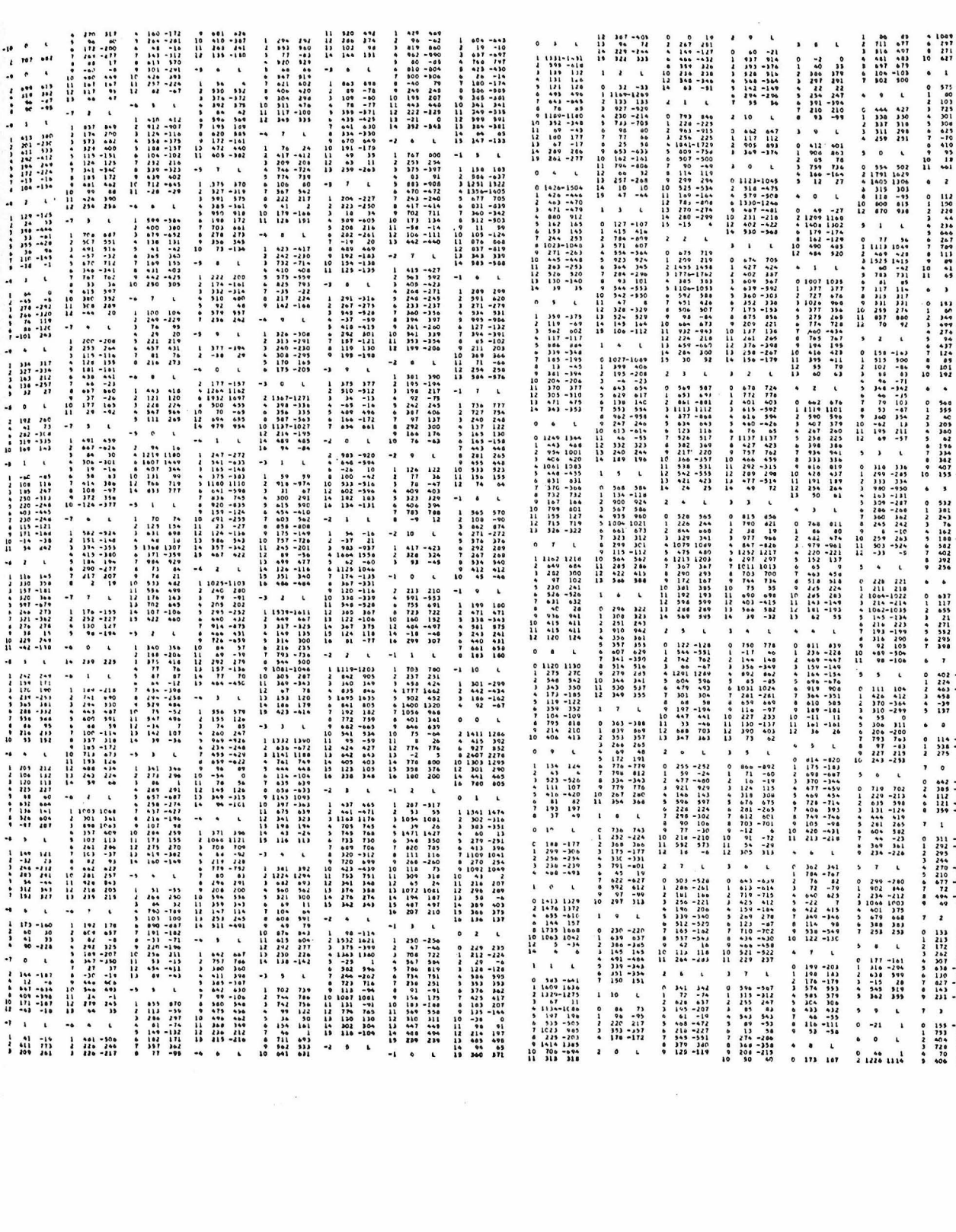

Table II. Observed and Calculated Structure Factors for $Co(diars)_2Cl_3$

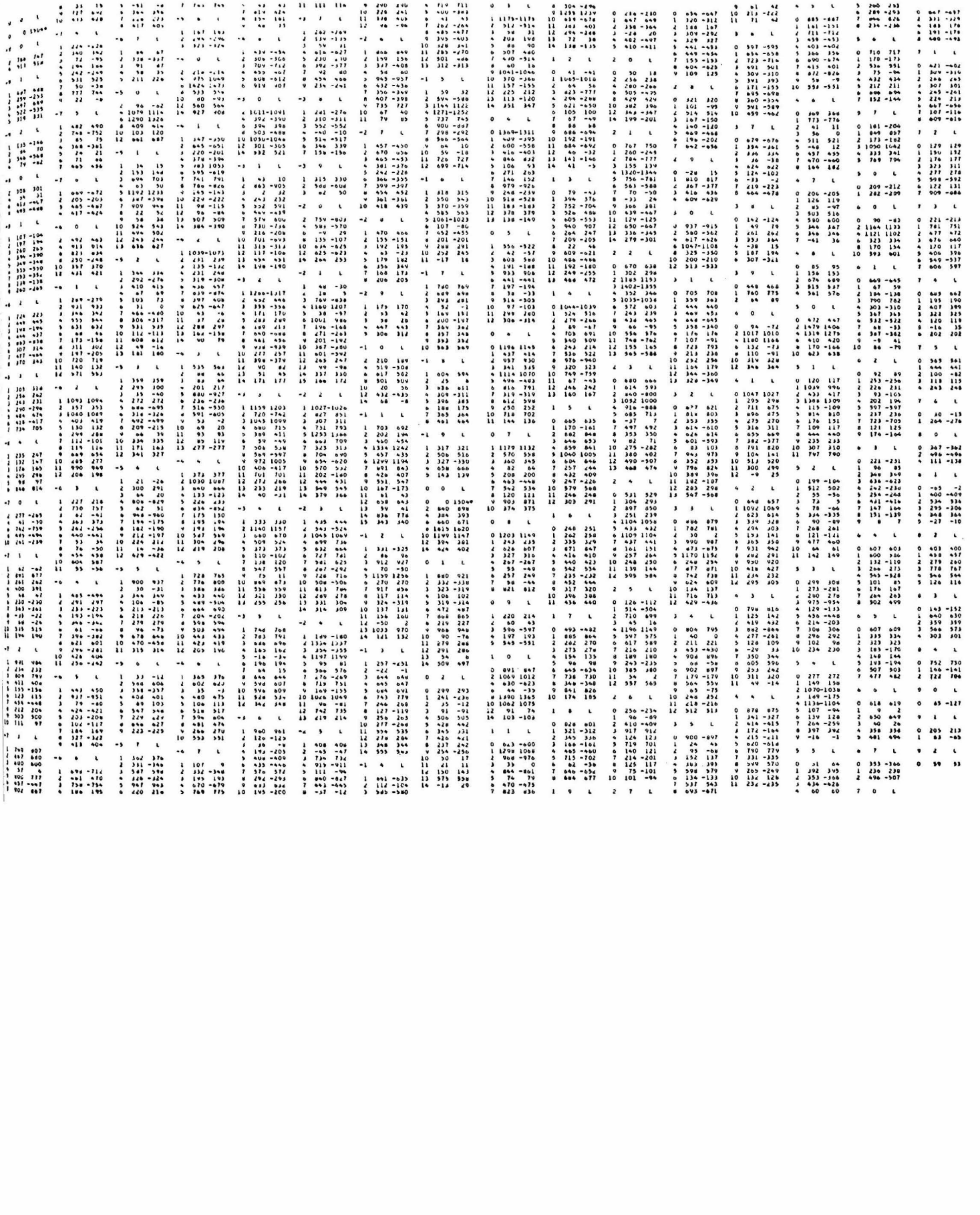

TABLE III.

Positional and Thermal Parameters of the Atoms and their Standard Deviations in $[Ni(diars)_2Cl_2]Cl$[a]

Atom	x	y	z	$B \times 10^2$
Ni	0 (0)	0 (0)	0 (0)	
As_2	19861 (11)	15108 (8)	-597 (5)	
As_3	7695 (12)	-11653 (8)	-12293 (6)	
Cl_4	14204 (28)	-14993 (20)	10995 (14)	
Cl_5	50000 (0)	0 (0)	50000 (0)	
C_6	22026 (103)	178 (78)	-16950 (54)	
C_7	27532 (104)	11397 (75)	-11783 (51)	
C_8	39050 (120)	19487 (89)	-14480 (58)	
C_9	44741 (128)	15917 (91)	-22230 (61)	
C_{10}	39089 (117)	4927 (100)	-27439 (59)	
C_{11}	27844 (125)	-3000 (89)	-24820 (60)	
C_{12}	15681 (141)	34697 (92)	-709 (81)	
C_{13}	-6442 (138)	-15418 (124)	-22597 (68)	

TABLE III (continued)

Atom	x	y	z	$B \times 10^2$
C_{14}	37465 (137)	13155 (110)	8062 (64)	
C_{15}	17799 (156)	-29255 (112)	-10321 (89)	
H_{16}	43222 (1228)	3446 (1077)	-31378 (687)	4.0
H_{17}	51075 (1158)	22294 (978)	-24073 (695)	4.0
H_{18}	42896 (1179)	26488 (983)	-10447 (700)	4.0
H_{19}	25208 (1188)	-10553 (989)	-27730 (674)	4.0
H_{20}	43871 (1155)	21162 (1063)	6765 (649)	4.0
H_{21}	41739 (1127)	3008 (1050)	7380 (627)	4.0
H_{22}	35555 (1198)	13699 (1017)	13474 (731)	4.0
H_{23}	6878 (1238)	36363 (953)	-4507 (657)	4.0
H_{24}	19760 (1319)	39302 (1220)	-599 (798)	4.0
H_{25}	14640 (1300)	38348 (1770)	4028 (705)	4.0
H_{26}	22988 (1274)	-28047 (1115)	-6090 (712)	4.0
H_{27}	20705 (1261)	-30515 (1108)	-14602 (743)	4.0
H_{28}	11739 (1211)	-37460 (1070)	-10232 (686)	4.0

TABLE III (continued)

Atom	x	y	z	$B \times 10^2$
H_{29}	-12843 (1155)	-6441 (1040)	-23952 (660)	4.0
H_{30}	-13372 (1122)	-23991 (992)	-20874 (659)	4.0
H_{31}	-2977 (1116)	-1874 (1008)	-27904 (672)	4.0

	β_{11}	β_{22}	β_{33}	β_{12}	β_{13}	β_{23}
Co	724 (28)	235 (17)	164 (7)	-71 (33)	-9 (23)	-20 (17)
As_2	689 (14)	264 (9)	173 (4)	-134 (17)	-36 (12)	-9 (9)
As_3	845 (16)	266 (9)	200 (4)	-149 (19)	61 (12)	-101 (9)
Cl_4	1096 (38)	469 (22)	293 (10)	64 (46)	-247 (32)	287 (23)
Cl_5	1096 (57)	872 (39)	328 (16)	752 (76)	193 (48)	173 (39)
C_6	799 (136)	414 (85)	212 (37)	1 (173)	-62 (117)	89 (88)
C_7	914 (135)	367 (81)	176 (35)	12 (181)	0 (113)	147 (87)
C_8	1002 (155)	512 (94)	265 (41)	-249 (198)	-8 (134)	29 (97)
C_9	1240 (173)	650 (98)	281 (43)	-100 (220)	-72 (142)	224 (111)
C_{10}	907 (151)	766 (108)	279 (44)	17 (210)	443 (132)	203 (112)

TABLE III (continued)

	β_{11}	β_{22}	β_{33}	β_{12}	β_{13}	β_{23}
C_{11}	1158 (173)	548 (94)	274 (43)	-3 (214)	-52 (141)	-80 (101)
C_{12}	1232 (185)	424 (100)	428 (53)	-178 (201)	-127 (162)	-154 (118)
C_{13}	1200 (190)	1369 (147)	271 (45)	-664 (284)	-7 (155)	-728 (145)
C_{14}	1330 (188)	938 (120)	209 (40)	83 (245)	-311 (146)	11 (120)
C_{15}	1683 (226)	542 (109)	545 (65)	240 (250)	820 (192)	-57 (146)

[a] All values except those for the isotropic temperature parameters have been multiplied by 10^5. The anisotropic temperature factors are of the form $\exp\{-(h^2b_{11} + k^2b_{22} + \ell^2b_3 + hkb_{12} + h\ell b_{13} + k\ell b_{23})\}$.

TABLE IV

Positional and Thermal Parameters of the Atoms and their Standard Deviations

$[Co(diars)_2Cl_2]Cl$[a]

Atom	x	y	z	$B \times 10^2$
Co	0 (0)	0 (0)	0 (0)	
As_2	19803 (6)	15042 (6)	-651 (4)	
As_3	7678 (6)	-11650 (6)	-12231 (4)	
Cl_4	13604 (15)	-13902 (14)	10080 (9)	
Cl_5	50000 (0)	0 (0)	50000 (0)	
C_7	27553 (53)	11442 (53)	-11835 (34)	
C_8	38956 (65)	19247 (66)	-14499 (42)	
C_9	44570 (70)	15749 (64)	-22307 (40)	
C_{10}	39064 (66)	4657 (66)	-27498 (42)	
C_{11}	27818 (71)	-3120 (70)	-24823 (43)	
C_{12}	15579 (75)	34776 (61)	-901 (52)	
C_{13}	-6690 (83)	-15574 (92)	-22691 (47)	
C_{14}	37350 (72)	13392 (81)	8028 (48)	
C_6	22201 (55)	-39 (53)	-16949 (35)	

TABLE IV (continued)

Atom	x	y	z	$B \times 10^2$
C_{15}	17913 (105)	-29079 (74)	-10433 (69)	
H_{16}	42969 (662)	28096 (630)	-32408 (409)	282 (143)
H_{17}	52007 (734)	20516 (669)	-23505 (409)	300 (148)
H_{18}	41382 (594)	25434 (576)	-11407 (363)	84 (133)
H_{19}	24871 (615)	-9030 (607)	-27578 (372)	112 (142)
H_{20}	44208 (832)	20350 (836)	7081 (463)	474 (187)
H_{21}	41572 (688)	5453 (725)	7052 (400)	302 (159)
H_{22}	34556 (792)	13827 (739)	14050 (523)	550 (195)
H_{23}	5796 (772)	35499 (654)	-5189 (426)	367 (155)
H_{24}	23634 (695)	40051 (658)	-2392 (364)	243 (134)
H_{25}	14914 (770)	37931 (730)	4614 (475)	443 (184)
H_{26}	25690 (853)	-28685 (829)	-6306 (493)	486 (226)
H_{27}	22354 (750)	-31529 (709)	-15323 (456)	364 (169)
H_{28}	10315 (880)	-36105 (830)	-9438 (486)	546 (198)
H_{29}	-14756 (1029)	-8792 (1010)	-23792 (589)	971 (303)
H_{30}	-13148 (700)	-23376 (677)	-19763 (411)	387 (147)

TABLE IV (continued)

Atom	x	y	z	$B \times 10^2$
H_{31}	-1501 (1012)	-19449 (954)	-27608 (595)	795 (243)

	b_{11}	b_{22}	b_{33}	b_{12}	b_{13}	b_{23}
Co_1	370 (16)	148 (14)	177 (6)	-21 (23)	-26 (15)	9 (14)
As_2	343 (18)	160 (8)	191 (13)	-133 (11)	12 (7)	-24 (7)
As_3	496 (9)	197 (8)	212 (3)	-133 (11)	140 (8)	-110 (7)
Cl_4	625 (19)	358 (17)	295 (7)	98 (27)	-202 (18)	262 (17)
Cl_5	800 (29)	752 (28)	355 (12)	772 (5)	322 (29)	167 (28)
C_6	423 (71)	332 (65)	220 (29)	126 (111)	249 (72)	74 (69)
C_7	322 (67)	305 (64)	207 (27)	-199 (108)	-30 (69)	122 (69)
C_8	659 (85)	393 (75)	280 (34)	-97 (130)	-115 (86)	46 (87)
C_9	591 (83)	588 (80)	305 (34)	-60 (139)	248 (85)	322 (85)
C_{10}	781 (98)	750 (82)	243 (31)	152 (144)	385 (88)	212 (89)
C_{11}	897 (96)	433 (77)	295 (35)	134 (146)	33 (94)	-212 (89)
C_{12}	723 (95)	196 (70)	477 (43)	-51 (131)	246 (103)	-146 (84)
C_{13}	832 (96)	1332 (113)	285 (34)	-563 (188)	61 (96)	-662 (103)

TABLE IV (continued)

	b_{11}	b_{22}	b_{33}	b_{12}	b_{13}	b_{23}
C_{14}	533 (85)	795 (99)	316 (37)	-220 (155)	-168 (86)	16 (92)
C_{15}	1318 (139)	442 (83)	657 (53)	624 (173)	943 (151)	61 (105)

[a] All values except those for the isotropic temperature parameters have been multiplied by 10^5. The anisotropic temperature factors are of the form $\exp\{-(h^2b_{11} + k^2b_{22} + \ell^2b_{33} + hkb_{12} + h\ell b_{13} + k\ell b_{23})\}$.

TABLE V

Values of Selected Interatomic Distances in $[Ni(diars)_2Cl_2]Cl$

Pair	R, Å
$Ni-As_2$	2.3390
$Ni-As_3$	2.3457
$Ni-Cl_4$	2.4262
As_2-C_7	1.9387
As_2-C_{14}	1.9353
As_2-C_{12}	1.9174
As_3-C_6	1.9381
As_3-C_{13}	1.9083
As_3-C_{15}	1.9290
C_6-C_7	1.3800
C_7-C_8	1.4141
C_8-C_9	1.3808
C_9-C_{10}	1.3702
$C_{10}-C_{11}$	1.3813
$C_{11}-C_6$	1.3939

TABLE VI

Values of Selected Interatomic Distances in $[Co(diars)_2Cl_2]Cl$

Pair	R, Å
$Co-As_2$	2.333
$Co-As_3$	2.336
$Co-Cl_4$	2.256
As_2-C_7	1.939
As_2-C_{14}	1.930
As_2-C_{12}	1.931
As_3-C_6	1.943
As_3-C_{13}	1.939
As_3-C_{15}	1.918
C_6-C_7	1.391
C_7-C_8	1.390
C_8-C_9	1.383
C_9-C_{10}	1.372
$C_{10}-C_{11}$	1.377
$C_{11}-C_6$	1.383

TABLE VII

Selected Bond Angles in $[Ni(diars)_2Cl_2]Cl$

A–B–C	∢(ABC), deg
As_2–Ni–As_3	86.8
As_2–Ni–Cl_4	96.62
As_3–Ni–Cl_4	93.40
C_7–As_2–Ni	107.28
C_7–As_2–C_{12}	105.57
C_7–As_2–C_{14}	101.14
C_{12}–As_2–Ni	116.86
C_{12}–As_2–C_{14}	104.36
C_{14}–As_2–Ni	119.74
C_6–As_3–Ni	107.24
C_6–As_3–C_{13}	103.77
C_6–As_3–C_{15}	103.44
C_{13}–As_3–Ni	118.76
C_{13}–As_3–C_{15}	102.50
C_{15}–As_3–Ni	119.16
C_7–C_6–C_{11}	119.48
C_6–C_7–C_8	119.83
C_7–C_8–C_9	119.25
C_8–C_9–C_{10}	120.85
C_9–C_{10}–C_{11}	120.00
C_{10}–C_{11}–C_6	120.56

TABLE VIII

Selected Bond Angles in $[Co(diars)_2Cl_2]Cl$

A–B–C	∢ (ABC), deg
As_2–Co–As_3	86.6
As_2–Co–Cl_4	91.8
As_3–Co–Cl_4	92.4
C_7–As_2–Co	107.9
C_7–As_2–C_{12}	104.7
C_7–As_2–C_{14}	101.2
C_{12}–As_2–Co	116.8
C_{12}–As_2–C_{14}	103.9
C_{14}–As_2–Co	120.2
C_6–As_3–Co	107.9
C_6–As_3–C_{13}	104.0
C_6–As_3–C_{15}	101.7
C_{13}–As_3–Co	118.7
C_{13}–As_3–C_{15}	102.1
C_{15}–As_3–Co	120.1
C_7–C_6–C_{11}	119.6
C_6–C_7–C_8	119.4
C_7–C_8–C_9	119.7
C_8–C_9–C_{10}	121.0
C_9–C_{10}–C_{11}	119.2
C_{10}–C_{11}–C_6	121.0

III. SPECTRAL AND MAGNETIC STUDIES OF SOME NICKEL AND COBALT DIARSINE COMPLEXES

Introduction

We have measured the u. v. and visible spectra of a series of d^6 and d^7 nickel and cobalt diarsine complexes in solution at 300°K and in clear frozen glasses at 77°K. A number of unstable complexes were examined in Nujol mulls at 300°K and at 77°K. The spectral results have been interpreted in terms of a qualitative M. O. scheme. We have also measured the magnetic susceptibility of a solid sample of $Ni(diars)_2Cl_3$.

Experimental

Preparation of Compounds

Reagents. O-phenylenebisdimethylarsine (diarsine) was purchased from Aldrich or City Chemical Company and used without further purification. When refrigerated in sealed ampules, diarsine remains stable for several months. The pure compound is a clear liquid which turns yellowish as it decomposes. All metal salts were reagent grade and used without further purification.

$Ni(diars)_2X_3$ (X = Cl, Br, SCN) was prepared by the method of Nyholm[1] and recrystallized from ethanol.

$Co(diars)_2X_3$ (X = Cl, Br) was also prepared by Nyholm's method[2] and recrystallized from ethanol (X = Br) or an ethanol-ether or ethanol-cyclohexane mixture (X = Cl).

$\underline{Ni(diars)_2X_3(ClO_4)_2}$ (X = Cl, Br) was prepared by Nyholm's method.[28] These salts were not recrystallized because they are quite unstable in solution, reverting in a matter of seconds to the Ni(III) complex.

All samples were analyzed for C, H, and X by Galbraith Microanalytical Laboratory, Knoxville, Tenn.

Physical Measurements

All electronic spectra were measured on a Cary Model 14RI spectrophotometer. Measurements at room temperature were made in matched 1 cm square cells of fused suprasil manufactured by Pyrocell Manufacturing Co. Weak bands were measured in cylindrical 10 cm quartz cells. Measurements at 77°K were done in a quartz dewar in which the sample was completely immersed. Bubbling of liquid N_2 was prevented by pumping on the dewar with a vacuum pump. thus cooling the nitrogen slightly below its boiling point. For low temperature measurements, we used quartz cells which had been made by molding round quartz tubing onto a solid, rectangular molybdenum form. Cells made in this way have been found to be much less susceptible to cracking at low temperatures and give nicely reproducible spectra.[29]

The solvents for room temperature spectra were anhydrous U.S.P.-N.F. grade ethanol (U. S. Industrial Chemical Co.) and spectrograde methanol (Matheson, Coleman and Bell). The low temperature spectral solvents were 2:1 mixtures of 2-methyltetrahydrofuran with methanol or ethanol. These mixtures have excellent

solvent properties and form transparent crack-free glasses at 77°K. The 2-MeTHF was chromatoquality (MCB) and was purified by distillation over lithium aluminum hydride. Extinction coefficients measured at 77°K were corrected for a 20% volume contraction factor. Complexes of Ni(IV) which decompose in solution, were measured in Nujol mulls. The solid was finely ground between two pieces of ground glass and spread thinly between two quartz plates. This technique produces reasonably good spectra in the visible region down to 400 nm. Unfortunately, there is no way to obtain the u.v. spectrum or the extinction coefficients for the visible spectrum.

Magnetic measurements were made on a solid sample of $Ni(diars)_2Cl_3$ using a Princeton Applied Research FM-1 Vibrating Sample magnetometer and an Andonian Associates LHe dewar. The sample is placed in a small Teflon sample holder which is attached to a rod assembly containing a Cu/constantan thermocouple. The heater boils the liquid N_2 or He and warms the resultant gas, thus regulating sample temperature. Variable temperature data were taken point by point, slowly reducing the power to the heater and permitting the sample to equilibrate between readings. The susceptibility is measured vs. a precalibrated thermocouple reading. Two runs were made, one using liquid nitrogen coolant from room temperature to 78°K, and a second using liquid He from 192°K to 4°K. The data were corrected for the diamagnetism of the holder and calibrated at room temperature with $HgCo(SCN)_4$. The diamagnetic corrections for diarsine and chloride were taken from Selwood.[30]

Results--Magnetic

The experimental values of the magnetic susceptibility over the temperature range 4°K to 300°K are given in Tables IX and X. Figures 3 and 4 are plots of $1/\chi$ vs. T. As is fairly obvious from the graph, the data obey the Curie-Weiss law

$$\chi = C/(T - \theta)$$

with a Weiss constant $\theta = 10°K$. The room temperature magnetic moment is 1.756 B. M. in good agreement with the value originally reported by Nyholm.[1]

The most important result of this experiment is that there is no antiferromagnetic interaction, i.e., no intermolecular interaction between the unpaired spins. This will be important later when we attempt to interpret the change which occurs in the ESR spectrum of this compound when it is diluted into an isomorphous diamagnetic matrix.

Results--Spectral

First let us define a coordinate system as follows:

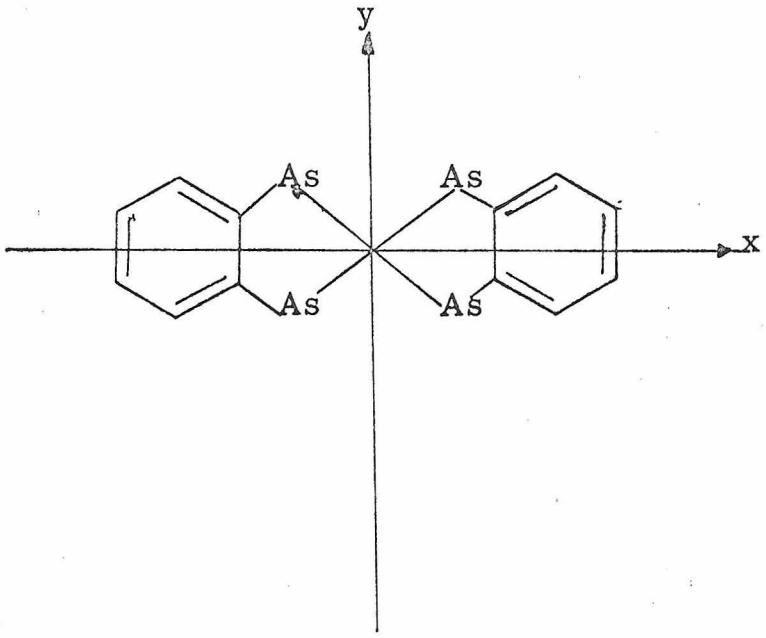

Figure 3. Susceptibility ($1/\chi$) vs. Temperature for $Ni(diars)_2Cl_3$ from 77°K to 260°K using liquid Nitrogen coolant.

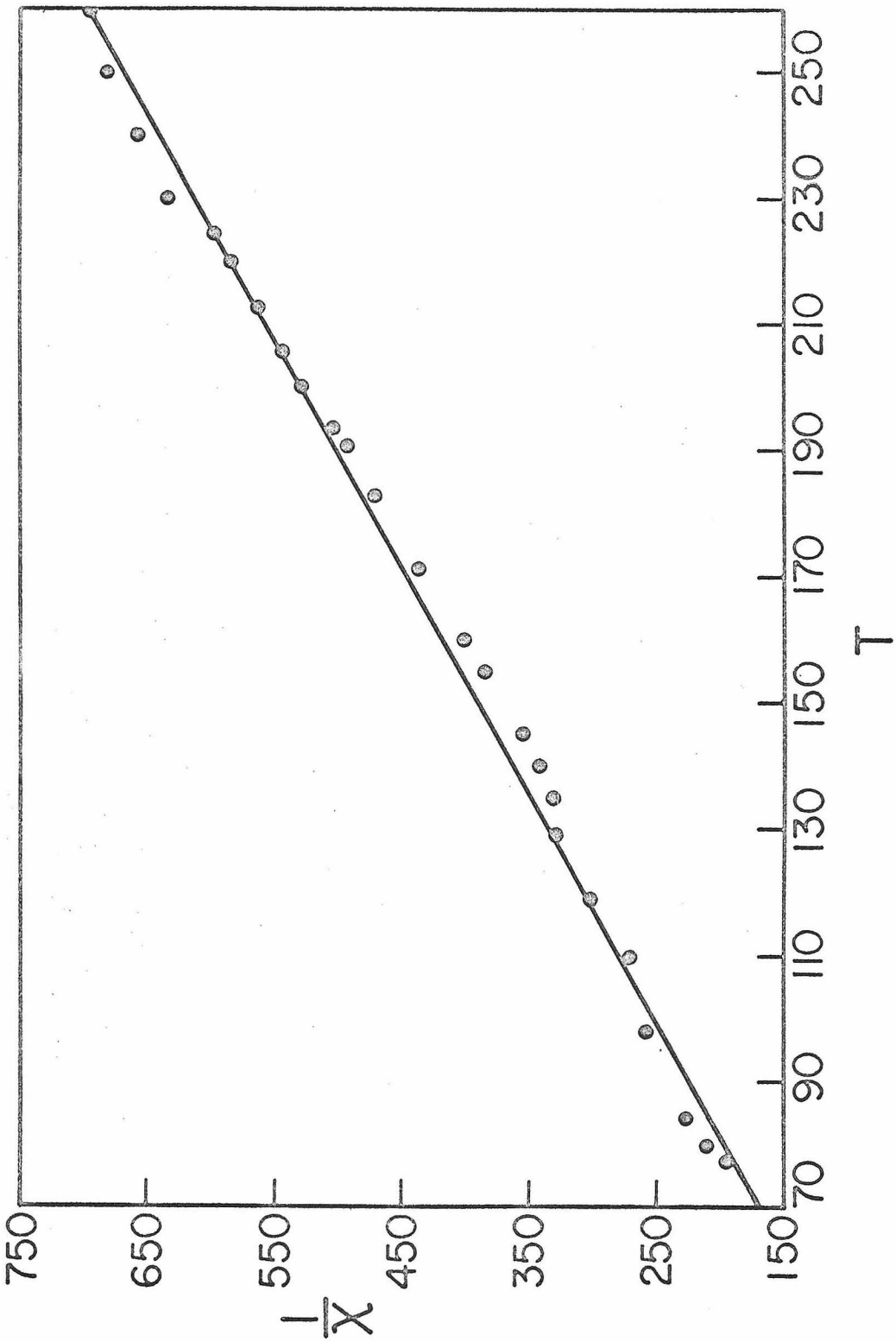
750
650
550
450
350
250
150
1/χ
70
90
110
130
150
170
190
210
230
250
T

Figure 4. Susceptibility ($1/\chi$) vs.
Temperature for $Ni(diars)_2Cl_3$ from 190°K to 15°K
using liquid Helium coolant.

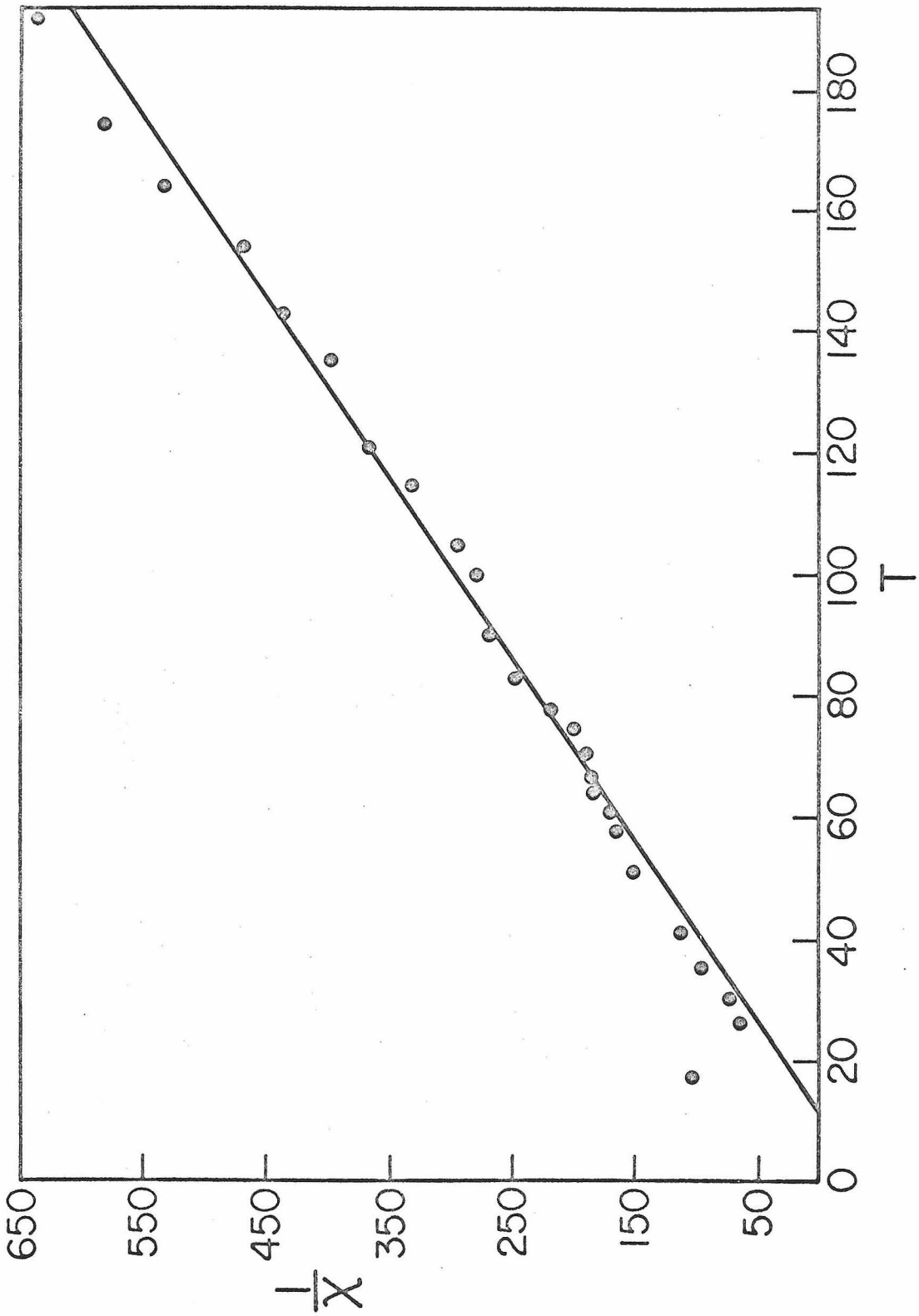
650
550
450
350
250
150
50
1/χ
0
20
40
60
80
100
120
140
160
180
T

TABLE IX

Susceptibility vs. Temp $Ni(diars)_2Cl_3$ Using Liquid N_2 Coolant

T in °K	χ_M(corrected for diamagnetism) $\times 10^{+2}$	μ
300	.129	1.756
260.2	.144	1.730
250.9	.147	1.717
241.2	.153	1.718
231.8	.159	1.718
225.8	.168	1.744
220.9	.171	1.741
213.4	.178	1.741
207.0	.184	1.744
201.6	.190	1.749
194.9	.199	1.762
191.0	.202	1.757
187.1	.205	1.752
183.3	.211	1.760
180.1	.217	1.770
176.7	.221	1.765
171.2	.230	1.773
167.8	.239	1.790
163.3	.245	1.789
160.8	.251	1.797

TABLE IX (continued)

T in °K	χ_M (corrected for diamagnetism) $\times 10^{+2}$	μ
157.5	.254	1.789
155.0	.260	1.796
151.8	.270	1.809
149.7	.273	1.807
147.4	.276	1.802
145.9	.282	1.813
142.2	.285	1.800
140.6	.288	1.799
135.1	.297	1.792
129.9	.303	1.775
125.8	.312	1.773
123.6	.322	1.783
119.9	.331	1.781
116.2	.343	1.785
113.6	.349	1.781
112.0	.352	1.777
109.0	.358	1.767
110.2	.374	1.815
104.9	.383	1.792
103.8	.386	1.790
98.4	.392	1.757
91.0	.411	1.728
87.3	.432	1.736

TABLE IX (continued)

T in °K	χ_M (corrected for diamagnetism) $\times 10^{+2}$	μ
84.2	.444	1.730
83.6	.453	1.742
81.3	.469	1.746
80.0	.481	1.755
79.7	.490	1.767
79.2	.496	1.773
78.8	.506	1.785
78.5	.518	1.803

TABLE X

Susceptibility vs. Temp

$Ni(diars)_2Cl_3$ Using Liquid He Coolant

T in °K	χ_M (corrected for diamagnetism) $\times 10^2$	μ
192.1	.158	1.557
174.7	.173	1.555
165.8	.188	1.580
155.7	.219	1.651
143.7	.234	1.640
135.4	.249	1.644
121.1	.275	1.631
115.1	.300	1.662
104.9	.341	1.691
100.8	.356	1.695
90.7	.372	1.642
83.3	.402	1.637
77.4	.453	1.674
75.5	.484	1.709
73.6	.489	1.697
71.7	.514	1.717
67.8	.545	1.719
64.5	.560	1.699
61.0	.596	1.704
58.1	.606	1.677

TABLE X (continued)

T in °K	χ_M (corrected for diamagnetism) $\times 10^2$	μ
56.2	.636	1.691
53.5	.641	1.657
51.1	.667	1.651
49.5	.703	1.668
48.7	.723	1.677
47.0	.753	1.683
43.0	.820	1.679
42.5	.840	1.690
42.5	.860	1.711
41.1	.881	1.702
39.7	.896	1.686
38.7	.927	1.693
37.7	.957	1.698
36.7	.988	1.702
35.6	1.020	1.703
34.5	1.04	1.694
34.0	1.07	1.705
34.5	1.11	1.751
34.0	1.15	1.768
33.4	1.18	1.777
32.3	1.23	1.780
31.7	1.26	1.786
31.1	1.30	1.801

TABLE X (continued)

T in °K	χ_M (corrected for diamagnetism) $\times 10^2$	μ
30.5	1.34	1.808
29.9	1.39	1.824
27.7	1.44	1.786
27.7	1.49	1.818
27.1	1.52	1.817
27.1	1.55	1.835
26.5	1.59	1.835
26.5	1.62	1.856
17.0	.942	1.130

The work of Preer[13] on 5-coordinate d^8 systems has indicated that for compounds of the form $Ni(diars)_2X^+$ (X = Cl, Br, I, NCS) the ordering of d levels (in C_{4v} microsymmetry) is

$$x^2-y^2\ (B_1) < xz, yz\ (E) < z^2\ (A_1) < xy\ (B_2)$$

The inversion of the x^2-y^2 and xz, yz levels has been attributed to the importance of metal $(d\pi) \rightarrow As(\pi)$ backbonding.

The addition of another halide to the system as in $Ni(diars)_2X_2^+$ or $Co(diars)_2X_2^+$ should further destabilize xz, yz and z^2 with respect to x^2-y^2, and one would therefore expect the ordering of metal levels to remain the same in these compounds.

Co(III)$(diars)_2X_3$. The visible and u.v. spectra of $Co(diars)_2Cl_3$ and $Co(diars)_2Br_3$ are reported in Table XI. The spectrum of the chloride is illustrated in Figure 5. Feltham[11] and Yamada[31] have previously examined the d^6 Co(III) diarsine complexes and assigned their visible spectra. Feltham assigns the weak band at 16,460 cm^{-1} in the chloride and 15,750 cm^{-1} in the bromide to the ligand field transition $^1A_{1g} \rightarrow {}^1E_g$. In the chloride, the second ligand field transition, $^1A_{1g} \rightarrow {}^1A_{2g}$, is hidden under the charge transfer band at 25,800 cm^{-1}. The bromide spectrum contains an asymmetric charge transfer band at 23,670 cm^{-1} which at low temperatures splits to reveal a band at 22,220 cm^{-1}. We assign this band to the second spin allowed ligand field transition $^1A_{1g} \rightarrow {}^1A_{2g}$.

The first charge transfer band was originally assigned by Yamada as an $As(\sigma) \rightarrow Co(d\sigma^*)$ transition.[31] He based this assignment on a spectrum of $[Co(diars)_3][ClO_4]_3$ which had a charge transfer

Figure 5. Electronic spectrum of $Co(diars)_2Cl_3$ at 300°K and 77°K.

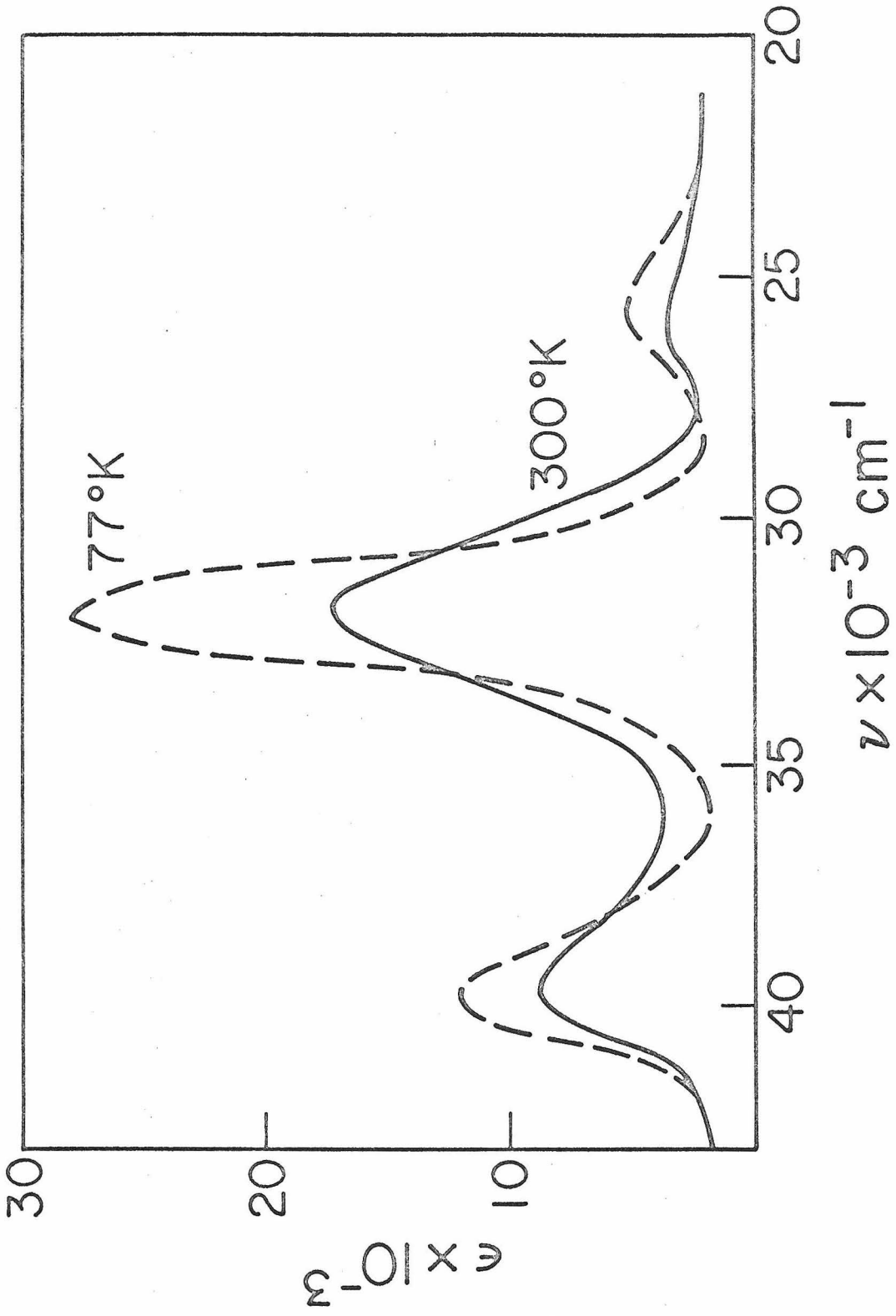
77°K
300°K
ε x 10⁻³
ν x 10⁻³ cm⁻¹
30
20
10
20
25
30
35
40

TABLE XI

Electronic Spectra of $Co(diars)_2X_3$

Assignment	300°K	77°K
X = Cl		
$^1A_{1g} \rightarrow {}^1E_g$	16,460 cm^{-1} (70)[a]	---
$X(\pi) \rightarrow M\sigma^*$	25,800 cm^{-1} (3500)	25,800 cm^{-1} (4800)
charge transfer and intraligand transitions	31,750 cm^{-1} (17,000)	31,750 cm^{-1} (28,000)
	39,840 cm^{-1} (8600)	39,840 cm^{-1} (12,000)
X = Br		
$^1A_{1g} \rightarrow {}^1E_g$	15,750 cm^{-1} (67)[b]	22,200 cm^{-1} (3200)[c]
$X(\pi) \rightarrow M\sigma^*$	23,670 cm^{-1} (3800)	23,670 cm^{-1} (5800)
charge transfer	30,530 cm^{-1} (20,000)	31,200 cm^{-1} (28,000)
and intraligand	35,398 cm^{-1} (17,000)	35,000 cm^{-1} (22,000)
transitions	42,105 cm^{-1} (14,100)[b]	---

[a] Measured in EtOH.

[b] Observed in MeOH.

[c] Assignment $^1A_{1g} \rightarrow {}^1A_{2g}$.

band at $\sim 25,000$ cm^{-1}. More careful work by Feltham[11] has indicated that on standing, $[Co(diars)_3](ClO_4)_3$ decomposes to form trans-$Co(diars)_2Cl_2^+$, and that the band at 25,000 cm^{-1} is associated only with the latter species. On the basis of the fact that the low-energy charge transfer band at $\sim$25,000 cm^{-1} is present in the bromide and chloride but not in the tris-diarsine, we assign this band to the $X(\pi) \rightarrow Co(d_{z^2})$ charge transfer transition $^1A_{1g} \rightarrow {}^1E_u$.

This assignment is consistent with the results of Preer[13] which indicate that the first charge transfer band in the $Ni(II)(diars)_2X_2$ complexes arises from the $X(\pi)$ level. Above 30,000 cm^{-1} intraligand transitions complicate the charge transfer spectrum considerably and we have not attempted further spectral assignments.

$Ni(diars)_2X_3$. The visible and u.v. spectra of $Ni(diars)_2X_3$ (X = Cl, Br) are reported in Table XII. Figure 6 is an illustration of the X = Cl spectrum. Spectra were also taken of $Ni(diars)_2(NCS)_3$ in solution. However, this species, which is not very stable in the solid form, appears to revert rapidly to $Ni(II)(diars)_2NCS^+$ in alcohol. The spectrum we measured was identical to the one reported by Preer[13] for $[Ni(II)(diars)_2NCS]ClO_4$.

The first charge transfer band in $Ni(diars)_2X_3$ occurs at 25,700 cm^{-1} (X = Cl) and 23,400 cm^{-1} (X = Br). We assign this transition to $X(\pi) \rightarrow Ni(d_{z^2})$ ($^2A_{1g} \rightarrow {}^2E_u$). We expect the $X(\pi)$ level in the Ni(III) compound to be destabilized with respect to the Co(III) compound since the Ni–X distance is appreciably longer than the Co–X distance. For the same reason, we expect the d_{z^2} level to be

Figure 6. Electronic spectra of $Ni(diars)_2Cl_3$ at 300°K and 77°K.

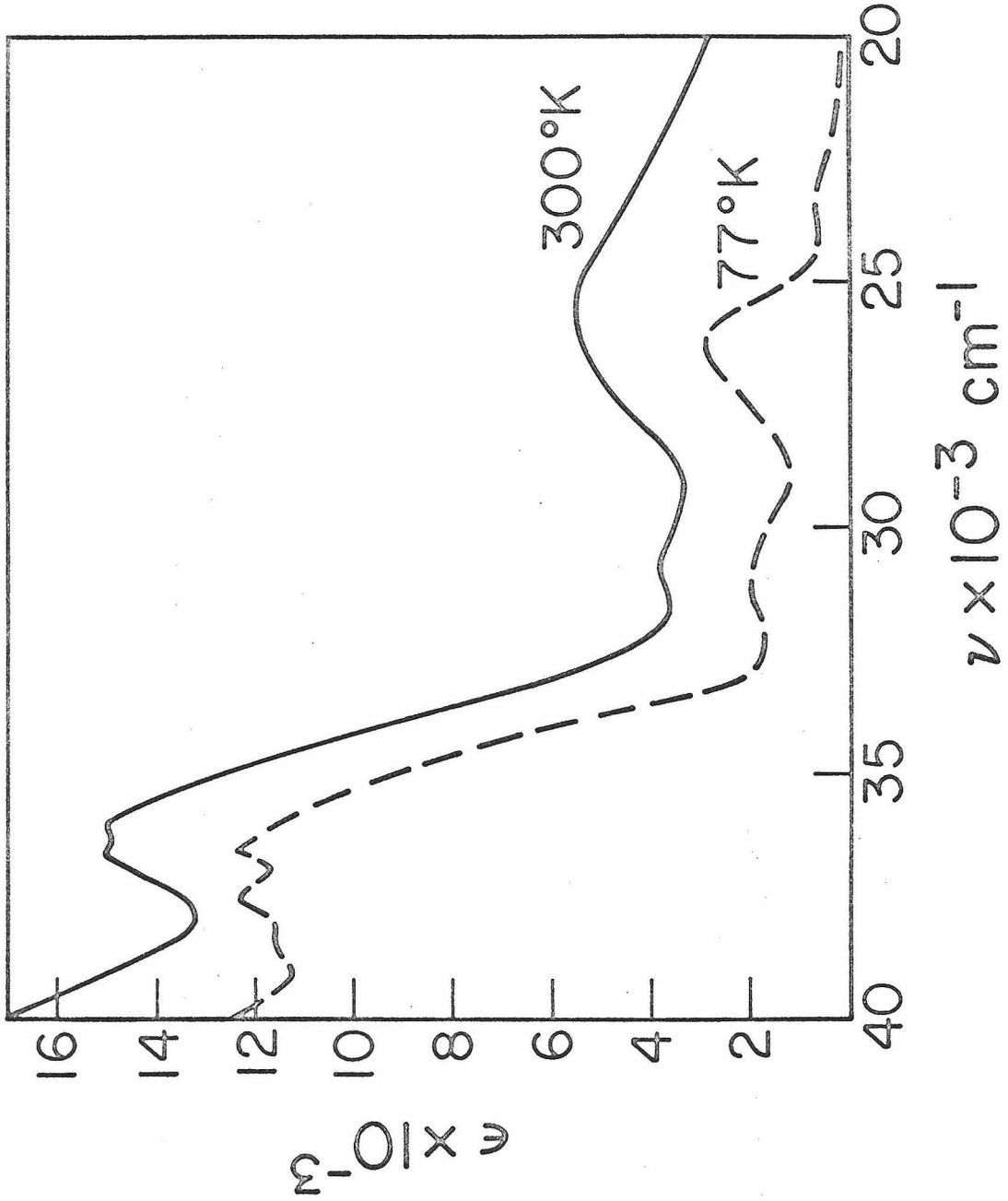
300°K
77°K
ν x10⁻³ cm⁻¹
ε x10⁻³
16
14
12
10
8
6
4
2
20
25
30
35
40

TABLE XII

Electronic Spectra of $Ni(diars)_2X_3$

Assignment	300°K	77°K
X = Cl		
xz, yz → z^2	13,200 cm^{-1} (20)[b]	------
X(π) → M(d_{z^2})	25,700 cm^{-1} (5650)	23,700 cm^{-1} (540)[c]
charge transfer	30,800 cm^{-1} (3880)sh	26,200 cm^{-1} (2960)
and intraligand	35,900 cm^{-1} (15,000)	31,300 cm^{-1} (1890)
transitions	36,600 cm^{-1} (15,100)	36,600 cm^{-1} (12,300)
		37,700 cm^{-1} (12,500)
		38,500 cm^{-1} (11,600)
X = Br		
xz, yz → z^2	12,600 cm^{-1} (150)[c]	------
X(π) → M(d_{z^2})	23,409 cm^{-1} (800)	22,200 cm^{-1} (483)
charge transfer	27,800 cm^{-1} (1200)	24,300 cm^{-1} (2200)
and intraligand	34,800 cm^{-1} (4000)	27,400 cm^{-1} (800)
transitions	41,200 cm^{-1} (2600)	36,400 cm^{-1} (a)
		41,600 cm^{-1} (a)

[a] ϵ cannot be measured because absorption is a shoulder on solvent band.

[b] Measured in EtOH.

[c] Measured in MeOH.

stabilized. These two effects combine to lower the energy of the Ni(III) X(π) $\rightarrow$ M(σ^*) charge transfer with respect to the corresponding Co(III) transition. This lowering of energy is partially cancelled by the increased electron repulsion for the d^7 case. Weighing the relative importance of these three factors, we predict that the first charge transfer band in Ni(III) should be at slightly lower energy than the one in Co(III) which is in fact the case.

Above 30,000 cm^{-1} as in the cobalt spectra, intraligand transitions complicate the band assignments.

The third intense band is vibronically split in the chloride showing two sharp peaks at 36,600 and 37,700 cm^{-1}. The energy difference = 1100 corresponds exactly to an IR peak which has been assigned by Rodley to a diarsine phenyl ring vibration.[32]

The ligand field spectra of these compounds are more difficult to assign. Yamada[31] reports three bands at 13,200 cm^{-1}, 16,600 cm^{-1}, and 19,200 cm^{-1} in $Ni(diars)_2Cl_2^+$ which he assigns as spin-forbidden bands. We were unable to locate the latter two transitions in solutions as concentrated as 2.5×10^{-2} M. The transition at 13,200 cm^{-1} has an $\epsilon \sim 20$. In the bromide, the same transition occurs at 12,600 cm^{-1} and has an ϵ on the order of 150. On this basis, we suggest that this transition is probably spin allowed. At liquid nitrogen temperatures two further ligand field bands can be observed. The asymmetric peaks at 25,700 cm^{-1} in the chloride and 23,400 cm^{-1} in the bromide split at 77°K into bands at 26,200 cm^{-1} and 24,300 cm^{-1} and lower intensity bands at 23,700 cm^{-1} and 22,200 cm^{-1}.

There are five possible spin allowed transitions in $Ni(diars)_2X_2^+$. The primary change in the energy levels in going from five coordinate Ni(II) to six coordinate Ni(III) complex should be the destabilization of the d_{z^2} level. In $Ni(II)(diars)_2Cl^+$, the $x^2 - y^2 \rightarrow xy$ transition occurs at 26,285 cm^{-1}. Since it is unlikely to move to lower energy in the Ni(III) case, we can eliminate it as a possible assignment for the two observed ligand field bands.

We tentatively assign the first ligand field band at 13,200 cm^{-1} in the chloride and 12,600 cm^{-1} in the bromide to the transition $^2A_{1g} \rightarrow {}^2E_g$ $(xz, yz \rightarrow z^2)$. This seems reasonable from the energy point of view. The same transition in the five coordinate d^7 complex $Co(II)(CN)_5^{-3}$ has been assigned by Tsay and Gray[33] to the band at 10,000 cm^{-1}. Although diarsine and chloride are both weaker ligands than cyanide, the Ni(III) complex is six coordinate and has a greater charge on the central metal. The $x^2 - y^2 \rightarrow z^2$ transition is probably buried under this ligand field transition. The band in the bromide compound in particular is very asymmetric. We assign the transition at 23,700 cm^{-1} in the chloride and 22,200 cm^{-1} in the bromide to $xz, yz \rightarrow xy$ $(^2A_{1g} \rightarrow {}^2B_{2g})$.

<u>$[Ni(diars)_2X_2][ClO_4]_2$</u>. We took the spectra of these compounds (X = Cl, Br) in a Nujol mull since they revert very rapidly to $Ni(diars)_2X_2^+$ in solution. The visible spectrum of the chloride consists of two equally intense bands with a shoulder. Unfortunately, it is impossible to measure extinction coefficients in a mull. We assign these transitions to the appropriate ligand field band for a d^6 complex.

Figure 7. Electronic spectra of $Ni(diars)_2Cl_2(ClO_4)_2$ in a mull at room temperature.

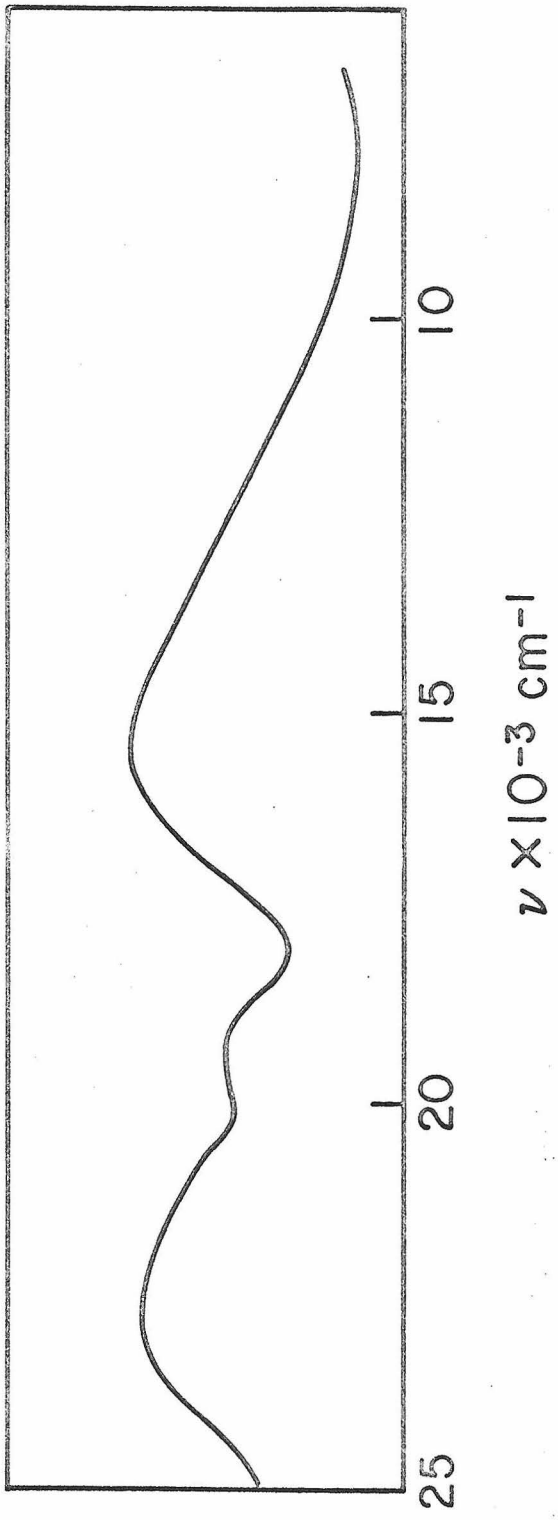
10
15
20
25
ν ×10⁻³ cm⁻¹

TABLE XIII

Electronic Spectra of $NiD_2X_2(ClO_4)_2$

Assignment	300°K	77°K
X = Cl		
$^1A_{1g} \rightarrow {}^1E_g$	15,400 cm^{-1}	15,400 cm^{-1}
$^1A_{1g} \rightarrow {}^1A_{2g}$	19,600 cm^{-1}	19,600 cm^{-1}
$^1A_{1g} \rightarrow {}^1E_g$	23,500 cm^{-1}	23,500 cm^{-1}
X = Br		
$^1A_{1g} \rightarrow {}^1E_g$	15,900 cm^{-1}	15,900 cm^{-1}
$^1A_{1g} \rightarrow {}^1E_g$	22,700 cm^{-1}	22,700 cm^{-1}

In the chloride, the band at 15,400 cm^{-1} is assigned to the $^1A_{1g} \rightarrow {}^1E_g$ transition. We assign the shoulder at 19,600 cm^{-1} to $^1A_{1g} \rightarrow {}^1A_{2g}$, and the band at 23,500 cm^{-1} to $^1A_{1g} \rightarrow {}^1E_g$. In the bromide, the band at 15,900 cm^{-1} is assigned to the first $^1A_g \rightarrow {}^1E_g$ transition and the band at 22,700 cm^{-1} to the second $^1A_{1g} \rightarrow {}^1E_g$ transition. The $^1A_{1g} \rightarrow {}^1A_{2g}$ transition would be expected at lower energy in the bromide and is probably hidden under the lowest energy band.

IV. ELECTRON SPIN RESONANCE OF DOPED CRYSTALS AND POWDERS CONTAINING $Ni(diars)_2Cl_2^+$

Introduction

We have examined the powder and dilute single crystal spectra of $Ni(diars)_2Cl_2^+$ in various cobalt matrices. The powder spectra indicate that a dramatic change takes place in the structure of this compound when it is doped into another crystal matrix. This phenomenon is described and an explanation for it is proposed. The single crystal spectra have been interpreted using computer simulation techniques and values for the superhyperfine tensor elements have been extracted.

Experimental

Preparation of Compounds

$Ni(diars)_2Cl_3$,[1] $Co(diars)_2Cl_3$,[2] $Ni(diars)_2Cl_2ClO_4$,[1] $Co(diars)_2Cl_2ClO_4$,[2] and $Rh(diars)_2Cl_3$[34] were all prepared according to methods described by Nyholm.

Preparation of Doped Crystals and Powders

We have examined the ESR spectra of doped crystals of 1% to 3% $Ni(diars)_2Cl_2^+$ in matrices of $Co(diars)_2Cl_3$ and $Co(diars)_2Cl_2ClO_4$. We have also examined the powder spectra of $Ni(diars)_2Cl_2^+$ doped into $Co(diars)_2Cl_3$, $Co(diars)_2Cl_2ClO_4$, and $Rh(diars)_2Cl_3$ in concentrations of approximately 75% Ni, 50% Ni, 25% Ni, 10% Ni, and 3% Ni.

Two different methods were used to grow the crystals. In one, appropriate amounts of both compounds were weighed and dissolved in a small quantity of 100% ethanol. The solution was placed in a

covered beaker or crystallizing dish and permitted to stand for several days. Large, well-formed crystals are obtained in this way. A somewhat faster method which produces smaller crystals was also used. An ethanol solution containing both compounds was placed in a sealed dessicator which also contained a beaker of ethyl ether. Ether evaporated and recondensed in the ethanol beaker, forcing the diarsine complexes out of solution. Good crystals can be obtained overnight. This method was used to prepare the more concentrated crystals.

All powders were prepared by grinding up crystals rather than by direct precipitation. This guaranteed that our samples were in fact doped powders and not mechanical mixtures.

Instrumental

ESR spectra were taken using both X band (~10 GHz) and K band (~34 GHz) instruments. The X band measurements were done on a Varian V-4502 spectrometer using 100 KC field modulation and a 9 inch Varian electromagnet with Fielddial. This system has a V-4532 Dual Sample Cavity. Microwave frequencies were measured using a wave meter attached to the microwave bridge. The field was calibrated in every experiment by using a standard sample of solid diphenyldipicrylhydrazyl (K & K Chemical Co.) placed in the rear compartment of the dual cavity. The DPPH signal was detected using a low frequency (20-400 cps) modulation and detection system. Low temperature experiments were done by passing a stream of nitrogen gas through a liquid nitrogen heat exchanger and then through

a quartz dewar containing the sample. A Varian V-4540 temperature controller was used to monitor the rate of gas flow.

K band measurements were obtained using a Varian V-4500 spectrometer and 100 Kc field modulation. The field was calibrated using an Alpha Model 675 NMR gaussmeter. No DPPH standard was used with the single crystal samples, however, a capillary containing DPPH was inserted in with the powder samples and g values were measured by comparison with DPPH as well as by using the cavity frequency and calibrated field. Low temperature measurements were done as in X band.

Single Crystal Apparatus

Single crystal measurements on the X band spectrometer were taken using an M-10 Rotating Sample Holder purchased from Magna Devices. The holder can be rotated about its axis over a 360° range, and a disc at the bottom of the holder can be rotated 180° by use of a 10-turn dial. These two rotational degrees of freedom enable one to obtain all the necessary angles with only one mounting of the crystal. The crystal itself was glued to the Teflon plug with rubber cement. The glue had been pretested to be sure it did not have an EPR signal. Both rotational angles can be reset and read to an accuracy of 1°. Spectra were taken on doped crystals of Ni/Co(diars)$_2$Cl$_3$ and Ni/Co(diars)$_2$Cl$_2$ClO$_4$. The crystals were rotated about their a, b, and c* axes and spectra recorded at 5° intervals.

Some data were also taken at K band frequencies on Ni/Co(diars)$_2$Cl$_3$. The crystal was placed in a 2 mm wide quartz capillary tube with a flat bottom so that the crystal rested with its

$\vec{a}$ axis parallel to the capillary axis. The magnet was then rotated about the cavity, and spectra taken every 5 degrees. It was impossible to orient the crystal about any other axis because nothing with a diameter larger than 2 mm can fit into the K band cavity.

Obtaining ⟨A⟩ and ⟨g⟩ Values From a Doped Single Crystal

Consider a single crystal with external crystal axes a, b, and c. If the crystal is orthorhombic or cubic, we may use these axes as they are. For a monoclinic crystal, we use the orthonormal set abc* where c* is perpendicular to both a and b. The molecule of interest in the crystal is defined by its symmetry axes x, y and z, which are related to a, b and c* by some angular transformation. In our case, we know how to transform abc* to xyz because we know the X-ray crystal structures of both $Co(diars)_2Cl_3$ and $Co(diars)_2Cl_2ClO_4$. Consider the expression for the Zeeman Hamiltonian for this system

$$\mathcal{H} = \beta \vec{H} \cdot g \cdot \vec{S} =$$

$$\beta[H_a H_b H_{c^*}] \begin{bmatrix} g_{aa} g_{ab} g_{ac^*} \\ g_{ba} g_{bb} g_{bc^*} \\ g_{c^*a} g_{c^*b} g_{c^*c^*} \end{bmatrix} \begin{bmatrix} S_a \\ S_b \\ S_{c^*} \end{bmatrix} =$$

$$\beta[H_x H_y H_z] \begin{bmatrix} g_{xx} & 0 & 0 \\ 0 & g_{yy} & 0 \\ 0 & 0 & g_{zz} \end{bmatrix} \begin{bmatrix} S_x \\ S_y \\ S_z \end{bmatrix}$$

Note that the g tensor is diagonal along the molecular symmetry axes. Let the vector $\vec{\ell} = (\ell_x \ell_y \ell_z) = (\ell_a \ell_b \ell_c)$ be the direction cosine vector of the magnetic field $\vec{H}$ with respect to the xyz or abc* axes.

$$\vec{H} = H\vec{\ell}$$

Since the spin is also quantized in this direction

$$\vec{S} = \pm \tfrac{1}{2} \vec{\ell}$$

The resonant frequency occurs at the transition between the $+\frac{1}{2}$ and $-\frac{1}{2}$ spin states.

$$E + \tfrac{1}{2} = + \frac{\beta H}{2} \vec{\ell} \cdot g \cdot \vec{\ell}$$

$$E - \tfrac{1}{2} = - \frac{\beta H}{2} \vec{\ell} \cdot g \cdot \vec{\ell}$$

$\Delta E = \pm \beta H \vec{\ell} \cdot g \cdot \vec{\ell} = \pm \beta g' H$ where g' is the effective g value that one measures. It is clear therefore that

$$g' = \pm [\ell_a \ell_b \ell_{c^*}] \begin{bmatrix} g_{aa} & g_{ab} & g_{ac^*} \\ g_{ba} & g_{bb} & g_{bc^*} \\ g_{c^*a} & g_{c^*b} & g_{c^*c^*} \end{bmatrix} \begin{bmatrix} \ell_a \\ \ell_b \\ \ell_{c^*} \end{bmatrix} =$$

$$\pm [\ell_x \ell_y \ell_z] \begin{bmatrix} g_{xx} & 0 & 0 \\ 0 & g_{yy} & 0 \\ 0 & 0 & g_{zz} \end{bmatrix} \begin{bmatrix} \ell_x \\ \ell_y \\ \ell_z \end{bmatrix}$$

Because of the ambiguity in sign, one usually determines g'^2 ($g'^2 = \vec{\ell} \cdot g^2 \cdot \vec{\ell}$). The principal values of the tensor, g_x, g_y, and g_z are almost always positive so that this ambiguity in fact is not a problem.

Suppose for example we are mounted with the z crystal axis perpendicular to the field (see Figure 8). Then the components of $\vec{\ell}$ are (cos θ, sin θ, o)

$$g'^2 = [\cos\theta,\ \sin\theta,\ o] \begin{bmatrix} (g^2)_{xx} & 0 & 0 \\ 0 & (g^2)_{yy} & 0 \\ 0 & 0 & (g^2)_{zz} \end{bmatrix} \begin{bmatrix} \cos\theta \\ \sin\theta \\ o \end{bmatrix}$$

$$= (g^2)_{xx} \cos^2\theta + (g^2)_{yy} \sin^2\theta$$

It is obvious that a study of the angular dependence of g′ will enable one to solve for the three principal values. Hyperfine constants are determined in a similar fashion.

Consider the spin Hamiltonian for the hyperfine interaction of an unpaired electron with a single nucleus of spin I.

$$\mathcal{H}_{SI} = \vec{S} \cdot T \cdot \vec{I} = g_N \beta_N \vec{H}_{eff} \cdot \vec{I}$$

Here T is the hyperfine tensor whose principal elements (diagonal in the x′ y′ z′ system) consist of an isotropic and a dipole part.

$$T_{x'x'} = A + t_{x'}$$
$$T_{y'y'} = A + t_{y'}$$
$$T_{z'z'} = A + t_{z'}$$

The trace of this tensor is simply A, since the dipole contributions sum up to zero.

The x′ y′ z′ system in which T is diagonal does not have to be the same as the xyz system in which g is diagonal. In our case, where we are dealing with the superhyperfine interactions of the

Figure 8. Position of the magnetic field with respect to the molecular symmetry axes.

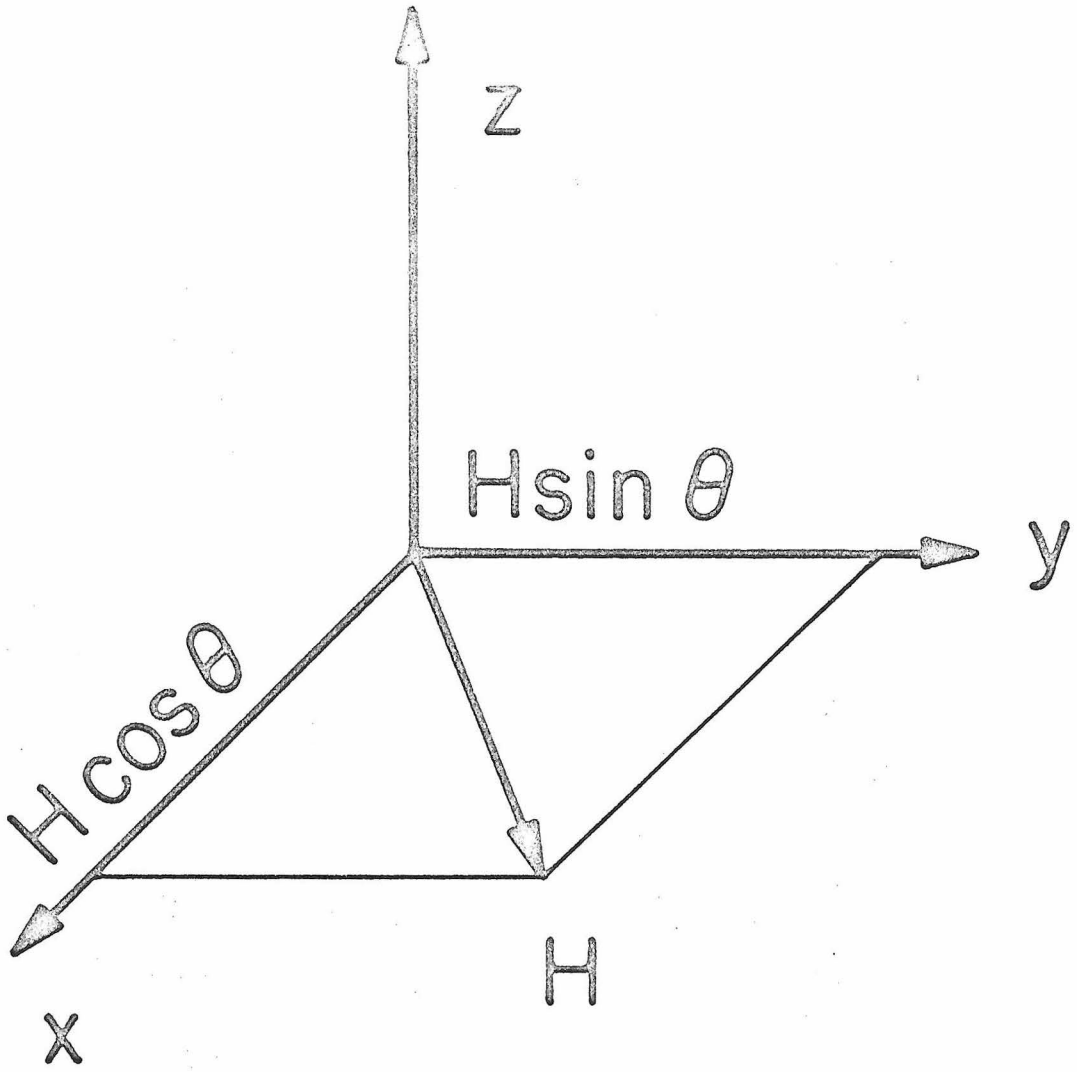
z
Hsin θ
y
Hcos θ
H
x

Figure 9. The principal directions of the g tensor and the ligand superhyperfine tensor.

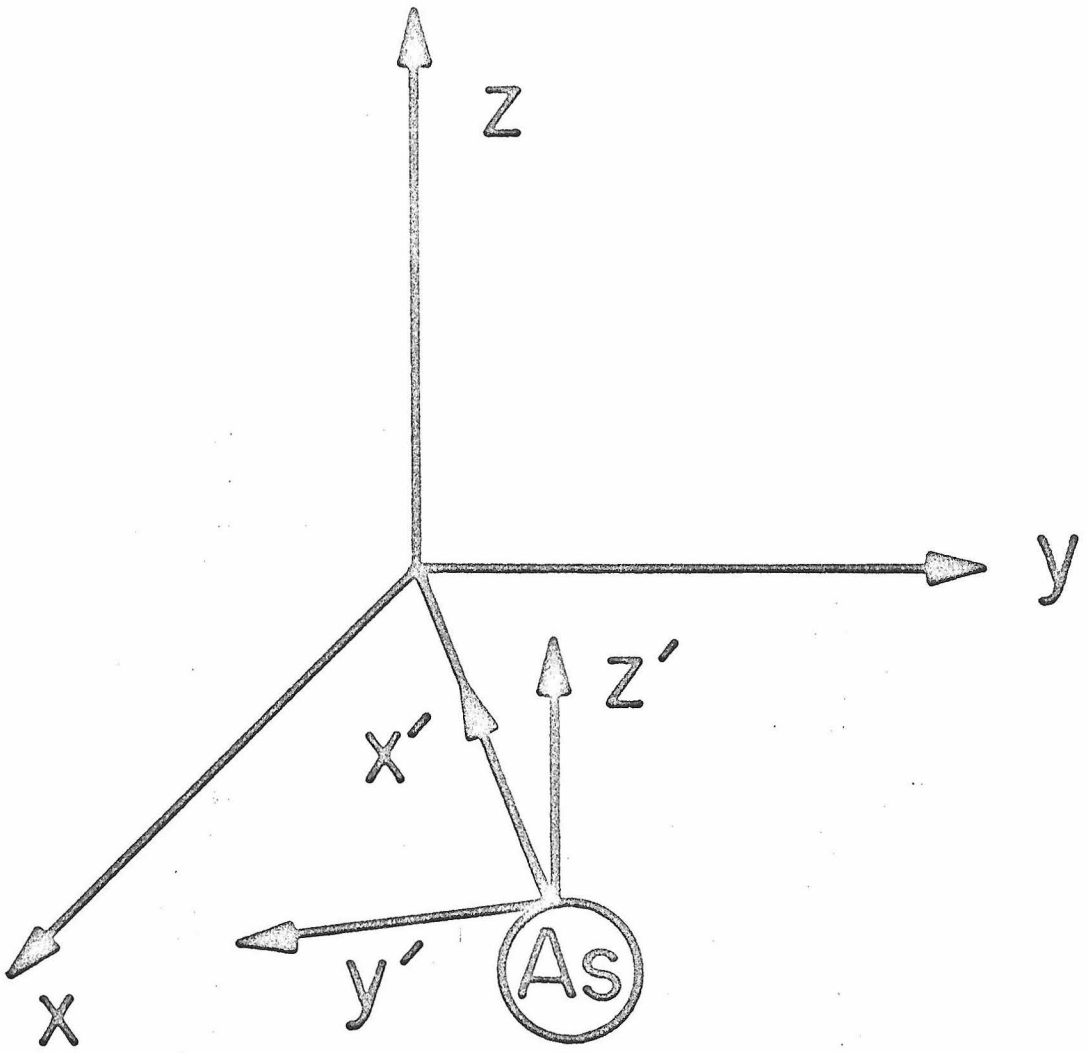
z
y
z′
x′
As
y′
x

ligands, they are different. (See Figure 9.) $\vec{H}_e$ is the effective magnetic field at the nucleus.

$$g_N\beta_N H_e = \vec{S} \cdot T = \pm \tfrac{1}{2} \vec{\ell} \cdot T$$

ΔE, the hyperfine splitting, is equal to $2g_N\beta_N H_e = \pm \ell \cdot T$

$$(\Delta E)^2 = (\ell \cdot T)^2 = \vec{\ell} \cdot T^2 \cdot \vec{\ell}$$

So, in principle, we measure the splitting ΔE at different orientations of the field with respect to the abc* or x′y′z′ axes. At each measurement, we know the components of $\vec{\ell}$, and with enough measurements we can solve for all the elements of the tensor T^2.

$$(\Delta E)^2 = [\ell_a \ell_b \ell_{c^*}] \begin{bmatrix} T^2_{aa} & T^2_{ab} & T^2_{ac^*} \\ T^2_{ba} & T^2_{bb} & T^2_{bc^*} \\ T^2_{c^*a} & T^2_{c^*b} & T^2_{c^*c^*} \end{bmatrix} \begin{bmatrix} \ell_a \\ \ell_a \\ \ell_{c^*} \end{bmatrix} =$$

$$[\ell_{x'}, \ell_{y'}, \ell_{z'}] \begin{bmatrix} T^2_{x'} & 0 & 0 \\ 0 & T^2_{y'} & 0 \\ 0 & 0 & T^2_{z'} \end{bmatrix} \begin{bmatrix} \ell_{x'} \\ \ell_{y'} \\ \ell_{z'} \end{bmatrix}$$

Of course the procedure becomes increasingly complicated when more than one ligand atom is involved because one can no longer measure ΔE directly. In our case, there are six ligand atoms involved, four arsenics in a square plane, and two chlorines in axial positions. These six atoms form three sets of equivalent pairs because of the center of inversion through the nickel atom. At any given angular orientation, therefore, there are three separate splitting constants contributing to the overall pattern. In order to determine what these

constants are, we must use computer techniques. Spectra are simulated using various possible combinations of constants until a spectrum is found which matches the line positions and intensities of the experimental spectrum. Needless to say, this process is time consuming and tedious. Once the constants have been extracted, there exists the additional problem of determining which splitting comes from which set of atoms, and of determining the absolute signs of the components of the T tensor. These problems will be discussed with reference to the particular case of $Ni(diars)_2Cl_2^+$ later in this chapter.

Preliminary ESR Spectra of $Ni(diarsine)_2Cl_3$

Preliminary spectra were taken of concentrated, powdered $Ni(diars)_2Cl_3$ at X band and K band frequencies. The X band spectrum is shown in Figure 10. The spectrum of $Ni(diars)_2Cl_2ClO_4$ has been studied by other workers[27] and is identical to that of the trichloride. Three g values are observed

$$g_1 = 2.0539 \pm .0005$$
$$g_2 = 2.0913 \pm .0005$$
$$g_3 = 2.1421 \pm .0005.$$

Work was begun on a single crystal of $Ni(diars)_2Cl_3$ doped into the isomorphous cobalt compound in a concentration of approximately 3%. This system was chosen initially because we knew the crystal structure of the nickel compound. Unfortunately, it proved to be an extremely difficult system to work in. The crystal space group is $P2_{1/c}$ and there are two inequivalent molecules per unit cell related

Figure 10. Powder spectrum of concentrated $Ni(diars)_2Cl_3$ at X band frequency.

to one another by a two-fold screw axis. This means that any given spectrum shows two separate, often overlapping, signals, each with a different hyperfine pattern. These two lines coalesce only in spectra taken with the "b" axis perpendicular to the field. In addition, the relationship between the external crystal axes and the symmetry axes of the molecule is not a simple one, and it is impossible to orient the crystal with the field parallel or perpendicular to the z axis. Consequently, we were unable to obtain enough well-resolved spectra to extract the hyperfine splitting constants. We were, however, able to measure the angular dependence of the g value in this system.

We measured the angular variation of g with the crystal mounted on both the "a" and "b" axes. The $\vec{a}$ axis data were obtained at K band and the $\vec{b}$ axis data at X band. We noted that the minimum value of g observed with the crystal $\vec{a}$ axis perpendicular to the field was 2.0304. This result was peculiar, because we expected the lowest measured g value to have been 2.0539.

We then ground up a number of dilute single crystals and examined the spectrum of a dilute powder at K band. This spectrum is illustrated in Figure 11. Instead of the three g value pattern seen in the concentrated powder, we now see a two g value spectrum with $g_{\parallel} = 2.008$ and $g_{\perp} = 2.142$.

We considered four possible explanations for this phenomenon:

1. A pseudo-zero field effect caused by intermolecular interactions of unpaired electrons in the concentrated crystal was causing an extra "pseudo" g value to appear. We rejected this explanation on the basis of the magnetic susceptibility data which indicated that no

Figure 11. ESR spectrum of a powder of 3% $Ni(diars)_2Cl_3$ doped into the isomorphous cobalt compound at K band frequency.

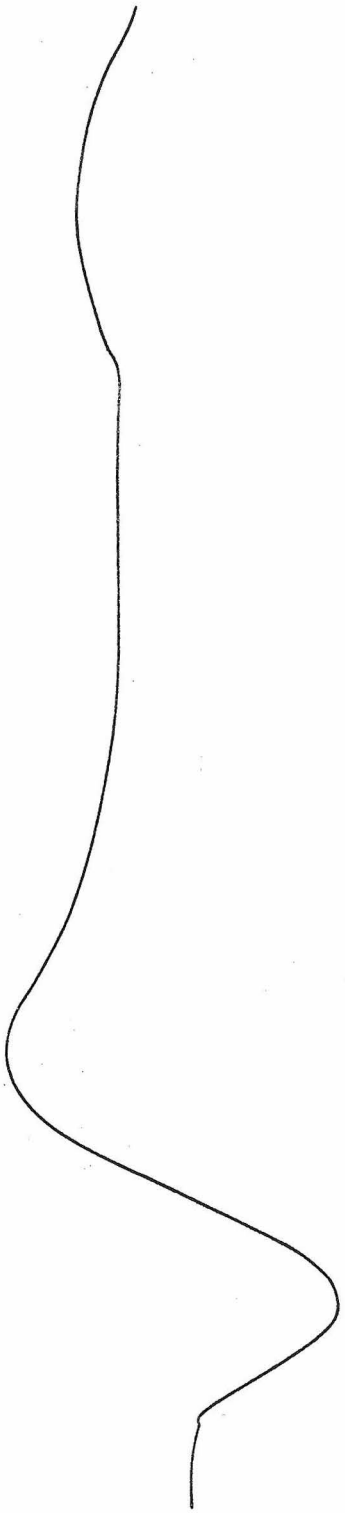

significant intermolecular interaction was taking place.

2. There had been a substitution of ethanol or water for chlorides in the course of the crystallization. To test this hypothesis, we examined the room temperature solution ESR spectrum of $Ni(diars)_2Cl_3$ in freshly prepared ethanol and water solutions. We then repeated the spectra after half an hour and again after two hours. It is fairly well established[1] that $Ni(diars)_2Cl_3$ is six coordinate in ethanol. Its spectrum shows both arsenic and chloride splittings. (See Figure 12.) The spectrum showed no appreciable change after two hours, and on this basis, we eliminated ethanol substitution as a possibility. The spectrum in water shown in Figure 13 is quite different from the ethanol spectrum. The lines are much sharper and the average g value is 2.12. After two hours, the signal becomes much less intense and the overall line shape changes. It is quite likely that an equilibrium between two and possibly three species is established in solution:

$$NiD_2Cl_2^{+} \rightleftharpoons NiD_2ClH_2O^{+2} \rightleftharpoons NiD_2(H_2O)_2^{+3}$$

This equilibrium does not account for our dilute powder spectrum, however, because its main product is a species with too high an average g value.

3. A third possibility we considered was that $Ni(diars)_2Cl_2^{+}$ was undergoing a dynamic distortion at room temperature which was averaging out the g anisotropy. To test this, we looked at the dilute powder spectrum at liquid nitrogen temperature. Since no appreciable change in the spectrum was observed, we abandoned this line of thought.

Figure 12. ESR spectrum of a solution of $Ni(diars)_2Cl_3$ in ethanol.

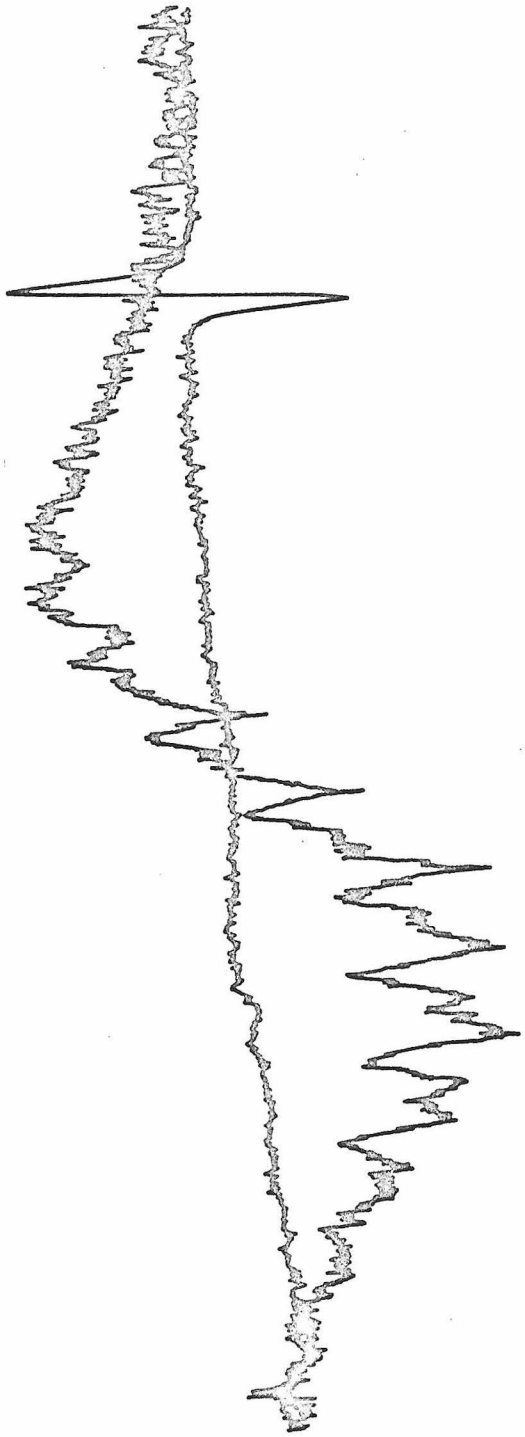

Figure 13. ESR spectrum of a solution of $Ni(diars)_2Cl_3$ in water.

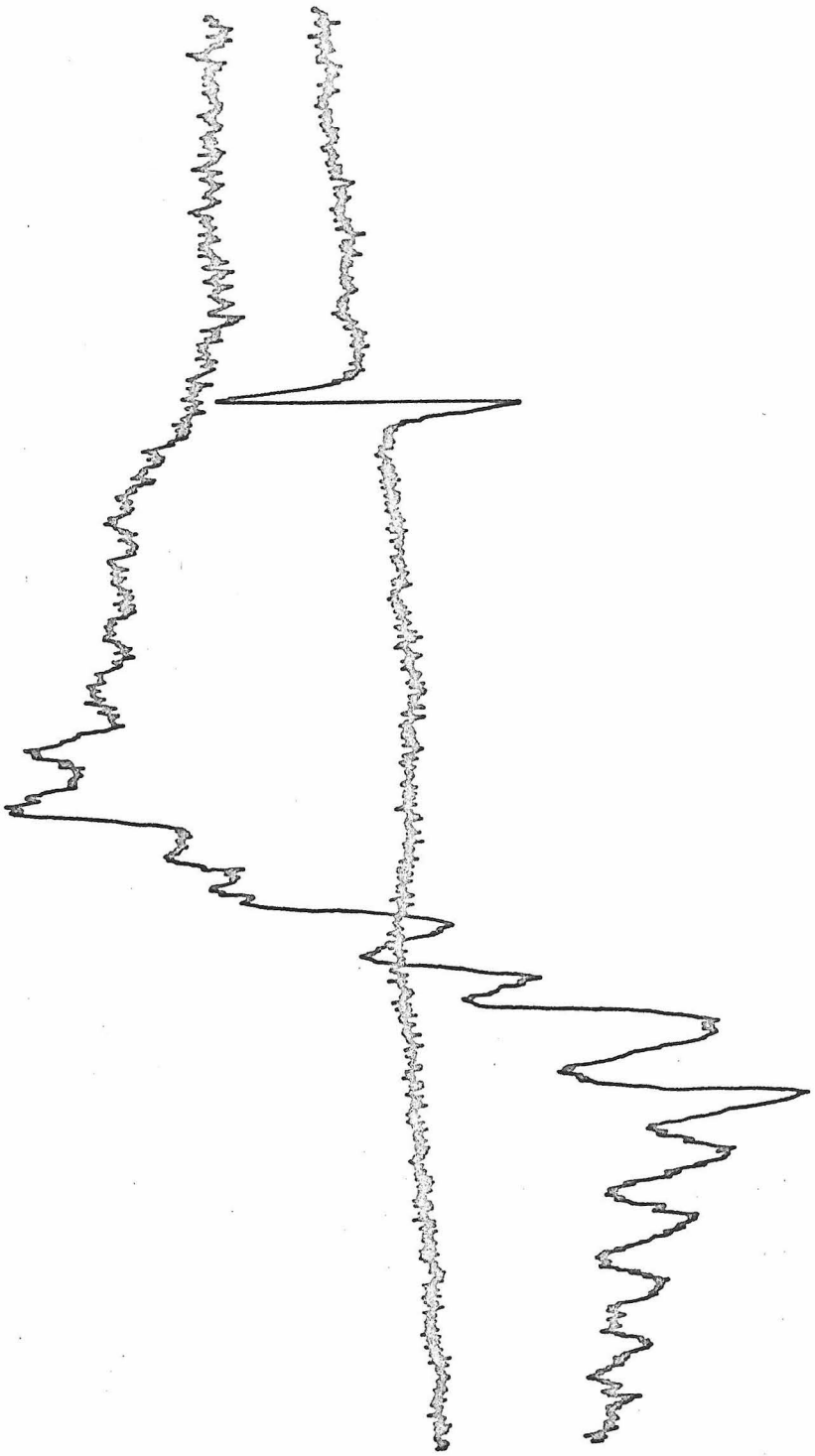

4. This left one other reasonable possibility; that the change in g value was due to a distortion imposed on the nickel by the cobalt matrix. This implied that the two salts could not be exactly isomorphous as had been previously thought. At this point, Dr. Gordon Rodley undertook the X-ray crystal structure of $Co(diars)_2Cl_3$ to test this hypothesis, and in fact found a significant difference in the metal-chloride distance in the two compounds. We believe that the change in g values can be adequately accounted for by assuming that the nickel chloride bond is contracted in the cobalt matrix. This point is amplified further in the next chapter.

Concentration Dependence of the Dilute Powder Spectrum of $Ni(diars)_2Cl_3$

If the hypothesis of a static distortion is valid, then the ESR spectra should have a concentration dependence. We grew mixed crystals of $Ni/Co(diars)_2Cl_3$, $Ni/Co(diars)_2Cl_2ClO_4$, and $Ni/Rh(diars)_2Cl_3$ in approximate concentrations of 75% Ni, 50% Ni, 25% Ni, 10% Ni, and 3% Ni. All three matrices showed essentially the same kind of concentration dependence. The spectra of 75% Ni and 50% Ni in $Co(diars)_2Cl_3$ show a three g value pattern. At 25% Ni, there is a marked increase in intensity of the peak at $g = 2.14$ and a decrease of intensity at $g = 2.09$ and $g = 2.05$. By 10% Ni, the two latter bands have completely disappeared and a weak band at $g = 2.00$ can be detected. The intermediate 25% spectrum is illustrated in Figure 14.

Figure 14. ESR spectrum of a powder of 25% $Ni(diars)_2Cl_3$ in a $Co(diars)_2Cl_3$ matrix.

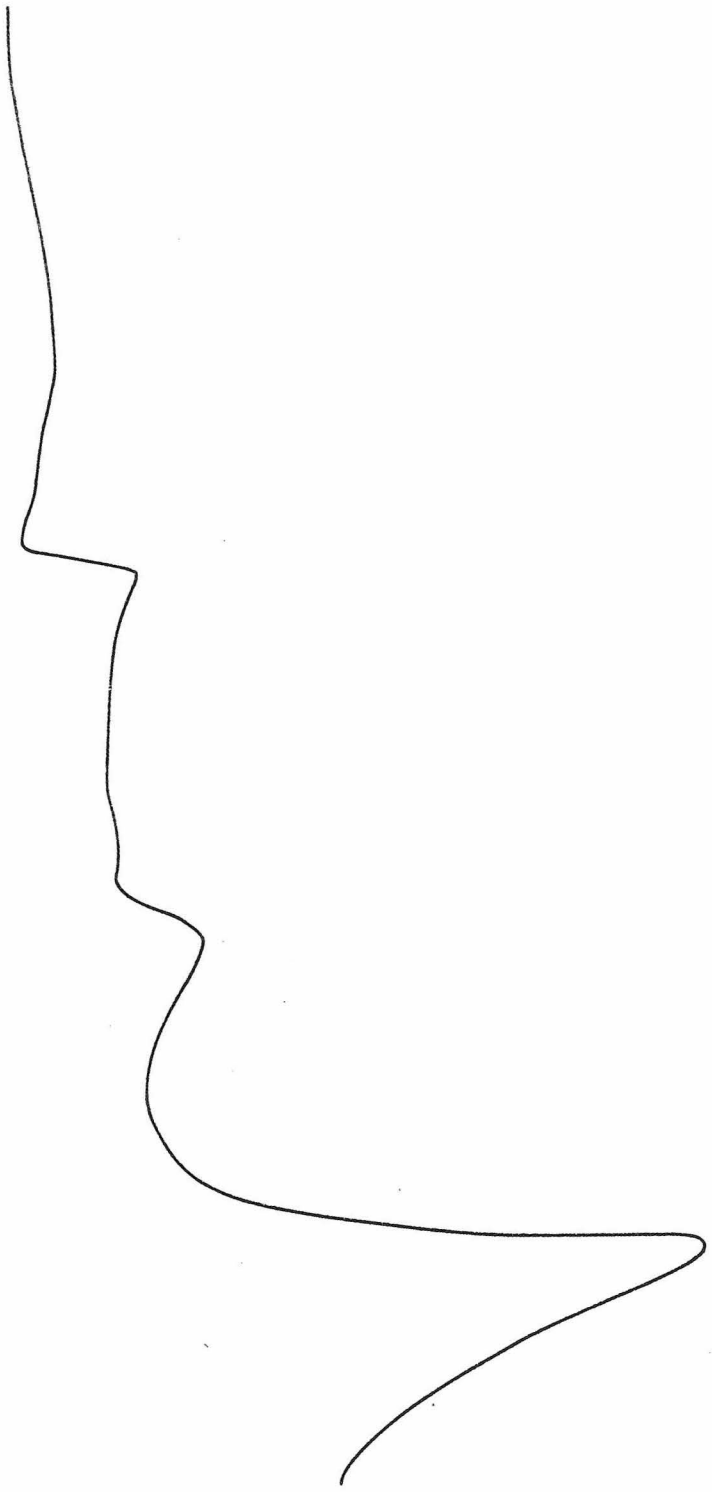

We suggest the following explanation: There are two electronically stable states for $Ni(diars)_2Cl_2^+$; the ground state with an elongated Ni–Cl bond and three g values, and an energy minimum at a shorter Ni—Cl distance which gives rise to the 2 g value spectrum. At concentrations of 50% or more, the nickel is dominant in the mixed crystal matrix and the ground state predominates. At 10% Ni or less, the smaller cobalt cell dominates and the two g value state is observed. At intermediate concentrations both species are present and their relative abundance is reflected in the intensities of the spectral lines. One might argue that the transition from one state to the other should be continuous, and that at intermediate concentrations there should be one intermediate state as opposed to a mixture of the two final states. In that case, however, one would expect to observe a gradual change in the g values. This is not seen. Only the intensities change, as if one species were disappearing while a second was being created. Although it is difficult at first to visualize the existence of two separate states in the same crystal, it becomes reasonable if one considers that the distribution of the nickel in the cobalt or rhodium matrix is not necessarily homogeneous. $Ni(diars)_2Cl_2^+$ is much less soluble than either $Co(diars)_2Cl_2^+$ or $Rh(diars)_2Cl_2^+$, and especially in concentrations as high as 25%, is likely to begin crystallizing first. This would result in micropockets of abnormally high nickel concentration in the mixed crystal.

The Angular Dependence of the g Value of $Ni(diars)_2Cl_3$

We have plotted our measured g values vs. angle for spectra of a single crystal of $Ni/Co(diars)_2Cl_3$ mounted on both the $\vec{a}$ and $\vec{b}$ axes. Figure 15 shows the data points for the $\vec{b}$ axis spectra. The solid line is a theoretical curve based on $g_{||} = 2.00$ and $g_{\perp} = 2.14$. It is apparent from this plot that the single crystal data are in excellent agreement with the principal g values measured in the dilute powder spectrum.

The Single Crystal Spectra of $Ni/Co(diars)_2Cl_2ClO_4$

Because of the many difficulties involved in solving the spectrum of $Ni/Co(diars)_2Cl_3$, we looked for a matrix with a simpler crystal structure. We chose $Co(diars)_2Cl_2ClO_4$. Its structure was done by Peter Pauling[26] but has not been published. Figure 16 shows the external morphology of the crystal and the relationship between the external and internal axes. Tables XIV to XVI give the pertinant structural data for this compound. $Co(diars)_2Cl_2ClO_4$ crystallizes in the pseudo-orthorhombic space group C_2, and the crystal b axis is parallel to the molecular z axis.

Spectra were taken of a doped single crystal of 3% $Ni/Co(diars)_2Cl_2ClO_4$ at 5° intervals about each of the three principal axes. The best of these spectra were chosen for computer simulation.

To simulate the spectra, we used a modified version of a computer program written by Gladney and Swalen. Splitting constants are assumed for each of the three ligand pairs. Each pair gives rise to seven equally spaced lines making a total of 343 possible lines.

Figure 15. The angular variation of the g value of a dilute single crystal of $Ni(diars)_2Cl_3$ mounted on the $\vec{b}$ axis.

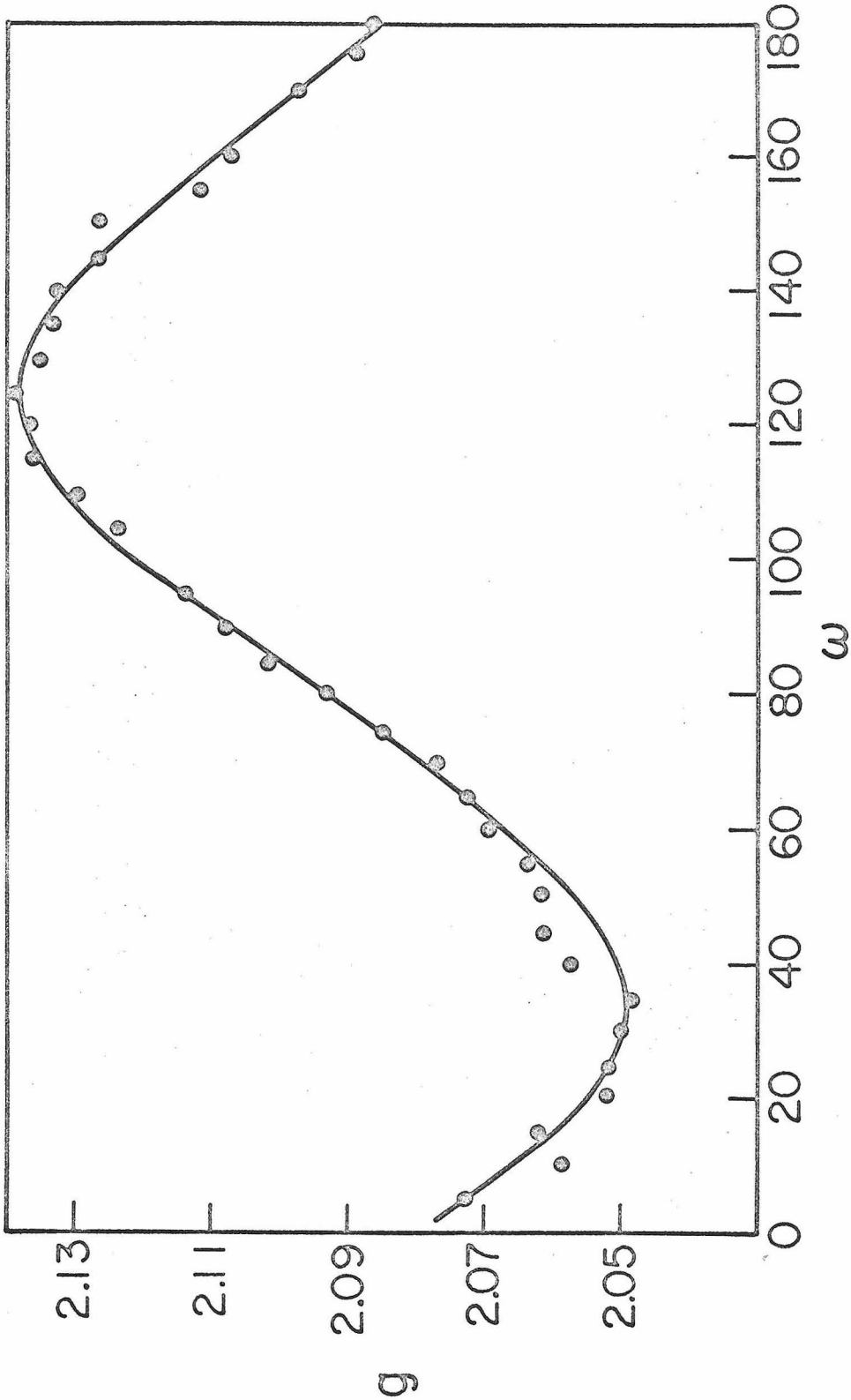
2.13
2.11
2.09
2.07
2.05
g
0
20
40
60
80
100
120
140
160
180
ω

Figure 16. The crystal structure of $Co(diars)_2Cl_2ClO_4$.

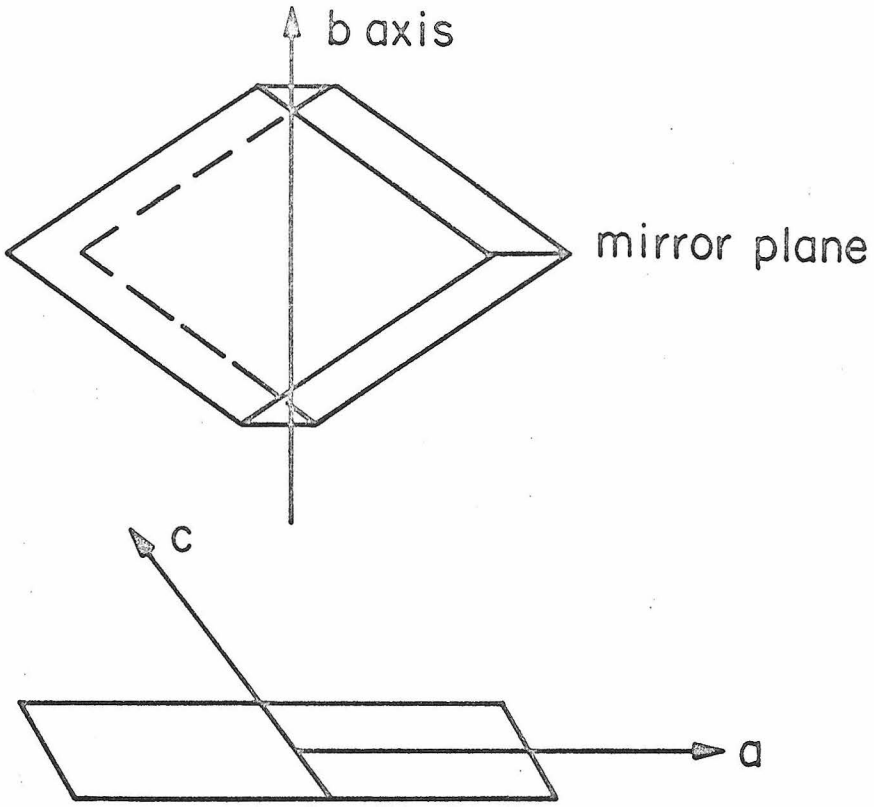
b axis
mirror plane
c
a

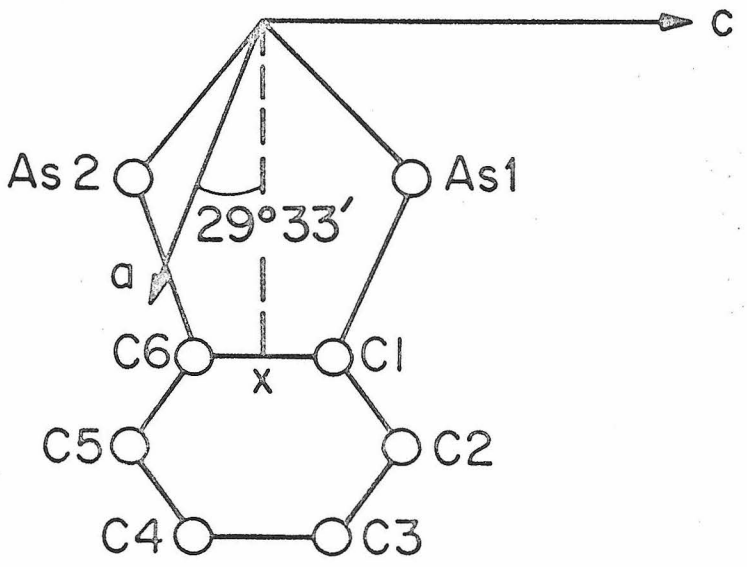
c
As 2
As1
29°33′
a
C6
C1
x
C5
C2
C4
C3

Table XIV

Structural Data for $[Co(diars)_2Cl_2]ClO_4$

Interatomic Distances in Å

$Co-Cl_1$	2.19
$Co-As_1$	2.36
$Co-As_2$	2.37
As_1-C_1	2.02
As_1-C_7	1.98
As_2-C_6	1.96
As_2-C_9	2.01
C_1-C_2	1.37
C_1-C_6	1.31
C_3-C_2	1.60
C_3-C_4	1.34
C_5-C_4	1.41
C_5-C_6	1.44

Table XV

Structural Angles for $[Co(diars)_2Cl_2]ClO_4$

A B C	∢ (ABC) Degrees
$As_1-Co-As_2$	94
$Co-As_1-C_1$	108
$Co-As_1-C_7$	118
$C_7-As_1-C_8$	107
$C_7-As_1-C_1$	101
$As_1-C_1-C_2$	117
$As_1-C_1-C_6$	117
$C_1-C_2-C_3$	117
$C_2-C_3-C_4$	110
$C_3-C_4-C_5$	122
$Co-As_2-C_6$	108
$Co-As_2-C_9$	118
$C_9-As_2-C_{10}$	105
$C_9-As_2-C_6$	104
$As_2-C_6-C_5$	121
$As_2-C_6-C_1$	121
$C_4-C_5-C_6$	122
$C_5-C_6-C_1$	118
$C_6-C_1-C_2$	126

Table XVI

Atomic Coordinates for $[Co(diars)_2Cl_2]ClO_4$

Atom	x/z	y/b	z/c
Co	0	0	0
Cl_1	0	.213	0
As_1	.188	0	.211
As_2	.144	0	-.055
C_1	.344	0	.210
C_2	.464	0	.325
C_3	.587	0	.325
C_4	.560	0	.211
C_5	.432	0	.099
C_6	.322	0	.101
Cl_3	0	0	.5
O_1	.058	.058	.455
O_2	.103	.103	.596

In practice, of course, one never resolves this many. The best resolved spectra are those in which the splitting constants are multiples of one another. At each calculated line position, one calculates a gaussian curve of specified amplitude and half width. The total hyperfine spectrum is the sum of all these curves. In addition, there is an overall line shape centered at $H = h\nu/g\beta$ on which the hyperfine spectrum is superimposed.

For a given spectrum, we calculated simulations for all possible combinations of the three splitting constants. This is not as time consuming as it sounds because certain constants may be eliminated immediately. For example, a spectrum consisting of equally spaced lines 10 gauss apart must arise from splitting constants which are multiples of 10. The original and simulated spectra were compared visually using a light box. The best match of positions and intensities was chosen for each.

Figure 17 shows the original and simulated spectra mounted on the $\vec{a}$ axis with the field parallel to the $\vec{b}$ axis. Figure 18 shows the spectra with the crystal mounted on the $\vec{b}$ axis and the field parallel to $\vec{a}$. Figure 19 shows the spectra with the crystal mounted on $\vec{b}$, and 9° from the molecular $\vec{y}$ axis. Figure 20 shows the spectra of $Ni/Co(diars)_2Cl_3$ mounted on the $\vec{b}$ axis with $\vec{H}$ parallel to the $\vec{x}$ axis.

Extracting the Hyperfine Constants

Figures 17, 18, 19, and 20 show the most important of the simulated spectra. A number of other spectra were also simulated as a check on our results. The best fit of constants for these four spectra were as follows:

Figure 17. Experimental and simulated spectra of dilute $Ni(diars)_2Cl_2ClO_4$ mounted on the $\vec{a}$ axis with $\vec{H} \parallel \vec{b}$.

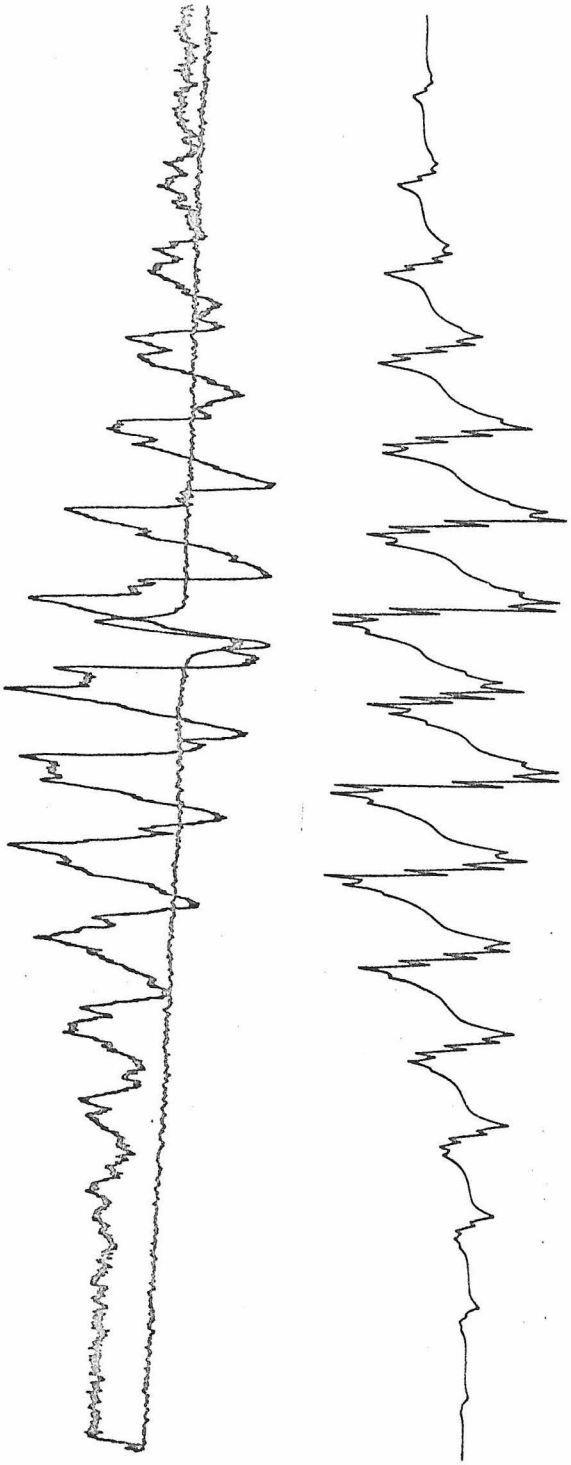

Figure 18. Experimental and simulated spectra of dilute $Ni(diars)_2Cl_2ClO_4$ mounted on the $\vec{b}$ axis with $\vec{H} \parallel \vec{a}$.

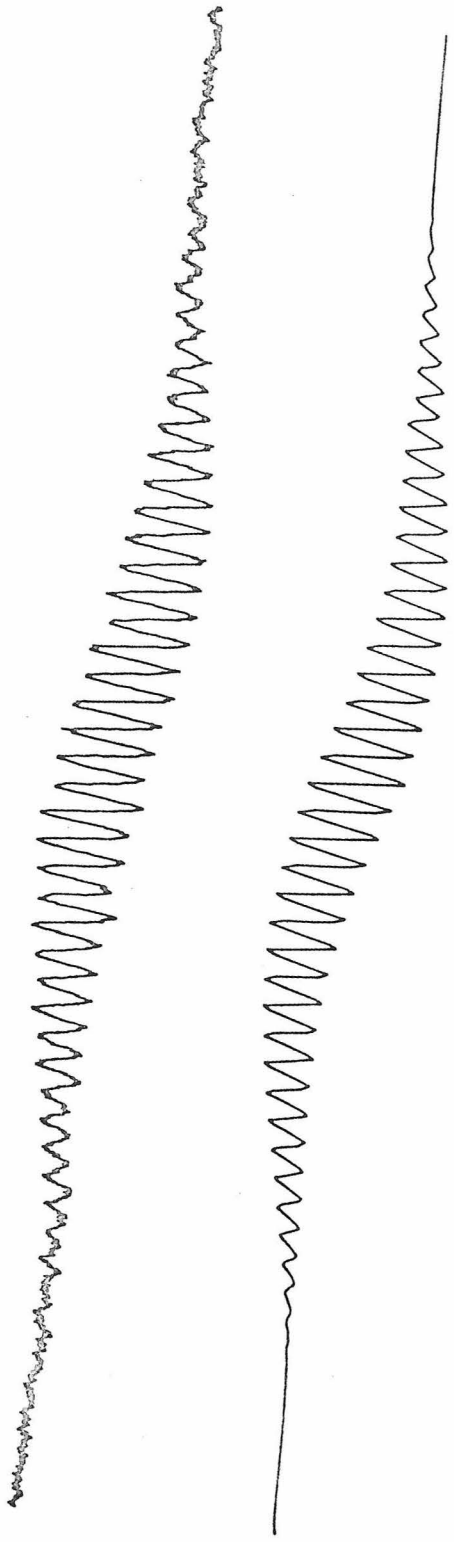

Figure 19. Experimental and simulated spectra of dilute $Ni(diars)_2Cl_2ClO_4$ mounted on $\vec{b}$ with $\vec{H}$ 9° from the molecular $\vec{y}$ axis.

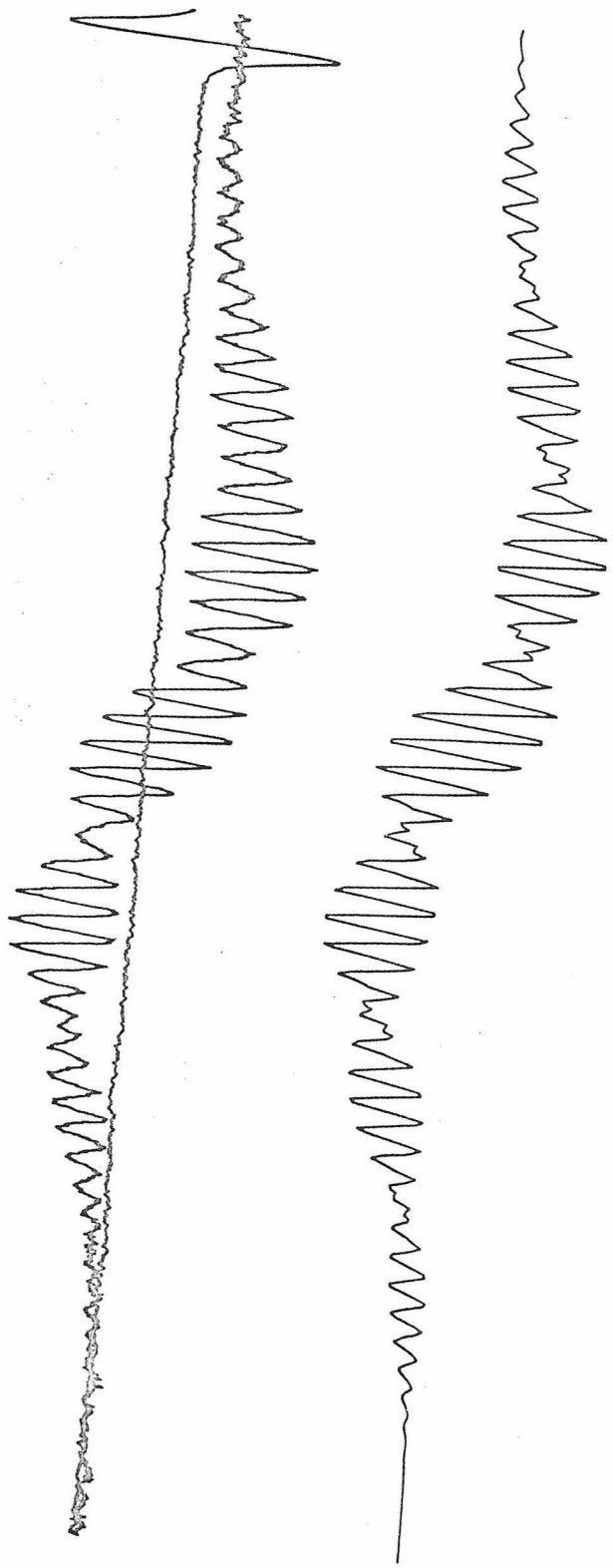

Figure 20. Experimental and simulated spectra of dilute $Ni(diars)_2Cl_3$ mounted on the $\vec{b}$ axis with $H \parallel$ to the molecular $\vec{x}$ axis.

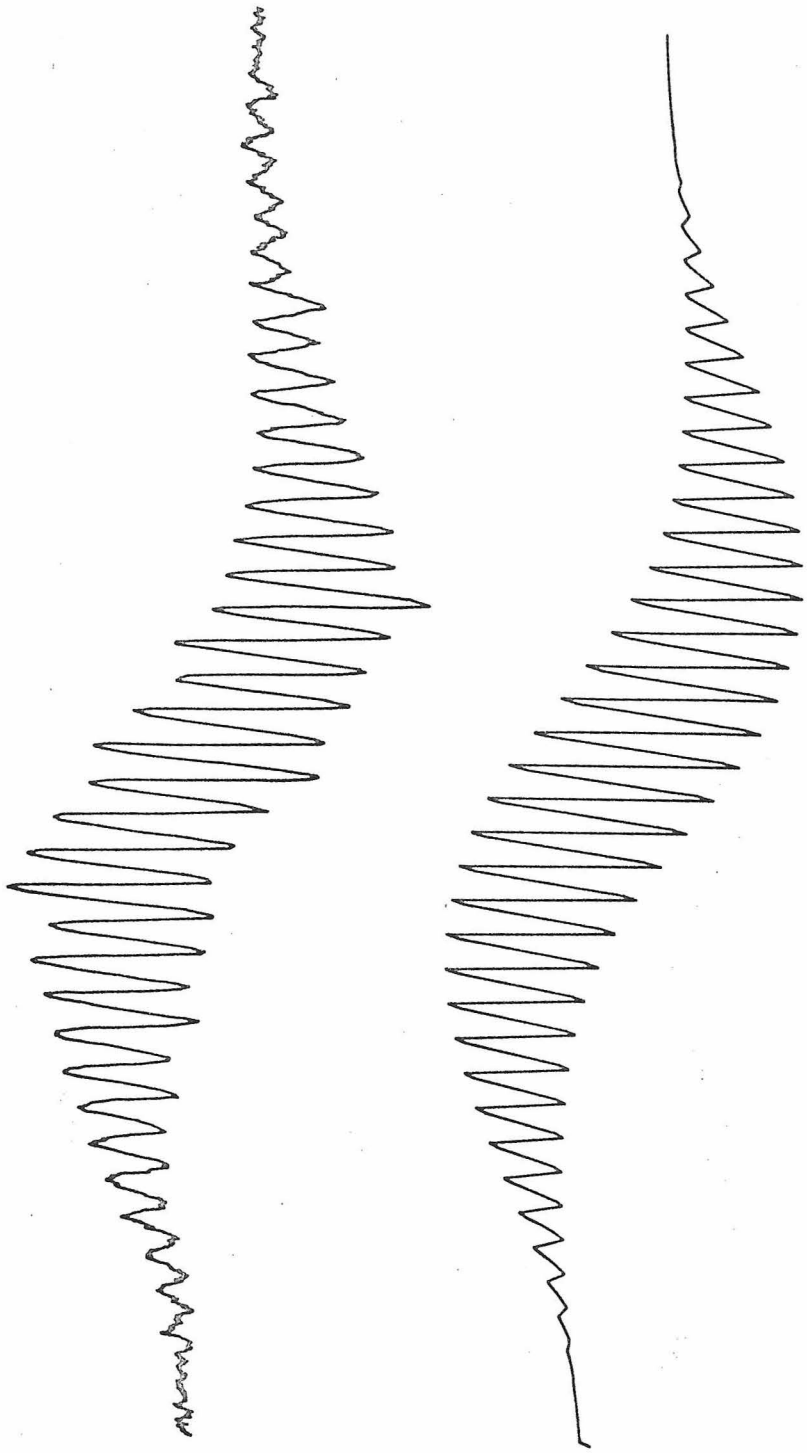

Orientation	Constants in Gauss
1) H ∥ to $\vec{b} = \vec{z}$	29, 32, 32
2) H ∥ to $\vec{a}$	37.5, 7.5, 7.5
3) H 9° from $\vec{y}$	50, 7.5, 8
4) H ∥ to $\vec{x}$	32, 8, 8

There are two immediate problems involved in interpreting these constants. The first is in deciding which constants belong to which ligand. The second is in determining the absolute orientation of the crystal, that is, we do not know if we are mounted on the $+\vec{b}$ or $-\vec{b}$ axis, and it does make an important difference. We do know our orientation exactly for spectra number one and number two where we are exactly parallel to the $\vec{a}$ and $\vec{b}$ axes. For the orientation in which H ∥ $\vec{b} = \vec{z}$ all four arsenic atoms are equivalent. Therefore, $A_z As = \pm 32$ gauss and $A_z Cl = \pm 29$ gauss.

In order to determine which splitting constants belong to which ligand, we examined the relationship between the two pairs of arsenic atoms.

$$\text{If} \quad \Delta E_1 = A + 2 \sin\theta \cos\theta B \quad \text{then}$$
$$\Delta E_2 = A - 2 \sin\theta \cos\theta B$$

where A refers to the diagonal element of the hyperfine matrix in the xy system and B is the off diagonal element. We chose the unambiguous orientation H ∥ to $\vec{a}$ and diagonalized the hyperfine matrix assuming both possibilities for the arsenic splitting constants. The combination 37.5, 7.5 resulted in an imaginary principal value for the hyperfine tensor thus establishing 7.5, 7.5 as the correct

combination. This means that for all spectra taken in the xy plane arsenic splittings on the order of 8 gauss are to be expected.

We next determined the exact orientation for spectrum number three by solving for the chloride hyperfine tensor assuming each possibility in turn. The principal values obtained in this way were used to predict chloride splittings at other orientations. An excellent fit was obtained to several spectra assuming that we were mounted along the +b axis.

The results of these calculations yielded the following principal values in gauss for the ligand superhyperfine tensors.

Cl	As
$A_x \pm 32$	$A_{\sigma} \pm 8.5$
$A_y \pm 50$	$A_{\pi} \pm 6.9$
$A_z \pm 29$	$A_z \pm 32$

The final problem is that of determining the absolute sign of these tensor components. From theoretical considerations we know that the sign of the dipole term in the z direction should be positive for chloride and negative for arsenic. Using this criterion, we can eliminate all but four possibilities. In Chapter V a final choice is made by examining the MO coefficients calculated from the four possibilities.

It is interesting that all four possibly correct choices of sign result in a negative contact term for both ligands. This point is discussed in the next chapter.

V. THE SINGLE CRYSTAL ESR SPECTRUM OF Ni(diarsine)$_2$Cl$_2^+$--THEORETICAL

Introduction

We have attempted to describe the bonding in Ni(diarsine)$_2$Cl$_2^+$ in terms of a molecular orbital scheme. The ground state is taken to be a combination of metal d_{z^2} and $d_{x^2-y^2}$ orbitals with chloride and arsenic p orbitals. Approximate molecular orbital coefficients have been calculated using the method and notation given by McGarvey.[35] The results of this calculation indicate that the electron is largely delocalized, spending approximately half its time in the vicinity of the six ligands.

The Molecular Orbital Scheme

Choosing the coordinate system shown in Figure 21, we can construct a qualitative molecular orbital scheme using the appropriate symmetry group. Because of the tipping of the benzene rings and the slight distortion of the chlorides, the true symmetry of the NiD$_2$Cl$_2^+$ cation is only C_i. Since a point group of such low symmetry is quite inconvenient for calculations, we have ignored the slight distortion of the chlorines and have used the point group C_{2h}. One might be tempted to proceed one step further in this approximation and work in D_{2h} symmetry. Unfortunately, this approach predicts an axially symmetric chlorine hyperfine tensor contrary to the experimental results. It appears that the tipping of the benzene rings, which permits chlorine $2p_x$ orbitals to enter the ground state, is quite important in accounting for the observed tensor anisotropy. This point will be discussed in more detail later on.

Figure 21. Coordinate system for $Ni(diars)_2Cl_2^+$

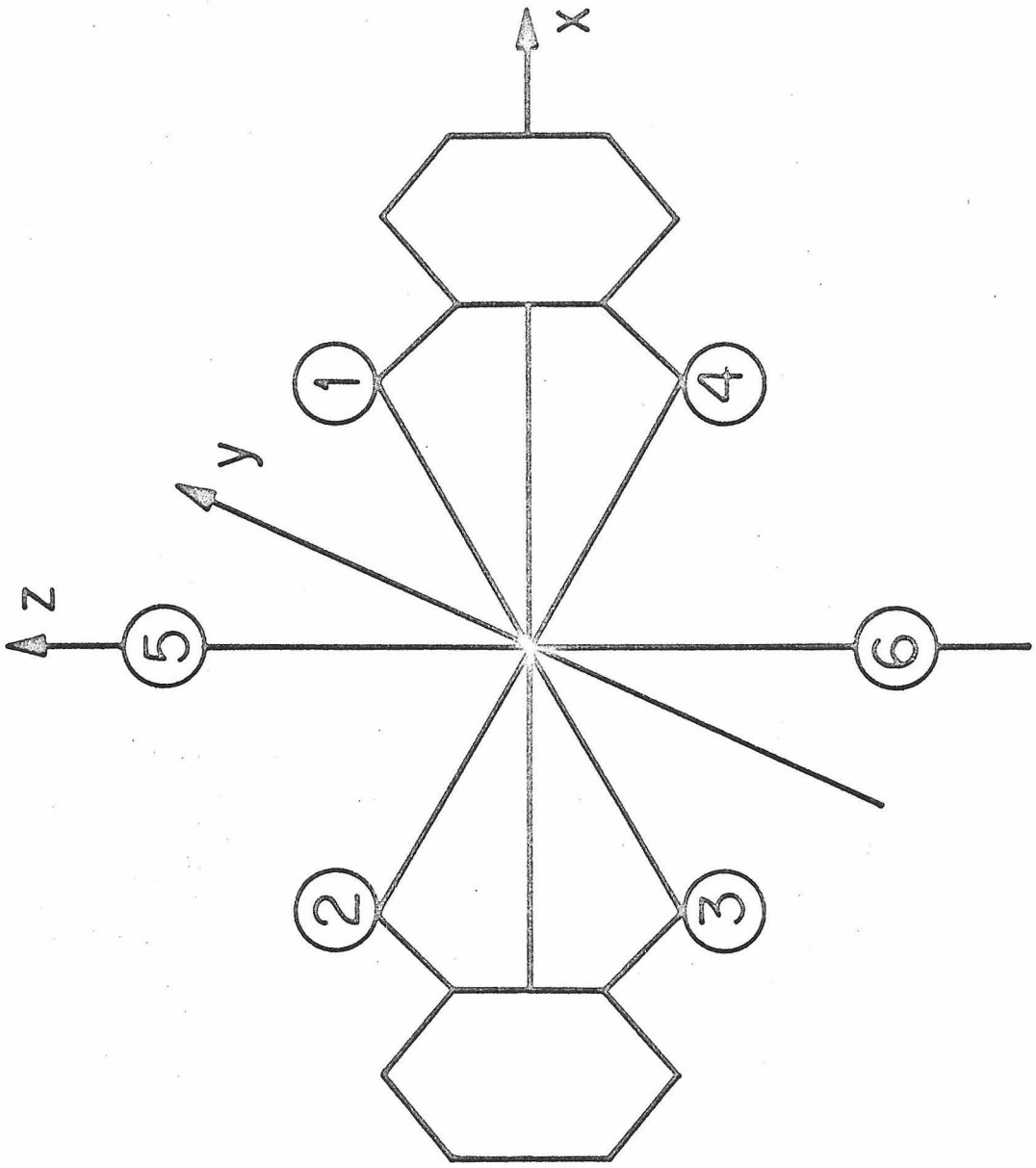
x
y
z
1
2
3
4
5
6

A number of approximations have been used to simplify this calculation. Before proceeding further, it will be useful to state and justify them.

1. We assume that the orbitals on the benzene ring do not contribute appreciably to those arsenic molecular orbitals which bond with the metal.

2. Secondly, we assume that the empty 4d levels of the arsenic atoms are at too high an energy to interact appreciably in the ground state. They have, therefore, not been included in our molecular orbital scheme.

3. The p_z orbitals of the arsenic atoms are primarily tied up in bonding with the methyl groups. They too have been neglected in this calculation.

Table XVII is a list of metal and ligand orbitals classified according to the symmetry designation of point group C_{2h}. Table XVIII shows a molecular orbital scheme for $Ni(diars)_2Cl_2^+$. Because of the complications involved in working in C_{2h} symmetry, most of our MO scheme is derived from D_{2h} orbitals. However, in the ground state $3A_g$ we have permitted ϕ_{pxCl} to mix with the other wave functions. This approximation is quite reasonable in view of the fact that only the ground state makes a first order contribution to the superhyperfine tensor elements. The coefficients have been chosen as positive in all cases, and the sign in front of each coefficient is appropriate for an antibonding combination of wave functions.

Table XVII

Molecular Wavefunctions Classified by

Symmetry in Point Group C_{2h}

	Ligand	Metal
A_g	$\phi_{sCl} = \frac{1}{\sqrt{2}}(s_5 + s_6)$	d_{z^2}
	$\phi_{p_zCl} = \frac{1}{\sqrt{2}}(p_{z_5} - p_{z_6})$	$d_{x^2-y^2}$
	$\phi_{p_xCl} = \frac{1}{\sqrt{2}}(p_{x_5} - p_{x_6})$	d_{xz}
	$\phi_{sAs} = \frac{1}{2}(s_1 + s_2 + s_3 + s_4)$	
	$\phi_{p_xAs} = \frac{1}{2}(p_{x_1} - p_{x_2} - p_{x_3} + p_{x_4})$	
	$\phi_{p_yAs} = \frac{1}{2}(p_{y_1} + p_{y_2} - p_{y_3} - p_{y_4})$	
B_g	$\phi_{p_yCl} = \frac{1}{\sqrt{2}}(p_{y_5} - p_{y_6})$	d_{xy}
	$\phi_{sAs} = \frac{1}{2}(s_1 - s_2 + s_3 - s_4)$	d_{yz}
	$\phi_{p_xAs} = \frac{1}{2}(p_{x_1} + p_{x_2} - p_{x_3} - p_{x_4})$	
	$\phi_{p_yAs} = \frac{1}{2}(p_{y_1} - p_{y_2} - p_{y_3} + p_{y_4})$	

Table XVIII

Molecular Orbital Scheme for $Ni(diarsine)_2Cl_2^+$

D_{2h}	C_{2h}	Wavefunction
B_{1g}	$2B_g$	$\alpha_1 d_{xy} + \alpha_2 \phi p_x As(B_g) + \alpha_3 \phi p_y As(B_g)$ $- \alpha_4 \phi S\, As(B_g)$
$2A_{1g}$	$3A_g$	$a_1 d_{z^2} + a_2 \phi p_z Cl(A_g) + a_3 \phi s\, As(A_g)$ $- a_4 \phi p_x As(A_g) - a_5 \phi p_y As(A_g)$ $- a_6 \phi s\, Cl(A_g) - a_7 \phi p_x Cl(A_g)$
B_{2g}	$2A_g$	$\beta_1 d_{xz} - \beta_2 \phi p_y Cl(A_g)$
B_{3g}	$1B_g$	$\gamma_1 d_{yz} - \gamma_2 \phi p_y Cl(A_g)$
$1A_{1g}$	$1A_g$	$\delta_1 d_{x^2-y^2} - \delta_2 \phi p_x As(A_g)$ $- \delta_3 \phi p_y As(A_g) - \delta_4 \phi s\, As(A_g)$

Corrections to the Ground State Due to Spin Orbit Coupling

Before proceeding to a detailed calculation of the superhyperfine tensor elements, it will be informative to calculate the corrections to the ground state wave function due to spin orbit coupling. All second order terms in the hyperfine tensor arise from this interaction. Because we are attempting only to give the reader a qualitative understanding of this process, and not to do a quantitatively rigorous calculation, we may make the following assumptions:

1. We will use the MO scheme previously outlined.

2. We will neglect all overlap.

3. We will assume that $E_{B_{3g}} \approx E_{B_{2g}}$. This is probably a good approximation for the doped crystal which exhibits an axially symmetric g tensor but is not valid for discussing the concentrated crystal.

The spin orbit coupling Hamiltonian is

$$H_{SL} = \sum_i \epsilon_i \ell_i \cdot s = (\epsilon_{Ni} + \sum_{i=1}^{4} \epsilon_{iAs} + \sum_{i=1}^{2} \epsilon_{iCl})$$

$$(\ell_z S_z + \tfrac{1}{2}(\ell_+ S_- + \ell_- S_+)$$

Since the ground state is now degenerate, we may use the expression for the first order wave function.

$$\psi^1 = \psi_n^0 - \sum_{m \neq n} \frac{\langle m | H_{SL} | n \rangle}{E_m - E_n} \phi_m$$

$$A_{1g}^{+} = A_{1g}\alpha\rangle - \sum_n \frac{\langle\psi_n|\epsilon L\cdot S|\psi_o\alpha\rangle|n\rangle}{E_n - E_o}$$

$$= A_{1g}\alpha\rangle - \tfrac{1}{2}\sum_n \frac{\langle\psi_n|\epsilon L_z|\psi_o\rangle}{E_n - E_o}|\psi_n\alpha\rangle$$

$$- \tfrac{1}{2}\sum_n \frac{\langle\psi_n|\epsilon(L_x + i\,L_y)|\psi_o\rangle}{E_n - E_o}|\psi_n\beta\rangle$$

$$A_{1g}^{-} = A_{1g}\beta\rangle + \tfrac{1}{2}\sum_n \frac{\langle\psi_n|\epsilon\,L_z|\psi_o\rangle}{E_n - E_o}|\psi_n\beta\rangle$$

$$- \tfrac{1}{2}\sum_n \frac{\langle\psi_n|\epsilon(L_x - iL_y)|\psi_o\rangle}{E_n - E_o}|\psi_n\alpha\rangle$$

In D_{2h} symmetry designation, the operator ℓ_z mixes A_{1g} with B_{1g}, ℓ_x mixes A_{1g} with B_{3g}, and ℓ_y mixes A_{1g} and B_{2g}. In C_{2h}, ℓ_z mixes A_g with B_g and ℓ_x and ℓ_y mix A_g with A_g. The result of this calculation yields the following Kramer's doublet.

$$A_{1g}^{+} = A_{1g}\alpha\rangle - \epsilon_1|B_{1g}\alpha\rangle - \epsilon_2|B_{2g}\beta\rangle$$

$$- \epsilon_3|B_{3g}\beta\rangle - \epsilon_4|B_{3g}\alpha\rangle$$

$$A_{1g}^{-} = A_{1g}\beta\rangle + \epsilon_1|B_{1g}\beta\rangle + \epsilon_2|B_{2g}\alpha\rangle$$

$$- \epsilon_3|B_{2g}\alpha\rangle + \epsilon_4|B_{3g}\beta\rangle$$

where

$$\epsilon_1 = \frac{-i\lambda_{As}(\alpha_3 a_4 - \alpha_2 a_5)}{2(E_{B_{1g}} - E_{A_{1g}})}$$

$$\epsilon_2 = \frac{-a_1\beta_1\sqrt{3}\,\lambda_{Ni} + a_2\beta_2\lambda_{Cl}}{2(E_{B_{2g}} - E_{A_{1g}})}$$

$$\epsilon_3 = \frac{-i a_1\gamma_1\sqrt{3}\,\lambda_{Ni} + i a_2\gamma_2\lambda_{Cl}}{2(E_{B_{3g}} - E_{A_{1g}})}$$

$$\epsilon_4 = \frac{i\lambda_{Cl} a_7\gamma_2}{2(E_{B_{3g}} - E_{A_{1g}})}$$

Calculation of the Superhyperfine Tensor Elements of the Chlorine and Arsenic Ligands

The electron spin nuclear spin interaction which gives rise to the experimentally observed hyperfine splitting may be expressed as follows.

$$\mathcal{H}_{SI} = g_e g_n \beta_e \beta_n \left(\frac{8\pi}{3}\sum_{i,k}\delta(r_{ik})\mathbf{I}_i \cdot \mathbf{S}_k - \sum_{i,k}\left[r_{ik}^2(\mathbf{S}_k \cdot \mathbf{I}_i) - 3(\mathbf{S}_k \cdot \mathbf{r}_{ik})(\mathbf{I}_i \cdot \mathbf{r}_{ik})\right] r_{ik}^{-5}\right)$$

Here, g_e is the free electron g value, g_n, the nuclear g value for the ligand in question, β_e, the Bohn magneton, β_n, the nuclear magneton, $\mathbf{I}_i$, the nuclear spin vector for nucleus i, and $\mathbf{S}_k$ the electron spin vector for the kth electron. In our case, k = 1. The first term containing the Dirac delta function is the so-called "contact term".

Figure 22. The principal coordinate systems for the g tensor and the A tensors.

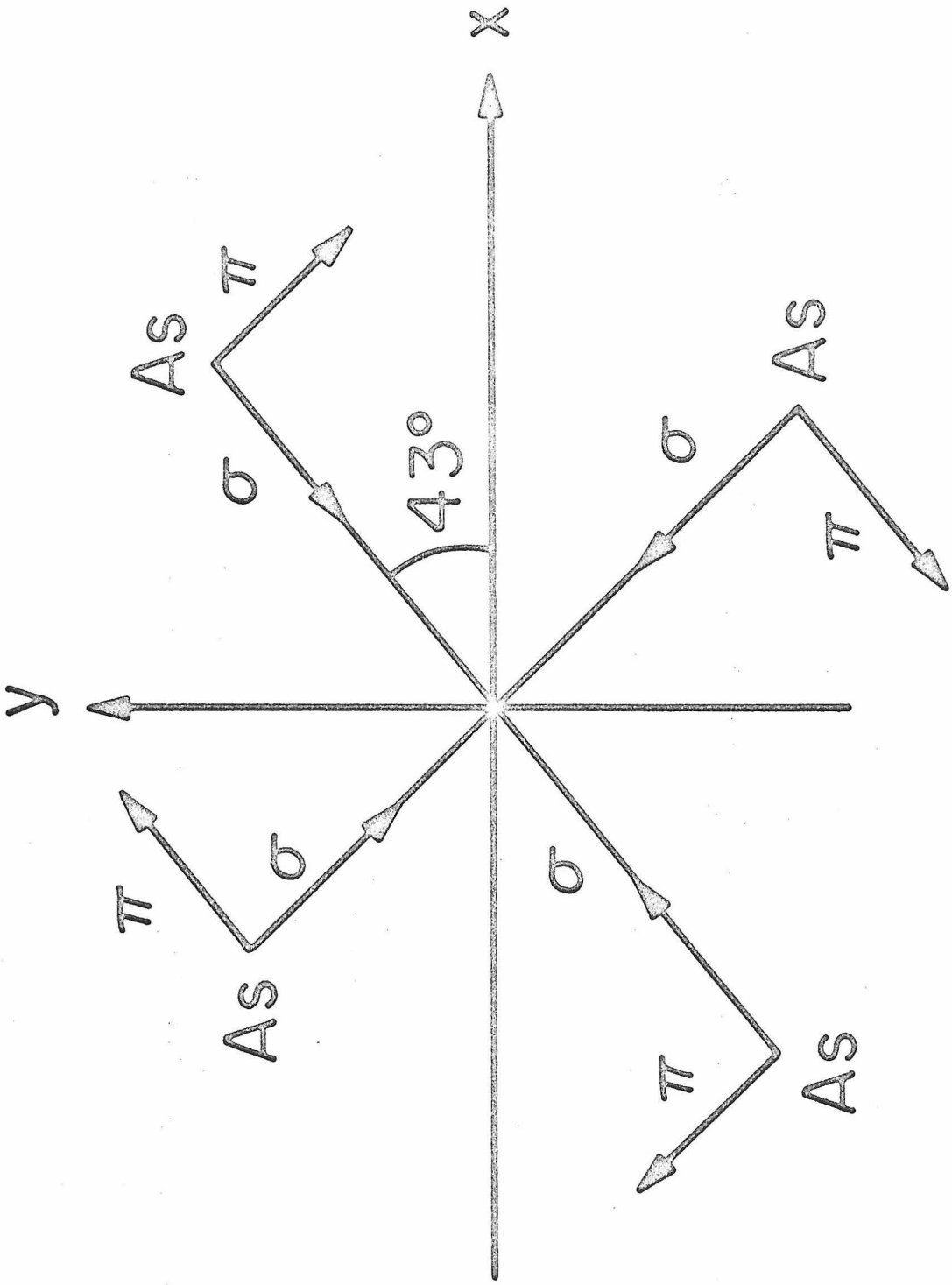
x
y
As
π
σ
43°
As
σ
π
π
σ
As
σ
π
As
As

This term expresses the interaction at the nucleus, i.e., at $r_{ik} = 0$. The second is the classical dipole term. Using spherical polar coordinates we may expand $\mathcal{H}_{SI}$ into a form more useful for calculations. The Hamiltonians for chlorine and arsenic will be different because their tensors are diagonal in different coordinate systems. Chlorine is diagonal along the symmetry axes of the molecule, xyz. Arsenic is diagonal in the $\sigma\pi z$ system illustrated in Figure 22. In deriving the arsenic Hamiltonian, we have followed McGarvey's treatment.[35]

The appropriate expressions for the superhyperfine tensors follow:

$$\underline{\text{Chlorine}} \qquad P' = g_e g_{Cl} \beta_e \beta_n$$

$$\begin{aligned}
\mathcal{H}_{SI} = {} & P'\left[\frac{8\pi}{3}\delta(r)S_z + \frac{(3\cos^2\theta - 1)}{r^3} S_z \right. \\
& \left. + \frac{3}{2}\frac{\sin\theta\cos\theta}{r^3}\left(e^{-i\phi}S_+ + e^{i\phi}S_-\right)\right] I_z \\
& + P'\left[\frac{8\pi}{3}\delta(r)S_x + \frac{(3\sin^2\theta\cos^2\phi - 1)}{r^3} S_x \right. \\
& \left. + \frac{3\sin^2\theta\sin\phi\cos\phi}{r^3} S_y + \frac{3\sin\theta\cos\theta\cos\phi}{r^3} S_z\right] I_x \\
& + P'\left[\frac{8\pi}{3}\delta(r)S_y + \frac{(3\sin^2\theta\sin^2\phi - 1)}{r^3} S_y + \right. \\
& \left. \frac{3\sin^2\theta\sin\phi\cos\phi}{r^3} S_x - \frac{3\sin\theta\cos\theta\sin\phi}{r^3} S_z\right] I_y
\end{aligned}$$

Arsenic $\qquad P' = g_e g_{As} \beta_e \beta_n$

$$\mathcal{H}_{SI} = P'\left[\frac{8\pi}{3}\delta(r)S_z + \frac{(3\cos^2\theta - 1)}{r^3}S_z + \right.$$

$$\left.\frac{3}{2}\frac{\sin\theta\cos\theta}{r^3}(e^{-i\phi}S_+ + e^{i\phi}S_-)\right]I_z$$

$$+ P'\left[\frac{4\pi}{3}\delta(r)(S_+ + iS_-) + \frac{1}{4}\frac{(1 - 3\cos^2\theta)}{r^3}(S_+ + iS_-)\right.$$

$$\left.+\frac{3}{4}\frac{\sin^2\theta}{r^3}(e^{2i\phi}S_- + ie^{-2i\phi}S_+) + \right.$$

$$\left.\frac{3}{2}(1 + i)\frac{\sin\theta\cos\theta}{r^3}(\cos\phi + \sin\phi)S_z\right]I_\sigma$$

$$+ P'\left[\frac{4\pi}{3}\delta(r)(S_+ - iS_-) + \frac{1}{4}\frac{(1 - 3\cos^2\theta)}{r^3}(S_+ - iS_-)\right.$$

$$\left.+\frac{3}{4}\frac{\sin^2\theta}{r^3}(e^{2i\phi}S_- - ie^{-2i\phi}S_+) + \right.$$

$$\left.\frac{3}{2}(1 - i)\frac{\sin\theta\cos\theta}{r^3}(\cos\phi - \sin\phi)S_z\right]I_\pi$$

Note that each of these expressions refers to only one of the ligand atoms with the θ and ϕ appropriate to that one atom. The vector, $\vec{r}$ refers to the distance between the ligand nucleus and the unpaired electron. The components of $\vec{r}$ are

$$r_x = \sin\theta\cos\phi$$

$$r_y = \sin\theta\sin\phi$$

$$r_z = \cos\theta$$

There is an alternative way of writing the Hamiltonian for the total hyperfine interaction in this system.

$$\mathcal{H}' = \sum_{i=1}^{4} A_{zi} I_{zi} S_z + A_{\sigma i} I'_{\sigma i} S_\sigma + A_{\pi i} I_{\pi i} S_\pi + \sum_{j=1}^{2} A'_{zj} I_{zj} S_z + A'_{xj} I_{xj} S_x + A'_{yj} I_{yj} S_y$$

Here, $A'_x A'_y A'_z$ are the principal elements of the chlorine tensor and $A_\sigma A_\pi A_z$ are the arsenic hyperfine constants. We may make use of these two different formulations of the Hamiltonian to obtain theoretical expressions for the tensor elements. The most convenient way to do this is to set the matrix elements of $\mathcal{H}_{SL}$ equal to the corresponding matrix elements of $\mathcal{H}'$. For example, let us obtain an expression for the chlorine A'_z element.

$$\langle A_{1g}^{+} | A'_z S_z I_z | A_{1g}^{+} \rangle =$$

$$P' \langle A_{1g}^{+} | \left(\frac{8\pi}{3} \delta(r) S_z + \frac{3\cos^2\theta - 1}{r^3} S_z + \frac{3}{2} \frac{\sin\theta\cos\theta}{r^3} (e^{-i\phi} S^{+} + e^{i\phi} S^{-}) \right) I_z | A_{1g}^{+} \rangle$$

In the calculation of superhyperfine parameters, it has been found satisfactory to use only first order terms.[36] That is, $A_{1g}^{+} = A_{1g}\alpha\rangle$ $A_{1g}^{-} = A_{1g}\beta\rangle$. Marshall has calculated the second order terms for some octahedral flourides and found them to be quite small. We have also calculated and estimated the magnitude of all

second order terms. The most generous estimate indicates that these terms cannot contribute more than ~1 gauss to the total splitting constant.

Therefore

$$\langle A_{1g}\alpha | A'_z S_z | A_{1g}\alpha \rangle =$$

$$P' \langle A_{1g}\alpha | \frac{8\pi}{3}\delta(r) S_z + \frac{3\cos^2\theta - 1}{r^3} S_z | A_{1g}\alpha \rangle$$

$$A_z^{Cl} = P' \langle A_{1g} | \frac{8\pi}{3}\delta(r) + \frac{3\cos^2\theta - 1}{r^3} | A_{1g} \rangle$$

Similarly

$$\langle A_{1g}^{+} | A'_x S_x I_x | A_{1g}^{-} \rangle =$$

$$\langle A_{1g}\alpha | A'_x S_x I_x | A_{1g}^{-} \rangle =$$

$$P' \langle A_{1g}\alpha | (\frac{8\pi}{3}\delta(r) S_x + \frac{3\sin^2\theta\cos^2\phi}{r^3} S_x) I_x | A_{1g}\beta \rangle$$

$$S_x I_x = \frac{S^+I^+ + S^-I^- + S^-I^+ + S^+I^-}{4}$$

We may choose either the S^+I^+ or the S^+I^- matrix element for comparison.

$$\langle A_{1g}\alpha | A'_x \frac{S^+I^-}{4} | A_{1g}\beta \rangle =$$

$$\langle A_{1g}\alpha | (\frac{8\pi}{3}\delta(r)\frac{S^+}{4} + \frac{3\sin^2\theta\cos^2\phi S^+}{4r^3}) I^- | A_{1g}\beta \rangle$$

$$A_x^{Cl} = \langle A_{1g} | \frac{8\pi}{3}\delta(r) + \frac{3\sin^2\theta\cos^2\phi}{r^3} | A_{1g} \rangle$$

$$A_y^{Cl} = \langle A_{1g} | \frac{8\pi}{3}\delta(r) + \frac{3\sin^2\theta\sin^2\phi}{r^3} | A_{1g} \rangle$$

The portions of the ground state wave function which contribute to the chlorine hyperfine tensor are

$$A_g^{Cl} = a_1 d_{z^2} + a_2 \phi p_{zCl} - a_6 \phi_{SCl} - a_7 \phi p_{xCl}$$

We have shown in the previous chapter that the contact terms here are negative. This means that the chlorine 3s orbitals do not make an appreciable contribution to the ground state and that we can set $a_6 \approx 0$. Most of the isotropic splitting is due to configuration interaction with lower level s orbitals. Because of the difficulties involved (see McGarvey[37]), we will not attempt to calculate the contact term.

Further expanding the expressions for the dipole terms, we obtain

$$A_{z\,dipole}^{Cl} = P' a_1^2 \langle d_{z^2} | \frac{3\cos^2\theta - 1}{r^3} | d_{z^2} \rangle$$

$$+ P' a_2^2 \langle p_z | \frac{3\cos^2\theta - 1}{r^3} | p_z \rangle +$$

$$P' a_7^2 \langle p_x | \frac{3\cos^2\theta - 1}{r^3} | p_x \rangle$$

$$A^{Cl}_{x\,dipole} = P' a_1^2 \langle d_{z^2} | \frac{3\sin^2\theta\cos^2\phi - 1}{r^3} | d_{z^2} \rangle$$

$$+ P' a_2^2 \langle p_z | \frac{3\sin^2\theta\cos^2\phi - 1}{r^3} | p_z \rangle$$

$$+ P' a_7^2 \langle p_x | \frac{3\sin^2\theta\cos^2\phi - 1}{r^3} | p_x \rangle$$

$$A^{Cl}_{y\,dipole} = P' a_1^2 \langle d_{z^2} | \frac{3\sin^2\theta\sin^2\phi - 1}{r^3} | d_{z^2} \rangle$$

$$+ P' a_2^2 \langle p_z | \frac{\sin^2\theta\sin^2\phi - 1}{r^3} | p_z \rangle$$

$$+ P' a_7^2 \langle p_x | \frac{\sin^2\theta\sin^2\phi - 1}{r^3} | p_x \rangle$$

Evaluating the integrals one obtains

$$A_{z\,dipole} = \frac{P' a_1^2}{R^3} + \frac{4}{5} P' a_2^2 \langle \frac{1}{r^3} \rangle_{3p} - \frac{2}{5} P' a_7^2 \langle \frac{1}{r^3} \rangle_{3p}$$

$$A_{x\,dipole} = \frac{-P' a_1^2}{2R^3} - \frac{2}{5} P' a_2^2 \langle \frac{1}{r^3} \rangle_{3p} + \frac{4}{5} P' a_7^2 \langle \frac{1}{r^3} \rangle_{3p}$$

$$A_{y\,dipole} = \frac{-P' a_1^2}{2R^3} - \frac{2}{5} P' a_2^2 \langle \frac{1}{r^3} \rangle_{3p} - \frac{2}{5} P' a_7^2 \langle \frac{1}{r^3} \rangle_{3p}$$

The integrals over the ligand atoms are quite straight forward. In order to calculate the metal contributions, we have used the method of Helmholz[38] which is explained in detail in appendix I. For this system

$$P'/\hbar = .06646 \times 10^{-16}$$

$$\frac{1}{R^3} = .0714 \times 10^{24}\ 1/cm^3 \text{ (R is the Ni–Cl distance)}$$

$$\langle \frac{1}{r^3} \rangle_{3p} = 55 \times 10^{24}\ el/cc$$

The components of A are in units of mc/sec.

An identical procedure may be followed in calculating the arsenic hyperfine tensor. The important parts of the wave function for arsenic are

$$A_g^{As} = a_1 d_{z^2} + a_4 \phi p_x As + a_5 \phi_y As$$

$$A_{z\ dipole}^{As} = P' a_1^2 \langle d_{z^2} | \frac{3\cos^2\theta - 1}{r^3} | d_{z^2} \rangle$$

$$+ P' a_4^2 \langle p_x | \frac{3\cos^2\theta - 1}{r^3} | p_x \rangle$$

$$+ P' a_5^2 \langle p_y | \frac{3\cos^2\theta - 1}{r^3} | p_y \rangle$$

$$A_{\sigma,\pi}^{As} = \frac{a_1^2 P'}{2} \frac{\langle d_{z^2} | 1 - 3\cos^2\theta | d_{z^2} \rangle}{r^3}$$

$$+ \frac{a_4^2 P'}{2} \frac{\langle p_x | 1 - 3\cos^2\theta | p_x \rangle}{r^3}$$

$$+ \frac{a_5^2 P'}{2} \frac{\langle p_y | 1 - 3\cos^2\theta | p_y \rangle}{r^3}$$

Note that to first order As_σ is identical to As_π. Small differences do arise in the second order terms. Most likely the small experimentally observed difference is a result of errors in the computer simulation.

$$A^{As}_{z\ dipole} = \frac{P'a_1^2}{R^3} - \frac{2}{5} P' (a_4^2 + a_5^2) \langle \frac{1}{r^3} \rangle_{4p}$$

$$A^{As}_{\sigma, \pi\ dipole} = \frac{-P'a_1^2}{2R^3} + \frac{P'}{5} (a_4^2 + a_5^2) \langle \frac{1}{r^3} \rangle_{4p}$$

$$P'/\hbar = .07745 \times 10^{-16}$$

$$\frac{1}{R^3} = .0790 \times 10^{24}\ 1/cm^3$$

$$\langle \frac{1}{r^3} \rangle_{4p} = 46.8 \times 10^{24}\ el/cc$$

The integrals $\langle \frac{1}{r^3} \rangle$ were calculated using a computer program written by Dr. T. Dunning. Clementi radial wavefunctions were used for Cl 3p[39] and Watson-Freeman functions for As 4p.[40]

Calculation of Molecular Orbital Coefficients

The three linearly independent dipole moment equations plus the normalization equation allows us to solve for four independent MO coefficients. We have set $a_4 = a_5$ in order to reduce the number of unknowns to four. From the molecular geometry we expect the As p_x mixing to be about the same as the As p_y mixing. In the previous chapter we established that there are two combinations of arsenic constants and two combinations of chlorine constants which predict the correct signs for the dipole terms. This means that there are four possible solutions to this set of equations. We have solved the four simultaneous linear equations for each possibility. Of the four combinations we tried, three predicted extremely low

Table XVIX

Molecular Orbital Coefficients and Tensor Elements for $Ni(diars)_2Cl_2^+$

Tensor Elements in Gauss		Molecular Orbital Coefficients	
A_x^{Cl}	= -32	a_1^2	= .4345
A_y^{Cl}	= -50	a_2^2	= .1335
A_z^{Cl}	= -29	$a_4^2 = a_5^2$	= .1584
A_{iso}^{Cl}	= -37	a_7^2	= .1151
A_σ^{As} } A_π^{As}	= -8.5, -6.9		
A_z^{As}	= -32		
A_{iso}^{As}	= -15.8		

values for a_1^2. The fourth solution, however, gave reasonable values for all the MO coefficients and we have selected these results as the best solution to the problem. The results are outlined in Table XVIX.

Calculation of g Values

For the dilute crystal which exhibits an axial g tensor, we can calculate the elements of g as follows.

$$g_{\parallel} = 2(A_{1g}^{+}|\ell_z + 2.0023 S_z|A_{1g}^{+})$$

$$g_{\perp} = 2(A_{1g}^{+}|\ell_x + 2.0023 S_x|A_{1g}^{-})$$

$g_{\parallel}$ and $g_{\perp}$ will be calculated to first order, i.e., terms of order ϵ^2 will be excluded.

$$\begin{aligned} g_{\parallel} &= 2.0023 + 4(A_{1g}|\ell_z|-\epsilon_1 B_{1g}) \\ &\quad + 4(A_{1g}|\ell_z|-\epsilon_4 B_{3g}) \\ &= -4i\epsilon_1[(2\alpha_2 a_1 - 2a_1\alpha_3)\int d_{z^2},\ p_{As}\sigma \\ &\quad + (a_4\alpha_3 - a_5\alpha_2)(1 + \int p_{As}p_{As}\pi - \int p_{As}p_{As}\sigma)] \\ &\quad - 4i\epsilon_4(a_7\gamma_1\sqrt{2}\int d_{xz}, p_x\pi - a_7\gamma_2) \end{aligned}$$

Since $a_4 \approx a_5$ and $\alpha_2 \approx \alpha_3$, we can set the first term ≈ 0.

$$g_{\parallel} = 2.0023 - 4i\epsilon_4(a_7\gamma_1\sqrt{2}\int d_{xz}, p_{x\pi} - a_7\gamma_2)$$

Similarly, for $g_{\perp}$

$$g_{\perp} = 2.0023 + 4(A_{1g}|\ell_x|-\epsilon_3 B_{3g})$$

$$g_{\perp} = g_x = 2.0023 - 4\epsilon_3(A_{1g}|\ell_x|\gamma_1 d_{yz} - \gamma_2\phi p_y)$$

$$\Delta g_{\perp} = -4i\epsilon_3[\sqrt{3}\, a_1\gamma_1 - a_2\gamma_2 + (a_2\gamma_1\sqrt{6} - a_1\gamma_2\sqrt{2})\int d_{z^2},\ p_{zCl}]$$

where $\int d_{z^2},\ p_{zCl}$ is the sigma overlap integral between chlorine 3p and nickel $3d_{z^2}$, and $\int d_{xz},\ p_{xCl}$ is the pi overlap integral. These were calculated using the VARIF program written by Basch.[41] The spin orbit coupling constants are 605 cm^{-1} for Ni[42] and 586 cm^{-1} for chloride.

In theory, using the a_i's obtained in our previous calculation, plus the value for $\Delta E\ B_{3g} - A_{1g}$ obtained from our spectral results (-13,200 cm^{-1}), we should be able to calculate values for γ_1 and γ_2 by simultaneously solving the equations for $g_{||}$ and $g_{\perp}$. We have done this and obtain the following results for the normalized values of γ_1 and γ_2:

$$\gamma_1^2 = .7380 \qquad \gamma_2^2 = .2619$$

It should be kept in mind that, due to the approximations necessary to reduce the number of unknowns to two, we cannot expect these coefficients to be a truly accurate representation of the configurational mixing of the B_{3g} molecular orbital into the ground state. In particular, we have completely neglected mixing with $d_{x^2-y^2}$. Such mixing should be of some importance since the arsenic atoms do make a large contribution. The addition of $d_{x^2-y^2}$ adds a potentially large term to the expression for $g_{||}$ and would have the effect of reducing the value of γ_2^2.

For this reason, although the coefficients we have obtained are quite reasonable, it does not seem profitable to attempt to draw any

rigorous quantitative conclusions from the g values in this system.

Discussion

A viable model of the electronic structure of $Ni(diars)_2Cl_2^+$ must be able to account for some rather unexpected experimental observations.

1) The chlorine superhyperfine tensor elements are not axially symmetric.

2) The isotropic arsenic splitting in $Ni(diars)_2Cl_2^+$ is 24 gauss while that in the diarsine radical cation is only 11 gauss.[13]

3) The concentrated powder spectrum of $Ni(diars)_2Cl_2^+$ shows a rhombic g tensor whereas the g tensor of the dilute powder is axially symmetric.

It was pointed out in Chapter II that almost all known d^7 and d^8 structures of diarsine complexes exhibit a departure from idealized D_{2h} symmetry. This occurs because the benzene rings are tipped and because the axial ligands are distorted from their octahedral positions. We propose that it is this distortion which is responsible for the unusual stability of the $Ni(diars)_2Cl_2^+$ cation.

The tipping of the rings lowers the symmetry from D_{2h} to C_{2h}. This allows the admixture of Clp_x and $Ni\,d_{xz}$ orbitals into the ground state. We have already seen that adding $Cl\ p_x$ to the ground state accounts very nicely for the unexpected anisotropy in the chlorine hyperfine tensor--a phenomenon which is not easily accounted for in any other way. We have also been able to explain the unusual change in g values by postulating a change in the extent of d_{xz} mixing in the

ground state. Let us assume that in the concentrated substance there is a small admixture of d_{xz}. When we dilute the paramagnetic species by putting it into a cobalt matrix, we expect the metal chloride distance to contract. This is the only reasonable change in view of the two crystal structures.

When the chlorides are in the pure crystal, they are two degrees off the z axis. As they move closer to the metal in the dilute crystal, they also move closer to the axis and bond with d_{z^2} to a greater extent. We therefore expect that the electronic ground state in the pure crystal will have a larger contribution from d_{xz} and $d_{x^2 - y^2}$ orbitals.

The presence of d_{xz} in the ground state should split the B_{2g} and B_{3g} orbitals by configuration interaction. This splitting should result in $g_y < g_x$. At the same time, the presence of d_{xz} and additional $d_{x^2 - y^2}$ in the ground state should raise the value of g_z.

We can therefore account for the rhombic g tensor observed in the concentrated powder simply by postulating that in this case there is d_{xz} in the ground state. When the crystal is diluted the chloride moves closer to the nickel and the complex rehybridizes eliminating most of the d_{xz}. We therefore return to an axially symmetric g tensor as observed.

It should be reiterated that $d_{x^2 - y^2}$ and d_{z^2} are both present in the ground state. We did not include $d_{x^2 - y^2}$ in the calculations only because we could not solve for five coefficients with only four equations. The large amount of mixing of the arsenic orbitals indicates that there is considerably more bonding in the metal arsenic

plane than would be expected if only d_{z^2} contributed to the ground state.

Finally, we come to the question of the negative contact term. We had been puzzled for some time over the observation that $Ni(diars)_2Cl_2^+$ seemed to have a larger isotropic arsenic splitting (24 gauss) than $diars^+$ (10 gauss). This result would be totally unexpected if both isotropic terms were positive. However, since we now know that $Ni(diars)_2Cl_2^+$ has a negative contact term, the explanation is obvious. Regardless of whether the contact interaction in $diars^+$ is positive or negative, it is still larger than the contact term in the nickel compound. This means that there is more arsenic 4s orbital in the ground state of the diarsine radical cation than in its complex, which is precisely what we expect.

It should be noted that the values of the contact term measured in our single crystal study ($A_{Cl} = -37$, $A_{As} = -15.8$) are not the same as those values observed in solution[43, 14] ($A_{Cl} = -17$, $A_{As} = -24$). In view of the rehybridization which we know must occur upon doping, this is to be expected. The spectra are undoubtedly quite sensitive to small distortions and are probably quite dependent upon the diamagnetic matrix which is used.

A negative contact term means that there is little ligand s orbital contribution to the ground state. This is not surprising for chlorine where we would expect primarily p bonding. However, at first it is somewhat puzzling for arsenic where we might be tempted to postulate that the orbitals are sp^3 hybrids. If we examine the crystal structure of $Ni(diars)_2Cl_2^+$ carefully, we note that the

metal-arsenic-methyl angles are all much greater than the tetrahedral angle. Apparently the s orbitals are involved largely with bonding to the methyl groups leaving primarily p orbitals to bond with the nickel.

To summarize we might say that the stability of the unusual d^7 $Ni(diars)_2Cl_2^+$ complex is due to its low symmetry which greatly facilitates the delocalization of the unpaired electron over the ligands.

APPENDIX I. THE CALCULATION OF METAL INTEGRALS

In the course of evaluating the hyperfine ligand splittings one must calculate a value for integrals of the form

$$\langle d_M \left| \frac{3\cos^2\theta' - 1}{r'^3} \right| d_M \rangle$$

where the d_M orbitals are expressed in coordinates centered on the metal and $f(\theta')$ refers to coordinates centered on the ligand.

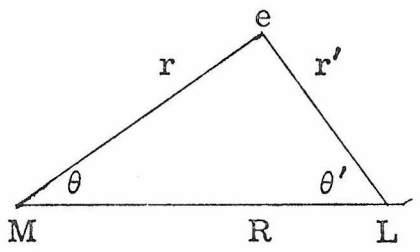

Figure 1

In Figure 1 r and r' are the distances of the electron from the metal atom and ligand atom, respectively, and R is the internuclear distance. Note that:

$$r \sin\theta = r' \sin\theta'$$

$$r'^2 = r^2 + R^2 - 2rR\cos\theta$$

Using the approach cited by Helmholz[38] we may consider two cases; $R > r$ and $r > R$. We may assume that the probability of finding the electron at a distance $r > R$ from the metal atom is quite small and

therefore it is only necessary to consider the first case. For $R > r$ we can show that

$$f(\theta') = \frac{1}{r'^3}(3\cos^2\theta' - 1) =$$

$$\frac{1}{2r^3}\frac{\partial^2}{\partial(\frac{R}{r})^2}\left[(\frac{r}{R})(1 + (\frac{r}{R})^2 - 2(\frac{r}{R})\cos\theta)\right]^{-\frac{1}{2}}$$

According to the spherical harmonic addition theorem

$$(R^2 + r^2 - 2rR\cos\theta)^{-\frac{1}{2}} =$$

$$\frac{1}{R}\sum_{n=o}^{\infty}(\frac{r}{R})^n Pn(\cos\theta) \qquad r < R$$

$$\text{or } \left[\frac{r}{R}(1 + (\frac{r}{R})^2 - \frac{2r}{R}\cos\theta\right]^{-\frac{1}{2}} =$$

$$\sum_{n=o}^{\infty}(\frac{r}{R})^{n+1} Pn(\cos\theta)$$

$$\frac{d^2}{(d\frac{R}{r})^2} = \frac{2r^3}{R^3}\frac{d}{d\frac{r}{R}} + \frac{r^4}{R^4}\frac{d^2}{(d\frac{r}{R})^2}$$

Taking the derivative of the polynomial series and dividing by $1/2r^2$ we obtain the expression for $f(\theta')$.

$$\frac{1}{R^3}\sum_{n=o}^{\infty}(n+1)(\frac{r}{R})^n Pn + \frac{r}{2R^4}\qquad (n+1)n(\frac{r}{R})^{n-1} Pn$$

where Pn are the Legendre polynomials of order n. Since the radial parts of the d functions consist of Legendre polynomials of order 2, we may automatically eleminate all terms in the series for which n is odd. For $n = 0$, $P_o = 1$ and the series reduces to $1/R^3$.

The integral $\langle d_M | \frac{1}{R^3} | d_M \rangle$ is just $\langle \frac{1}{R^3} \rangle$ which is known. For $n = 2$, the terms are on the order of $1/R^5$. For most cases $\langle 1/R^3 \rangle$ is a reasonable approximation for the metal integral.

APPENDIX II. AN ABORTIVE ATTEMPT TO SYNTHESIZE A PLATINUM(III) DIARSINE COMPLEX

It was felt that it would be useful to have a platinum analogue of our Ni(III) complex. Since stable Pt(II) and Pt(IV) derivatives were known, we proceeded to try to synthesize a Pt(III) derivative. $[Ni(IV)(diars)_2Cl_2][ClO_4]_2$ and $[Pt(IV)(diars)_2Cl_2][ClO_4]_2$ can both be made by oxidizing the divalent complexes with concentrated nitric acid or chlorine gas and then precipitating with $HClO_4$.[3] We felt that a sensible approach to the synthesis of the intermediate Pt(III) oxidation state might simply involve the use of a milder oxidizing agent.

We began by synthesizing $Pt(diars)_2Cl_2$ by Nyholm's method.[3] This compound was dissolved in ethanol and refluxed with a stoichiometric amount of iodine. After several hours the solution decolorized and a yellow precipitate formed. Unfortunately, this precipitate was diamagnetic and did not analyze for any of the possible products: $Pt(diars)_2I_3$, $Pt(diars)_2Cl_2I$, or $Pt(diars)_2ClI_2$, or $Pt(diars)_2I_4$. To avoid the obvious problems posed by the possibility of mixtures, we decided to attempt the following three syntheses.

1. $Pt(diars)_2I_2 + \frac{1}{2} I_2 \rightarrow Pt(diars)_2I_3$
2. $Pt(diars)_2Br_2 + \frac{1}{2} Br_2 \rightarrow Pt(diars)_2Br_3$
3. $2Pt(diars)_2(NO_3)_2 + 2HNO_3 + 4H^+ \rightarrow$
   $2Pt(diars)_2(NO_3)_2^+ + 2H_2O + N_2O_4$

All three starting materials were synthesized from $Pt(diars)_2Cl_2$ by exchange reactions.[3] Our attempts to make the Pt(III) derivatives are outlined below:

1. $Pt(diars)_2I_3$. Freshly prepared $Pt(diars)_2I_2$ was added to ethanol. The fresh precipitate was light green in color but turned yellow in ethanol. The concentrated solution was dark brown. After several hours of refluxing with I_2 a purplish-black precipitate was formed. This precipitate was completely insoluble in both EtOH and H_2O. This behavior seems to parallel the behavior of the Ni iodide derivatives noted by Nyholm.[1] $Ni(diars)_2I_2$ occurs in two forms; one is green and unstable, the other brown and stable. When $Ni(diars)_2Cl_3$ is treated with KI, a black insoluble precipitate is formed which was thought to be some sort of polymer. No further work was done on the compound resulting from the $Pt(diars)_2I_2$ reaction with iodine because its insolubility made purification impossible.

2. $Pt(diars)_2Br_3$. $Pt(diars)_2Br_2$ dissolved in ethanol decolorizes Br_2 instantly with the formation of a yellow precipitate. The precipitate was washed with H_2O and ethanol and recrystallized from DMF. The compound was diamagnetic and gave no ESR signal in solution at room temperature or at liquid nitrogen temperature. It did not analyze properly either for $Pt(diars)_2Br_3$ or $Pt(diars)_2Br_4$. It is interesting to note here that Nyholm[28] reported, in the course of his preparation of Ni(IV) and Pt(IV) derivatives, that the use of halogens as oxidizing agents led to products of indefinite composition which appeared to be impure.

3. $\underline{Pt(diars)_2(NO_3)_3}$. A solution of $Pt(diars)_2(NO_3)_2$ was treated with dilute (~3M) nitric acid in stoichiometric amounts. An oxidation reduction reaction took place as evidenced by the evolution of brown NO_2 gas. A yellow-white precipitate was obtained which analyzed as $Pt(diars)_2(NO_3)_3$.

	C	H	N
Theor.	25.18	3.35	4.40
Exp	25.23	3.47	4.13

Unfortunately, none of its other properties were compatible with this formulation. Again the compound was diamagnetic and gave no ESR signal. We considered the possibility that it might be a metal-metal dimer, a bridged dimer, or a hydride. However, these possibilities were ruled out. No M–H stretch could be found in the IR region appropriate for a Pt–H stretching frequency; no Pt–Pt stretch was visible in the Raman spectrum, and Beers law is followed in ethanol solution. The conductivity in nitromethane indicated that there are three ions in solution. This would be compatible with either

$$\underset{\text{monomer}}{Pt(diars)_2(NO_3)_3} \rightarrow Pt(diars)_2NO_3^{+2} + 2NO_3^-$$

$$\text{or} \quad [Pt(diars)_2(NO_3)_3] \rightarrow 2Pt(diars)_2NO_3^{+2} + 4NO_3^-$$

Unfortunately, $Pt(diars)_2NO_3^{+2}$ should be paramagnetic and give an ESR signal. When KI is added to the solution, a yellow ppt is formed. If I^- were reducing Pt(III) to Pt(II), I_2 should be released. To detect I_2, we added CCl_4 to the solution. It remained colorless. If I_2 had formed and been oxidized by excess I^- to I_3^-, the I_3^- could be detected using the starch test. This too was negative. Either the original

complex was Pt(II) and incapable of being further reduced by I^-, or it was undergoing only an anion exchange reaction with no reduction. We examined the IR of the compound in a KBr pellet and compared it to the IR of $Pt(diars)_2(NO_3)_2$. Apart from a few bands in the region where uncoordinated nitrate absorbs, the spectra were virtually identical.

An attempt to repeat the preparation failed to produce a compound with the same analysis.

Discussion

It is apparent that $Pt(II)(diars)_2X_2$ is oxidized in solution by I_2, Br_2, and dilute HNO_3. The evidence for this is the visible decolorization of the halogens and the evolution of NO_2 gas. The oxidation products of the halogens are probably impure Pt(IV) derivatives. Nyholm managed to isolate some pure Pt(IV) derivatives by precipitating with $HClO_4$. Although some of the impurities may well contain Pt(III), oxidation with halogens does not appear to be a good synthetic route to Pt(III) complexes. Dilute HNO_3 also appears to oxidize Pt(II). However, the product of this reaction seems to contain simply impure Pt(II) rather than Pt(IV). One concludes this from the IR spectrum and also from the fact that I^- does not reduce the compound at all. Pt(IV) should be a very strong oxidizing agent. Apparently if a Pt(III) derivative is formed it is very unstable and reverts by some other mechanism to Pt(II).

If Pt(II) does indeed proceed by a two-step oxidation reduction reaction to Pt(IV), the strength of the oxidizing agent is apparently crucial. If the oxidizing agent is too strong, the reaction goes to

Pt(IV). At room temperature Br_2 is too strong and I_2 is too weak. One might attempt a synthesis at room temperature using oxidizing agents intermediate in strength between the two, or using oxidizing agents weaker than I_2 at higher temperatures. We did attempt to generate a Pt(III) complex by u. v. irradiation of EtOH solution of $Pt(II)(diars)_2Cl_2$. No ESR signal could be detected apart from one at g = 2, which can be attributed to the solvent.[13] This approach might be extended further. For example, one could try different solvents or irradiate a dilute single crystal containing Pt(II) in a diamagnetic nonoxidizable matrix, for example $Co(III)(diars)_2Cl_2ClO_4$. One might also attempt these syntheses beginning with Pd(II) rather than Pt(II).

BIBLIOGRAPHY

1. R. S. Nyholm, J. Chem. Soc., 851, 2061 (1950).
2. R. S. Nyholm, J. Chem. Soc., 851, 2071 (1950).
3. C. M. Harris, R. S. Nyholm, and D. J. Phillips, J. Chem. Soc., 4379 (1960).
4. R. J. H. Clark, W. Errington, J. Lewis, and R. S. Nyholm, J. Chem. Soc., 989 (1966).
5. J. Lewis, R. S. Nyholm, and P. W. Smith, J. Chem. Soc., 2592 (1962).
6. R. S. Nyholm, Nature, 183, 1039 (1959).
7. R. V. Parish and R. S. Nyholm, Chem. and Ind., 470 (1956).
8. R. S. Nyholm and G. J. Sutton, J. Chem. Soc., 572 (1958).
9. V. F. Duckworth and N. C. Stephenson, J. Inorg. Chem., 8, 1661 (1969).
10. R. S. Nyholm, Nature, 168, 705 (1951).
11. R. D. Feltham and W. Silverthorn, J. Inorg. Chem., 7, 1154 (1968).
12. R. D. Feltham and W. Silverthorn, J. Inorg. Chem., 9, 1207 (1970).
13. James Preer, Ph.D. Thesis, California Institute of Technology, 1970.
14. P. Kreisman, R. E. Marsh, J. Preer, and H. B. Gray, J. Am. Chem. Soc., 90, 1067 (1968).
15. E. I. Stiefel, J. H. Waters, E. Billig, and H. B. Gray, J. Am. Chem. Soc., 87, 3016 (1965).

16. D. C. Olson and J. Vasilevskis, J. Inorg. Chem., 8, 1611 (1969).

17. A. Wolberg and J. Manassen, J. Am. Chem. Soc., 92, 2982 (1970).

18. D. J. Duchamp, (1964) ACA Meeting, Bozeman, Montana, paper B-14, p. 29.

19. J. A. Ibers, "International Tables for X-ray Crystallography," Kynock Press, Birmingham, England, 1962, Vol. 3, Table 3.3.1.

20. R. F. Stewart, E. R. Davidson, and W. T. Simpson, J. Chem. Phys., 42, 3175 (1965).

21. N. C. Stephenson, Acta Cryst., 17, 592 (1964).

22. N. C. Stephenson, Acta Cryst., 17, 1517 (1964).

23. N. C. Stephenson, J. Inorg. Nucl. Chem., 24, 791 (1962).

24. N. C. Stephenson, J. Inorg. Nucl. Chem., 24, 797 (1962).

25. F. W. B. Einstein and G. Rodley, J. Inorg. Nucl. Chem., 29, 347 (1967).

26. P. Pauling, unpublished results.

27. C. Corvaja and P. L. Nordio, La Ricerca Scientifica, 44 (1968).

28. R. S. Nyholm, J. Chem. Soc., 2602 (1951).

29. W. H. Hamill in "Radical Ions," ed. E. T. Kaiser and L. Kevan, Interscience Pub., New York, 1968, Chap. 9.

30. P. W. Selwood, "Magnetochemistry," Interscience, New York, 1956.

31. S. Yamada, Coord. Chem. Rev., 2, 83 (1967).

32. G. Rodley, private communication.

33. F. D. Tsay and H. B. Gray, to be published.

34. R. S. Nyholm, J. Chem. Soc., 857 (1950).

35. B. McGarvey, Transition Metal Chemistry, 3, 90 (1966).

36. W. Marshall and R. Stuart, Phys. Rev., 123, 2048 (1961).

37. B. McGarvey, J. Phys. Chem., 71, 51 (1967).

38. L. Helmholz, A. Guzzo, and R. Sanders, J. Chem. Phys., 35, 1349 (1961).

39. E. Clementi, "Tables of Atomic Functions," Supplement to IBM Journal of Research and Development, 9, 2 (1965).

40. R. E. Watson and A. J. Freeman, Phys. Rev., 124, 117 (1961).

41. C. J. Ballhausen and H. B. Gray, "Molecular Orbital Theory," W. A. Benjamin, Inc., New York, 1964.

42. H. Brooks, Ph.D. Thesis, Columbia University, 1968.

43. P. T. Manoharan, private communication.

Proposition 1

Abstract It is proposed that the technique of Photoelectron Spectroscopy be used to determine the mode of oxygen -iron binding in Hemoglobin.

The technique of Photoelectron Spectroscopy or ESCA was developed by Siegbahn and coworkers [1] at the University of Uppsala in Sweden. In principle, when a substance is irradiated with x-rays photoelectrons are emitted. The energy of an emitted electron is characteristic of the element from which it originates, and also characteristic of the particular atomic energy level from which it has been ejected. By monitoring the number of electrons ejected as a function of the x-ray energy, one can measure the binding energy of an inner electron shell with a precision of a few tenths of an electron volt. The peak obtained is extremely narrow, and thus the technique is quite sensitive and capable of extremely high resolution. For example, using ESCA one can easily detect the cobalt atom in a small sample of vitamin B12 or the sulfur atoms in insulin. [1]

The position of the electron peak is sensitive to the charge on the atom. The formation of a chemical bond, which changes the charge distribution of the outer electrons, effects a change in the screening of the core electrons. Thus, the photoelectron spectrum reflects changes in valence state. In a complex organic molecules one can distinguish CH_3 carbon from CH_2, CH, or carbon bonded to any other group. One can use these results in two ways. Since ESCA shifts are characteristic for a given group, the technique may be applied to detailed qualitative analysis. ESCA shifts can also be calculated theoretically using Hartree Fock methods and can be correlated with a semiempirical determination of effective charge. In this way one can make some estimate of the nature of the chemical bond involved.

In general, the bonding energies of core electrons increase with increasing oxidation state. ESCA shifts have been correlated directly with oxidation number for inorganic sulfates, sulfites, perchlorates and perchlorites. For covalently bonded compounds, the shifts may be correlated with modified oxidation numbers based on differences in electronegativity.

ESCA has enormous potential for qualitative and quantitative analysis of complicated molecules. Each atom in each of its valence states makes a characteristic contribution to the spectrum. The relative intensities of the peaks gives a quantitative measure of the percent of each kind of atom in the molecule. Klein and Kramer have used this technique in the analysis of proteins.[2] They have been able to estimate quantitatively the nitrogen and sulfur content of several different proteins and have been able to distinguish between amine and amide nitrogen.

There has been much debate in the literature about the method by which oxygen binds to iron in hemoglobin. Griffith[3] has suggested that oxygen binds symmetrically. This model is compatible with Fe(IV) peroxide.

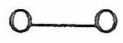

Griffith Model

Pauling[4] has suggested that oxygen binds asymmetrically as superoxide.

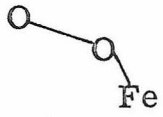

Pauling Model

A cobaltihemoglobin has recently been synthesized and has been shown by EPR to contain superoxide.[5] We propose to use ESCA to attempt to determine whether O_2^{-2} or O_2^{-1} is present in the hemoglobin molecule.

We propose first to study a series of model peroxide and superoxide compounds in order to determine the shift of the oxygen 1s level in each case. These model compounds should include H_2O_2, CaO_2, BaO_2, Na_2O_2, KO_2, RbO_2, and the recently characterized cobalt dimers[6] $((NH_3)_5Co\text{-}O_2\text{-}Co(NH_3)_5)^{+4}$ and $((CN)_5Co\text{-}O_2\text{-}Co(CN)_5)^{-5}$. There also exists an unstable $Fe(III)(EDTA)O_2^{-3}$ monomer which might be examined in solution.[7] Hopefully these studies will provide a criterion for distinguishing peroxide and superoxide from each other and from organic oxygen.

The difficulty in this experiment is, of course, the

presence of oxygen in the protein portion of hemoglobin. Organic oxygen should give rise to a fairly inten se peak and it may prove difficult to resolve the less intense peroxide or superoxide unless its position is appreciably shifted from the protein peak. One would want to examine the cobaltihemoglobin carefully to see whether superoxide is resolvable in this case. Obviously one would also want to examine deoxyhemoglobin to be certain that a ligand O_2 peak has been correctly assigned.

If either the Pauling or the Griffith model is valid, one should be able to distinguish between them using ESCA. In the Griffith model the oxygens are equivalent and should give rise to only one peak. In the Pauling model they are not equivalent and a splitting should be observed.

Ideally one would prefer to work with the iron peak. Kramer and Klein have measured the ESCA chemical shifts of some iron complexes.[8] These complexes showed the expected changes in binding energy verses oxidation state for complexes of the same ligand but were extremely difficult to correlate with complexes of different ligands. Although it might be possible to estimate th e charge on iron in hemoglobin using ESCA, this experiment would not offer any conclusive proof of the method of oxygen binding.

References

1. Siegbahn et al., "ESCA, Atomic, Molecular and Solid State Structure Studied by means of Electron Spectroscopy," Almquist and Wiksells, Uppsala(1967).

2. L.N. Kramer and M.P. Klein, to be published.

3. Griffith, Proc. Royal Soc. (London), A 235, 23 (1956).

4. Pauling, Haemoglobin, Sir Joseph Barcroft Memorial Symposium, p. 57, London, Butterworths, (1949).

5. Basolo, Conference on Inorganic Biochemistry, Blacksburg Virginia, (1970).

6. W.P. Shaefer and R.E. Marsh, J. Am. Chem. Soc., 88, 178(1966).

7. C. Walling, M. Kurz and H. Schugar, J. Inorg. Chem., 9, 931(1970).

8. L.N. Kramer and M. P. Klein, J Chem Phys., 51, 3618(1969).

Proposition II

Abstract It is proposed that the technique of thin film single crystal u. v. spectroscopy be used to facilitate the assignment of the charge transfer spectra of d^6 and d^7 diarsine complexes.

The ligand field and charge transfer spectra of known d^6 and d^7 diarsine complexes are quite difficult to assign.[1, 2] In particular the charge transfer spectra are complicated by the presence of intraligand transitions of fairly high intensities above 30, 000 cm^{-1}.[3] The assignment of the charge transfer spectra would be greatly facilitated if it were possible to determine the polarizations of these bands. Single crystal polarization work in the u. v. region has proved difficult because of the high intensities of the charge transfer bands. Workers in single crystal spectroscopy have previously used sections of single crystals cut to a thickness of about 10μ with a rotatory microtome.[4] This is sufficient for work in the visible region but too thick to be satisfactory in the u. v. region. Recently however, a technique has been developed using thin film single crystals[5] which has been successful in interpreting the spectra of the tetrachloroplatinates. Thin film crystals are grown by evaporating a solution on a saphire plate and single crystal regions are selected using a polarizing microscope. The rest of the plate is masked off. Crystals grown in this way are less than 10μ thick. They can be cooled to 77°K by conduction from a brass block immersed in liquid nitrogen.

The microsymmetry of all known d^6 and d^7 diarsine complexes with the exception of $Co(diars)_2Cl_2ClO_4$ [6] is C_{2h}.

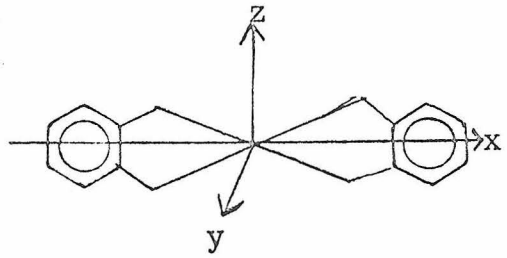

Because the benzene rings are tipped, the y axis is the two-fold axis, and the xz plane the σh. In this notation the orbitals transform as

follows:

A_g :	xz, z^2, x^2-y^2
B_g :	xy, yz
Au :	y
B_u :	x, z

The ground state for the d^6 complexes is ^1A_g and for the d^7 complexes ^2A_g. The fully allowed charge transfer transitions are

$A_g \longrightarrow A_u$ y polarized and

$A_g \longrightarrow B_u$ xz polarized.

There are two fully allowed As$\longrightarrow$M charge transfers, and two fully allowed X$\longrightarrow$M transitions in the system. The crystal structures of the isomorphous series $Ni(diars)_2X_3$ and $Co(diars)_2X_3$ (X=Cl, Br, N CS) are known[1] as is the crystal structure of ($Cl(diars)_2X_2)ClO_4$.[6]

Piper[7] has discussed the problem of how to determine polarizations in crystals of low symmetry. Let the crystal axes be x, y, z and let the molecular axis make an angle θ with the crystal z axis.

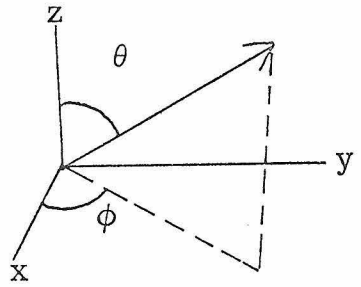

$\frac{I}{I_o} = 10^{-A}$ where I_o = incident intensity, I= transmitted intensity, and A = absorbance. If the incident ray is parallel to the crystal y axis and is polarized parallel or perpendicular to z, then the fraction of light transmitted may be resolved into components parallel(π) and perpendicular (σ) to the molecular axes.

$$10^{-A}_{\parallel} = \cos^2\Theta\, 10^{-A\pi} + \sin^2\Theta\, 10^{-A\sigma}$$

$$10^{-A}_{\perp} = \sin^2\Theta\cos^2\phi\, 10^{-A\pi} + (1-\sin^2\Theta\cos^2\phi)\, 10^{-A\sigma}$$

Experimentally, the plane of polarization of the light is rotated with respect to the crystal and the absorbance of a given band is measured as a function of angle. The equations are then solved for $A\sigma$ and $A\pi$.

References

1. P. Bernstein, Thesis, California Institute of Technology, (1970).

2. Feltham and Silverthorn, J. Inorg. Chem., 7, 1154 (1968).

3. J. Preer and H. B. Gray, to be published.

4. Ferguson, J. Chem. Phys., 34, 1609 (1961).

5. C. Cowman and H. B. Gray, to be published.

6. P. Pauling, unpublished results.

7. Piper, J. Chem. Phys., 35, 1240 (1961).

Proposition III

Abstract It is proposed to use the ligands NNN'N' tetramethyl-o-phenylenediamine and o-phenylenebisdimethylphosphine to prepare Co, Ni, Pd and Pt analogues to diarsine complexes and to study their properties.

Considering the wide variety of complexes formed by o-phenylenebisdimethylarsine ($o\text{-}C_6H_4(As(CH_3)_2)_2$) [1] it is surprising that little work has been done on complexes of the analogous nitrogen and phosphorus ligands NNN'N' tetramethyl o-phenylene diamine and o-phenylenebisdimethylphosphine. This scarcity of information is undoubtedly due in part to difficulties associated with synthesizing the ligands. A reasonably good synthesis for the phosphine in particular was only reported in 1960, [2] and even this synthesis gives only an 11% yield.

It would be extremely interesting to compare the properties of the Co, Ni, Pd, and Pt diarsine complexes with those of their diamine and diphosphine analogues. Since the electronic structure of the diarsine compounds is now known, [3, 4] one ought to be able to make some definite predictions about the properties of the complexes as the energies of the donor orbitals decrease in going from arsenic to phosphorus to nitrogen. In particular, one would expect that four or five coordinate complexes would form. Diarsine forms four coordinate complexes $(M(diars)_2)(ClO_4)_2$ where M=Pd, Pt [5, 6] and also complexes of the form $(M(diars)_2)X_2$ where X=Cl, Br, CNS, NO_2, and M=Ni, Pd, and Pt which exhibit five coordination in nitrobenzene solution. The complex $Pd(diars)_2I_2$ has been shown by x-ray crystallography to be six coordinate in the solid state. [7]

Diarsine is capable of stabilizing unusually high coordination numbers. This is due to the fact that the orbital energy of arsenic σ bonding orbitals is close to the energy of the metal d orbitals. This permits extensive covalent bonding and substantial delocalization over the ligand framework. $Ni(diars)_2X_2^+$ for example [3] is a stable six coordinate Ni(III) complex with a ^2A_g ground state. Because the electron in the dz^2 orbital is not localized on the

metal, electron repulsion is sufficiently reduced to permit the axial ligands to coordinate. One would not expect the diamine to be capable of stabilizing this structure. It would be particularly interesting to see whether one could obtain a five coordinate Ni(III) derivative of the diphosphine. Although the phosphorus ligand cannot participate in σ bonding as extensively as diarsine does, it can achieve additional stabilization via π backbonding between filled metal and empty phosphorus 3d orbitals. This stabilizing factor is not possible in the diamine and of doubtful importance in diarsine because of the high energy of the empty arsenic 4d orbitals. An unstable five coordinate complex of Ni(III) has in fact been reported with the phosphorus ligand $P(Et)_3$.[8] This complex was postulated to have a tetragonal pyramid structure.

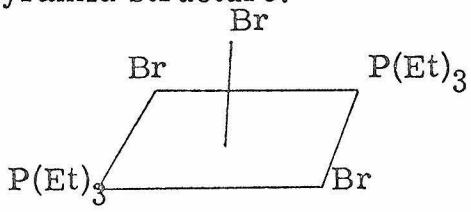

A few complexes have been reported recently with these ligands.

NNN'N' tetramethyl phenylene diamine forms a four coordinate complex with Pd(II)[9] of the form

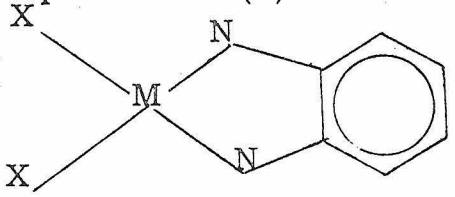

M= Pd
X= Cl, Br, I

Its diarsine analogue exists.[10] Graziani[11] et al. have reported preliminary space group data but not crystal structures for compounds with the formulation; $Ni(II)(o\text{-}C_6H_4\text{-}(N(CH_3)_2)_2)Cl_2H_2O)_2$, $Cu(II)(o\text{-}C_6H_4\text{-}(N(CH_3)_2)_2)Cl_2$, and $Hg(II)(o\text{-}C_6H_4\text{-}(N(CH_3)_2)_2)Cl_2$. Rizzardi describes the synthesis of Cr and W carbonyl compounds; $Cr(CO)_3L$ and cis $W(CO)_4L$.[12] Clark has made diamine derivatives of Ti, Zr and Sn.[13] $(TiF_4)_2L$ is probably a six coordinate halogen bridged dimer, $SnCl_4L$ is also probably six coordinate, and $ZrCl_4 \cdot 1\ 1/2\ L$ has been postulated to be eight coordinate like the analogous diarsine complex. A few non-transition metal complexes

of the diamine have also been reported with magnesium,[14] dimethylberyllium[15] and diphenylberyllium.[16]

Several interesting complexes have also been made with o-phenylenebisdimethylphosphine and the similar diethyl derivative. Four coordinate Ni(II) and Pd(II) complexes have been reported.[17] Both $Pd(o\text{-}C_6H_4(P(Et)_2)_2)_2Br_2$ and $Ni\ (o\text{-}C_6H_4(P(Et)_2)_2)_2(NO_3)_2$ are four coordinate. Complexes also exist with tungsten $(cisW(CO)_2L)$[18], cobalt,[19] and iron.[20] Cobalt forms a five coordinate hydride L_2CoH which can be converted into a six coordinate diaryl boron comples $L_2Co(BPh_2)_2$.[19] Bancroft[20] has studied the Mossbauer spectra of several interesting low spin Fe(II) derivatives of the form FeX_2Y_2, X= H, Cl, Br Y= o-phenylene-bisdimethylphosphine.

We propose to prepare Ni, Co, Pd and Pt derivatives of these two ligands and to study their optical and magnetic properties via electronic spectroscopy, ESR, and magnetic susceptibility.

References

1. R. S. Nyholm, J. Chem. Soc., 2061(1950).

2. F. A. Hart, J. Chem. Soc., 3324(1960).

3. P. Bernstein, Thesis, California Institute of Technology(1970).

4. J. Preer, Thesis, California Institute of Technology (1969).

5. C. M. Harris and R. S. Nyholm, J. Chem. Soc., 4375(1956).

6. C. M. Harris, R. S. Nyholm, and D. J. Phillips, J. Chem. Soc., 4379(1960).

7. N. C. Stephenson, J. Inorg. Nucl. Chem., 24, 797 (1962).

8. K. Jenson and B. Nygaard, Acta Chem. Scand., 3, 474 (1949).

9. F. H. C. Stewart, Chem. and Ind., 264 (1958).

10. J. Chatt and F. G. Mann, J. Chem. Soc., 1622(1939).

11. Graziani, Bombieri and Forsellina, Ric. Sci. 36, 855(1966).

12. Rizzardi et al, Gazz. Chem. Ital., 98, 1231 (1968).

13. R. H. Clark, and W. Errington, J. Chem. Soc., A, 258(1967).

14. G. E. Coates and J. A. Heslop, J. Chem. Soc., 26(1966).

15. N. A. Bell and G. E. Coates, Canad. J. Chem., 44, 744(1966).

16. G. E. Coates and M. Tranah, J. Chem. Soc., A, 236 (1967).

17. J. Chatt, F. A. Hart, and H. R. Watson, J. Chem. Soc., 2537 (1962).

18. Adams, J. Chem. Soc. A, 87 (1969).

19. Schmid and Noeth, Chem. Ber. 100, 2899 (1967).

20. Bancroft, Mays and Prater, Chem. Comm., 39(1969).

Proposition IV

Abstract It is proposed to study the bonding characteristics of molecular nitrogen in its transition metal complexes.

Since Allen and Senoff reported the synthesis of the first molecular nitrogen complex[1], $(Ru(NH_3)_5N_2)Cl_2$, a large number of nitrogen complexes with transition metals have been prepared. Some of the more important include the following:

Ruthenium: In addition to $Ru(NH_3)_5N_2^{2+}$ [1], a dinitrogen complex[2] $Ru(NH_3)_4(N_2)_2^{2+}$ and a nitrogen bridged dimer[3] have been prepared. The structure of the dimer was recently confirmed by x-ray crystallography.[4]

Osmium: Osmium analogues exist to the pentamine and tetramine ruthenium complexes, $Os(NH_3)_5N_2^{2+}$ [5] and $Os(NH_3)_4(N_2)_2^{2+}$ [6]. Osmium complexes of the form $OsX_2N_2L_3$, X=Cl, Br, L=PMe_2Ph, PEt_2Ph, PPr_2Ph, PBu_2Ph, $PEtPh_2$, PEt_3 have also been reported[7]. All these complexes are extraordinarily stable.

Rhenium: Another important series are the rhenium complexes. Chatt et al have prepared $ReCl(PPh_3)_2(CO)_2N_2$ [8] and also a series of complexes of the form $ReXN_2L_2$, X=Cl, Br, and L=$Ph_2PCH_2CH_2PPh_2$, $Ph_2PCH_2PPh_2$, $Ph_2PCH=CH-PPh_2$, and $PMePh_2$ [9]. These can be oxidized with quantitative evolution of N_2. One complex, $ReClN_2(PPh_2CH_2CH_2PPh_2)_2$, oxidizes to give a paramagnetic monomer $(ReClN_2L_2)^+Cl^-$ with a magnetic moment of 1.9.

Cobalt: Cobalt forms an interesting series of mixed nitrogen-hydride complexes $CoHN_2L_3$ [10] and $CoHN_2L_2$ [11], L=PPh_3, $PMePh_2$, $PEtPh_2$, $PBuPh_2$, PEt_2Ph and other phosphorous ligands. The paramagnetic species $CoN_2(Ph_3P)_3$ [12] has also been reported. Misono et al. have observed that in the $CoHN_2L_2$ system, the N-N stretch is shifted to lower positions with an increase in the electron donating power of L.

Iron and Molybdenum: These elements are present in trace quantities in all biological systems capable of fixing nitrogen.[13] For this

reason, the electronic structure of simple adducts of molecular nitrogen containing these metals is of particular interest. $Mo(acac)_3$ can be reduced in the presence of $Ph_2PCH_2CH_2PPh_2$ under nitrogen to give trans $MoL_2(N_2)_2$ [14]. This complex has been characterized by its IR spectrum. Bancroft et al[15] have described the preparation of the very reactive species trans $FeHN_2(depe)_2$, depe=$Et_2PCH_2CH_2PEt_2$, and Sacco and Oresta[16] have prepared $FeN_2H_2L_3$ with L=$PEtPh_2$ and $PBuPh_2$. Just recently Bell and Buntzinger described the first stoichiometric reduction of molecular nitrogen to ammonia in a system containing iron. The system contained $FeCl_3$ and Dilithium naphthalene as the reducing agent. No iron complex was isolated in this reaction but one presumably occurs as an intermediate. None of the other iron or molybdenum complexes are susceptible to reductive cleavage.

The work in this field thus far has been mainly preparative. Nitrogen complexes can be characterized by the N-N stretch in the IR approximately 200 cm^{-1} lower than in free nitrogen[1]. In $Ru(NH_3)_5N_2^{+2}$ this band is at 2170 cm^{-1}. The frequency of this band depends on the other ligands in the system. As the other ligands increase their donating power, more electron density is fed into the nitrogen π^* orbitals, thus decreasing the overall bond order and decreasing the frequency of the N-N stretch [12]. Bancroft et al[15] have concluded on the basis of Mossbauer spectra that CO is both a better σ donor and a better π acceptor than N_2.

It would be interesting to do a detailed spectroscopic study of the well-characterized nitrogen complexes and their isoelectronic CN^-, CO and NO^+ analogues. CN^- is an excellent σ donor and NO^+ an excellent π acceptor. A comparison of UV and visible spectra could shed light on the relative importance of σ and π bonding in the nitrogen system.

Of particular interest would be a study of the photoelectron spectra of molecular nitrogen complexes. Thus far it has proved extremely difficult to achieve cleavage of the nitrogen molecule

followed by reduction to ammonia. Most efforts to reduce these complexes have resulted in their decomposition with evolution of nitrogen. In their original paper[2], Allen and Senoff thought that they had achieved reduction to ammonia, but Chatt later showed by N^{15} substitution that none of the ammonia was from the nitrogen molecule[18]. A good nitrogenase model should have the following characteristics: The metal-nitrogen bond should be strong enough for the compound to form from atmospheric nitrogen, but not so strong as to make the compound totally unreactive. Once complexed, the N-N bond should be sufficiently weakened to be susceptible to cleavage. There should be some charge separation between the nitrogens, since a positive charge will facilitate reduction. Presumably, one could achieve these conditions if the correct combination of metal and ligands were available. It would be interesting to try to correlate the reactivity of known nitrogen complexes with the position of the nitrogen 1s band in the photoelectron spectrum. If there is a charge separation, it should be reflected by a doublet rather than a singlet in this position.

We propose therefore to examine the electronic and photoelectron spectra of the known nitrogen complexes in an attempt to elucidate the important bonding features of the nitrogen molecule. Hopefully these studies will provide some insight into the design of a simple transition metal complex which can perform the functions of nitrogenase.

References

1. A.D. Allen and C.V. Senoff, Chem. Comm., 621 (1965).

2. J. Fergusson and J.L. Love, J. Chem. Soc. D, 399 (1969).

3. D.E. Harrison, H. Taube and E. Weissberger, Science, 159, 320 (1968).

4. I. Treitel, M. Flood, R. Marsh and H.B. Gray, J. Am. Chem. Soc. 91, 6512 (1962).

5. P.K. Das, J.M. Pratt, R.G. Smith, G. Swinden and W. Woolcock, Chem. Comm., 1539 (1968).

6. H.A. Scheidegger, J.N. Armor and H. Taube, J. Am. Chem. Soc. 90, 3263 (1968).

7. J. Chatt, G. Leigh and R. Richards, J. Chem. Soc. D, 515 (1969).

8. J. Chatt, Dilworth, G. Leigh, J. Organometal Chem., 21, 149 (1970).

9. J. Chatt, Dilworth and G. Leigh, J. Chem. Soc. D, 687 (1969).

10. M. Rossi and A. Sacco, J. Chem. Soc. D, 471 (1969).

11. A. Misono, Y. Uchida, Saito, M. Hidai and M. Araki, Inorg. Chem. 8, 168 (1969).

12. Speier and Marko, Inorg. Chim. Acta, 3, 126 (1969).

13. R. Murray and D.C. Smith, Coord. Chem. Rev. 3, 429 (1968).

14. M. Hidai, Tominari, Y. Uchida and A. Misono, J. Chem. Soc. D, 1392 (1969).

15. Bancroft, Mays and Prater, J. Chem. Soc. D , 585 (1969).

16. A. Sacco and M. Arista, Chem. Comm. , 1223 (1968).

17. L. Bell and H. Brintzinger, J. Am. Chem .Soc. 92, 4464 (1970).

18. J. Chatt, R. Richards, J. Fergusson and J.L. Love, Chem. Comm. , 1522 (1968).

Proposition V

Abstract It is proposed to use electron spin resonance to study the paramagnetic product of the reaction between K_2PdI_4 and EDM (N, N-ethylenedimorpholine).

Recently Lott and Rasmussen[1] reported what they believed to be the first paramagnetic, tetrahedral complex of Pd(II). They reacted the ligand N, N ethylenedimorpholine (EDM) with K_2PdI_4 in acetone.

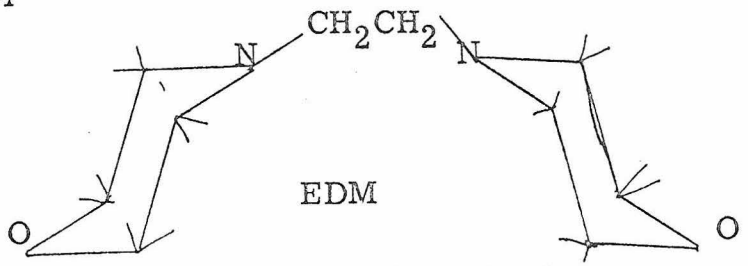

EDM

The reaction product is a diamagnetic solid 2 with stoichiometry PdI_2EDM. When dissolved in acetone, 2 gives a light red solution 3, which darkens after two hours to give a dark red solution 4. 2, 3, and 4, are all diamagnetic. Addition of excess EDM to 4 gives a light red paramagnetic solution 5. A reaction scheme is shown as follows:

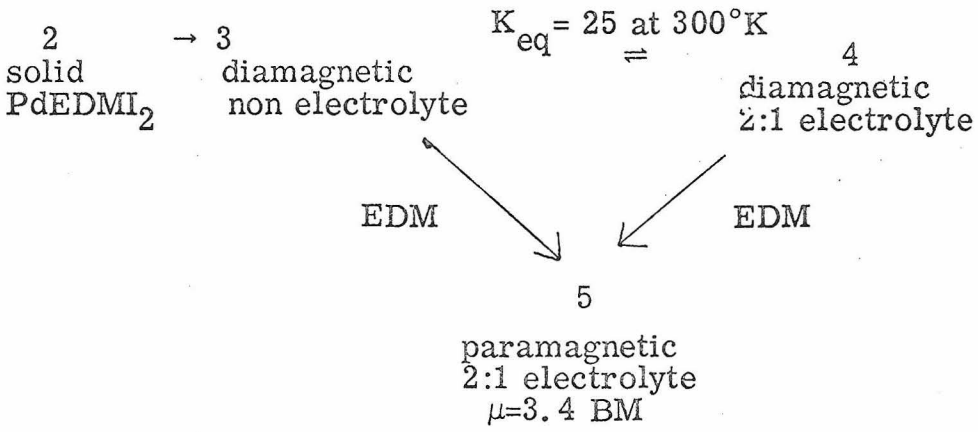

On the basis of conductivity data and knowledge of the steric requirements of the ligand, Lott and Rasmussen suggested the following probable structures for the species 2-5. They postulate that 2 and 3 are square planar monomers, that 4 is a dimer with bridging iodides, and that 5 is the tetrahedral species $Pd(II)(EDM)_2^{2+}$.

They suggest a tetrahedral structure because the steric requirements of the ligand and the paramagnetism (μ= 3.4 BM) make either an octahedral or a square planar structure unlikely.

If 5 is in fact tetrahedral $Pd(EDM)_2^{2+}$ then it would be of interest to measure and interpret its ESR spectrum. It should be possible to fit the spectrum to the following spin hamiltonian.[2]

$$H= g_{\parallel}\beta_e H_z S_z + g_{\perp}\beta_e(H_x S_x + H_y Sy) + D(S_z^2-2/3) + E(S_x^2-S_y^2) +$$

$$A_{Pd}S_z I_z + B_{Pd}(S_x I_x + S_y I_y) + \sum_{i=1}^{4} A_N S_z I_{zi} + B_N(S_x I_{xi} + Sy I_{yi})$$

(Pd has a nuclear spin of 5/2 and N a nuclear spin of 1.)

One expects to encounter the same difficulties in measuring the ESR spectrum of a tetrahedral d^8 system as one finds in an octahedral d^2 system. Both have a ^3F ground state with three lowest orbital levels connected by spin orbit coupling. This gives rise to short spin lattice relaxation times and large values of the zero field splitting constant, both of which make it difficult to detect an ESR signal. To optimize conditions for obtaining a spectrum one should work at liquid Nitrogen or even at liquid helium temperatures, and one should use a K band instrument. The low temperatures will lengthen the spin-lattice relaxation time and a K band instrument facilitates the detection of fine structure lines occuring at very high field strengths.

One would prefer to work with a crystal of the material rather than a solution, since lower temperatures may be achieved in a solid sample. Lott and Rasmussen did not isolate the tetrahedral species from solution, however it seems likely that it will be possible to do so. If the compound can be crystallized, an x-ray crystal structure would be desir able.

We propose therefore to attempt to isolate and crystallize this complex, to determine its structure, and to try to obtain its ESR spectrum as a solid and in solution at low temperatures.

References

1. A. Lott and P. Rasmussen, J. Am. Chem. Soc., 91, 6502(1969).

2. B. McGarvey, Transition Metal Chemistry, 3, 89 (1966).